Title
Ecological processes driving the structure and function of marine algal communities: from species traits to species invasions

Author
Ryznar, Emily Rose

Publication Date
2021

Peer reviewed|Thesis/dissertation

UNIVERSITY OF CALIFORNIA

Los Angeles

Ecological processes driving the structure and function of marine algal communities: from species traits to species invasions

A dissertation submitted in partial satisfaction
of the requirements for the degree Doctor of Philosophy
in Biology

by

Emily Rose Ryznar

2021

ABSTRACT OF THE DISSERTATION

Ecological processes driving the structure and function of marine algal communities: from species traits to species invasions

by

Emily Rose Ryznar
Doctor of Philosophy in Biology
University of California, Los Angeles, 2021
Professor Peggy Marie Fong, Chair

Marine ecosystems are complex and diverse, with multiple, often simultaneous processes influencing community structure and functioning. While algae play pivotal roles in supporting biodiversity and ecosystem function, dramatic population increases due to human-induced factors are causing shifts to undesirable alternate states that may not be reversable, motivating research into understanding the processes shaping algal communities in the Anthropocene.

Functional groups cluster species assumed to have similar responses to environmental drivers and effects on ecosystem functioning, but these assumptions are rarely tested for marine algae. In Chapter 1, I evaluated the Functional Group Model (FGM), which groups species based on morphological complexity, and makes predictions for traits assumed to correspond with ecological function. We tested these predictions by measuring growth, toughness, and tensile strength across tropical and temperate algae. Only toughness aligned with FGM predictions. Further, there was significant within-group variability among species for all traits, implying the

FGM does not predict community responses to ecological drivers and/or contributions to ecosystem function.

Marine algal invasions pose severe threats to marine communities, but mechanisms driving invasion success are poorly understood. In Chapter 2, I evaluate how community diversity, herbivory, and interactions with the foundational kelp, *Macrocystis pyrifera*, influence success of the invasive alga, *Sargassum horneri*, in southern California. I found neither herbivory nor diversity provide strong explanations for invasive success, suggesting *S. horneri* requires disturbance to invade. In Chapter 3, I use stage-structured population models to assess whether interactions between kelp and *S. horneri* influence invasion success and kelp persistence. Modeled relationships between temperature and intraspecific competition for light resulted in accurate predictions of *S. horneri* population structure. Life history differences mediated *S. horneri* invasion success and kelp reestablishment, demonstrating *S. horneri* invasion is dependent on disturbances that remove kelp.

My research suggests that new approaches are needed to understand the link between algal community change and ecological drivers, particularly as algal communities are shifting in the Anthropocene. Further, as disturbances are predicted to increase in frequency and intensity with global change, my research implies that invasive species such as *S. horneri* will persist if the native community is disproportionately impacted.

The dissertation of Emily Rose Ryznar is approved.

Kyle C. Cavanaugh

Nathan Jared Boardma Kraft

James O. Lloyd-Smith

Peggy Marie Fong, Committee Chair

University of California, Los Angeles

2021

To mom, dad, and Elana:

None of this would have been possible without your love, guidance, and the Club Ryznar playlist on repeat. Thank you for supporting me throughout this grand adventure.

TABLE OF CONTENTS

LIST OF ACRONYMS

Acronym	Description
ANOVA	Analysis of Variance
CCA	Crustose Coralline Algae
±D±U	High/low Diversity, high/low Urchin density site
ENSO	El Niño Southern Oscillation
FG	Fast Growth phase of *Sargassum*
FGM	Functional Group Model (Littler and Littler 1980)
HSD	Honestly Significant Difference (for Tukey post-hoc)
PERMANOVA	Permutational Analysis of Variance
PISCO	Partnership for the Interdisciplinary Study of Coastal Oceans
RSR	Reproduction, Senescence, and Recruitment phase of *Sargassum*
SG	Slow Growth phase of *Sargassum*
WIES	University of Southern California's Wrigley Institute for Environmental Studies

LIST OF TABLES

LIST OF FIGURES

Chapter 1

Main text

Supplemental text

Supplemental text

ACKNOWLEDGMENTS

This dissertation and my growth as a scientist would have been impossible without help. I am extremely grateful for those who have provided guidance, funding, field assistance, and comic relief.

First and foremost, I want to acknowledge my wonderful coauthors. Chapter 1 is a version of Ryznar, E.R., Fong, P., and Fong, C.R. 2021. When form does not predict function: Empirical evidence violates functional form hypotheses for marine macroalgae. *Journal of Ecology* 109(2): 833-846. Both Peggy Fong and Caitlin Fong provided valuable guidance and support in project conceptualization and development, experimental design, data collection and interpretation, and manuscript writing and review. I would also like to thank Lauren Smith for field support on Catalina while collecting data for this manuscript.

Chapter 2 is a version of Ryznar, E.R., Smith, L.S., and Fong, P. Disturbance, not herbivory, may facilitate the invasion of a marine algal "passenger" on temperate rocky reefs. *In submission to Marine Environmental Research*. Lauren Smith was integral during methods development and preparation, implementing each experiment and survey in the field, data collection, and overall troubleshooting. Peggy Fong served as the P.I. for this chapter, and assisted in every step of the process from helping brainstorm ideas and hypotheses to data analysis and interpretation. In addition to my coauthors, I would also like to thank Kelcie Chiquillo, Ashley Hailer, Yubin Raut, Kathryn Scafidi, and Timothy Buchanan for the field support and valuable Catalina wisdom.

Chapter 3 is a version of Ryznar, E.R., Fong, P., and Lloyd-Smith, J.O. A simulation model demonstrates life history and abiotic factors mediate competition between a perennial foundational alga, giant kelp, and an annual invasive alga. *In preparation*. Jamie Lloyd-Smith

provided critical guidance in model design and development, model analysis, and troubleshooting, and served as the P.I. for this project. Peggy Fong provided valuable assistance during model conceptualization, biological interpretation, and model analysis. All authors provided valuable input in writing this manuscript. In addition to my coauthors, I would like to thank SBC LTER et al. (2018) for the field data used to inform the single-species *Sargassum horneri* model, Burgman and Gerard (1990) for the *M. pyrifera* model structure, and Mark Burgman for guidance. Finally, thank you Ana Gomez for the valuable support while developing this model.

In addition to the above acknowledgements, I want to specifically recognize many people and organizations that truly made this dissertation possible. First and foremost, Peggy Fong I cannot begin to express how much I have learned from you as my advisor. From underwater experimentation, proper grammar (e.g., uses of "which" vs. "that"), and maintaining a healthy work-life balance to exercising patience and persistence in the face of hardship, you have been instrumental in my growth as a scientist and as a person. You truly are an inspiring woman and I feel so lucky to have had you as a mentor during these last six years. Among many other memories, I will never forget snorkeling with you on my birthday around the Motus and spotting that sleeping thresher shark. So cool (but scary)! I will miss our weekly meetings.

I also indebted to my dissertation committee members Jamie Lloyd-Smith, Nathan Kraft, and Kyle Cavanaugh for all of their assistance and support. Kyle, thank you for all of your guidance throughout my graduate career and "kelp-y" inspiration. Nathan, thank you in particular for all of the recommendations and advice as I was taking a step into the functional trait-based realm. Jamie, thank you for teaching me the fundamentals of ecological modeling. I

have had so much fun developing my modeling chapter and am excited to continue learning in this space. Thank you for being patient (and so helpful) through my many, many struggles.

I would also like to acknowledge the UCLA La Kretz Center for California Conservation Science, the Phycological Society of America, the Santa Monica Audubon Society, and the UCLA Ecology and Evolutionary Biology Department for providing me crucial funding that made my dissertation possible, as well as the UC Berkeley Gump Research Station for logistical support. I want to give a special thank you to the University of Southern California Wrigley Institute for Environmental Studies for supporting me for three years as a Graduate Fellow on Catalina. In particular, thank you Lauren Oudin, Kellie Spafford, Trevor Oudin, Juan Aguilar, Eric Castillo, and Lorraine Sadler for all of your expert knowledge and assistance that helped get my projects in the water and for making Wrigley such a welcoming place. Thank you, Linda Duguay, for wrangling all of the fellows and facilitating an unforgettable fellowship. My time on Catalina as a Wrigley fellow will always stand out as the highlight of my graduate experience and I feel so fortunate to have been a part of such a special place.

This dissertation would also not be possible without the help of many others. Lauren Smith, thank you for being such an excellent research partner-in-crime and great friend. Your expert organization and problem-solving skills, limitless positivity, broad marine ecology knowledge, and fun spirit has been an integral part of my research and overall graduate experience. From fish tacos and pizzookies in Two Harbors, spending many, many hours spinning salad, making algae traps while listening to “Take it Easy”, untangling said traps underwater, poking algae, and eating brownies to talking through issues associated with underwater field experimentation, graduate school, and life, I will truly miss work alongside you. Also, thank you to Caitlin Fong for being a constant source of inspiration and a great teacher and

collaborator in the algal functional trait and ecological interactions realm. Also thank you for all of the crucial statistics advice!

In addition to my coauthors, I have been fortunate to have had the assistance of many others during the course of my graduate career. Kelcie Chiquillo ("Huey"), thank you for being an amazing field assistant, friend, "DCP", and adventure buddy. You provided integral help with my research while helping me maintain a healthy work-life balance through basically every activity under the sun (e.g., surfing, fishing, diving, rock climbing, hiking) and endless laughter. I would also like to acknowledge past and present members of the Fong lab including Shayna Sura, Shalanda Grier, Regina Zweng, Ashlyn Ford, Camille Gaynus, Tiara Moore, Sarah Joy Bittick, and Tonya Kane. Thank for the valuable input while I was formulating research ideas and conference presentations, and for all of the memories.

Last but certainly not least, thank you mom, dad, and Elana for always believing in me. You instilled a deep love and curiosity for the natural world from an early age, and that has without a doubt been the central motivation for my life trajectory, including pursuing a Ph.D. Elana, you are the best sister in the universe. Thank you for always being there through my many trials and tribulations and for being a constant inspiration through your creativity, determination, and adventurous spirit. Thank you grandma, grandpa, Uncle Jim, Aunt Martha, Adeline, and Nick for all of your support and for motivating my interest for science and the outdoors. Also, thank you James for your patience, your boundless positivity, and for fostering an adventurous life. Finally, thank you Hamiki and Oskar for the comic relief and cuddles. I love you all.

BIOGEOGRAPHICAL SKETCH

Previous Degrees Awarded

2014 B.S. in Marine Biology and a Minor in Language Studies (Spanish), University of California-Santa Cruz

Awards and Honors

2021 NOAA Sea Grant California State Fellowship

2020 Best Talk in Aquatic Sciences, Ecological Society of America Annual Meeting

2020 Schechtman Award for Distinguished Teaching

2020 Best Graduate Student Poster, UCLA EEB Research Symposium

2019 Honorable Mention for Best Student Talk in Community Ecology, Western Society of Naturalists Annual Meeting

2019 George A. Bartholomew Fellowship for Outstanding Field Biologists

2017-20 University of Southern California Wrigley Institute Graduate Fellowship

Publications

Ryznar, E.R., Fong, P., and Fong, C.R. 2021. When form does not predict function: Empirical evidence violates functional form hypotheses for marine macroalgae. *Journal of Ecology* 109(2): 833-846.

Fong, C.R., Chiquillo, K.L., Gaynus, C.J., Grier, S.R., Hà, B.A., **Ryznar, E.R.**, Smith, L.L, Sura, S.A., Zweng, R.C., Anggoro, A.W., Moore, T.N., and Fong, P. 2021. Flip it and reverse it: Reasonable changes in designated controls can flip synergisms to antagonisms *Science of the Total Environment* 772: 145243.

Barr, K., Goldberg, A., Ndefru, B., Philson, C.S., **Ryznar, E.R.**, and Zweng, R. 2020. Water in Los Angeles: Rethinking the current strategy. *Journal of Science Policy and Governance*

17(2). doi: 10.38126/JSPG170202

Conference presentations

Ryznar, E.R., Smith, L., and Fong, P. 2020. "Rapid growth, competitive release via disturbance, and low herbivory pressure facilitate the invasion of a brown marine alga into forests of giant kelp". Oral presentation. Ecological Society of America Annual Meeting, Virtual.

Ryznar, E.R., Smith, L., and Fong. P. 2020, May. "Rapid growth, competitive release via disturbance, and low herbivory pressure facilitate the invasion of a brown marine alga into forests of giant kelp". Poster. UCLA EEB Annual Research Symposium, Virtual.

Ryznar, E.R., Smith, L., and Fong. P. 2019, October. "Rapid growth, competitive release via disturbance, and low herbivory pressure facilitate the invasion of a brown marine alga into forests of giant kelp". Oral presentation. Western Society of Naturalists Annual Meeting, Ensenada, MX.

Ryznar, E.R., Fong, P., and Fong, C.R. 2019, June. "When form does not predict function: Empirical evidence violates functional form hypotheses for marine macroalgae". Oral presentation. Phycological Society of America Annual Meeting, Ft. Lauderdale, FL.

Ryznar, E.R., Fong, P., and Fong, C.R. 2018, October. "When form does not predict function: Empirical evidence violates functional form hypotheses for marine macroalgae". Oral presentation. Western Society of Naturalists Annual Meeting, Tacoma, WA.

Professional Experience

2015 **Scientific Aid,** California Department of Fish and Wildlife, Monterey, CA

2014 **Research Assistant**, Huinay Scientific Field Station, Los Lagos, Chile

2012 -14 **Research Aid**, California Department of Fish and Wildlife, CA and WA

CHAPTER 1

When form does not predict function: empirical evidence violates functional form hypotheses for marine macroalgae

Abstract

Functional groups are widely used to reduce complexity and generalize across ecological communities. These models assume that shared traits among species correspond to some ecological role, process, or function, and that these traits can be leveraged to generate meaningful and distinct functional groups so that intergroup trait variation exceeds intragroup variation. We sought to validate the assumptions of the widely used Functional Group Model (FGM) for marine macroalgae, which groups species based on morphological complexity, by testing the predictions of the FGM for several traits assumed to correspond with morphological complexity. The FGM predicts increased resistance to disturbance and herbivory as morphological complexity (tensile strength and thallus toughness, respectively) increases. The FGM also predicts a tradeoff between complexity and growth rate. To test predictions, we measured: 1) thallus toughness (force to penetrate), 2) tensile strength (force to break) and 3) relative growth for both tropical and temperate macroalgae from different functional groups. Thallus toughness followed model predictions at the functional group level, though there was significant variability among species. However, the model did not predict tensile strength at any level for either tropical or temperate macroalgae. Further, relative growth did not follow predictions; rather it was highly variable among species and functional groups. The assumptions of the FGM that differences in morphological complexity can be used to generate distinct

functional groups and that intergroup trait variation outweighs intragroup variation were violated, providing strong evidence that individual species responses need to be considered. Further, violations of assumptions indicate that functional groups should not be used to predict community responses to ecological drivers and/or species contributions to ecosystem function. Our study challenges the usefulness of functional form groups for marine macroalgae and emphasizes the need for a different conceptual framework.

Introduction

Functional groups have been used extensively in ecology as a means of simplifying often complex, speciose communities in order to make broader generalizations or comparisons, especially across ecosystems (McLaren and Turkington 2010; Pokorny et al. 2005; Smith et al. 2010). Functional groups organize species into groups that respond similarly to environmental drivers and have similar effects on ecosystem functioning (e.g., Naeem 2008; Tilman 2001). While species within functional groups may be related evolutionarily, phylogenetic relatedness is generally not a determining factor (Root 1967; Shipley et al. 2016; Tilman et al. 1997). As functional groups are a valuable approach to ecological research, it is critical to validate their underlying assumptions and emergent predictions.

In diverse systems, functional groups can be particularly useful in overcoming methodological and/or conceptual challenges. For example, use of functional groups can help simplify studies in speciose systems by grouping shared species' responses to environmental drivers and their ecological roles into larger functional units that can then be quantified and compared across ecosystems (Balata et al. 2011; Phillips et al. 1997; Thomas et al. 2019). Additionally, in systems where it is difficult or time-consuming to classify taxa to the species level, identifying functional groups can save time and effort without sacrificing critical

information on functional roles (Harrison et al. 2010; Padilla and Allen 2000; Thomas et al. 2019). However, while functional groups can be powerful simplifying tools in both complex systems and study design, evidence indicates that functional groups can change when different grouping criteria and ecosystem functions are considered, minimizing their predictive power (Anderegg 2015; Murray et al. 2014; Padilla and Allen 2000; Sullivan and Zedler 1999; Thomas et al. 2019). Therefore, close examination of criteria used to assemble function groups is needed.

Different criteria have been used to generate groups depending on the question and system of interest (Voille et al. 2007). One common way functional groups are generated is around criteria assumed to correlate to individual responses to ecosystem drivers and collective influences on ecosystem function (Chang et al. 2016; Murray et al. 2014; Padilla and Allen 2000). For example, common schemes include morphological traits (e.g., specific leaf area and maximum height in plants (Boulangeat et al. 2012); mouth structure and body size in animals (Bellwood et al. 2019; De Graaf et al. 1985)), life-history strategies (e.g., perennial vs. annual in plants (Sullivan and Zedler 1999); plant phenology (Cleland et al. 2006); lifespan and time to first reproduction in animals (Blaum et al. 2011), and physiology (e.g., nutrient uptake and growth rates in plants (Pokorny et al. 2005); metabolic rates and aerobic capacity in animals (Carey et al. 2013)). Further, groups defined by methods of resource utilization are generally classified as functional guilds and often pertain to animal species (Blondel 2003; Root 1967).

However, in some disciplines, no overarching consensus has been reached as to which types of traits are best to generate functional groups, and species can often fulfil multiple functional roles across spatial and temporal scales that correlate with multiple traits (Adler et al. 2014; Eviner and Chapin 2003; Gitay and Noble 1997; Levine 2016; Sullivan and Zedler 1999).

As the advantages of using functional groups are perceived to exceed their limitations, functional groups are used widely across many ecosystems and taxa. For example, functional groups have been applied to ecological studies as diverse as resource partitioning in grasslands (McLaren and Turkington 2010) and forests (López-Martinez et al. 2013), community assembly in marine macroalgae (Phillips et al. 1997; Littler and Littler 1984), feeding strategies in birds (De Graaf et al. 1985) and herbivorous fishes (Cheal et al. 2010), habitat use of terrestrial vertebrates (García-Llamas et al. 2019), and seasonal dynamics of phytoplankton (Reynolds 1984). Further, functional groups have been used in applications such as long-term community monitoring (Green and Bellwood 2009; Jaksic et al. 1996), community distribution and abundance models (García-Llamas et al. 2019), and biodiversity shifts in response to environmental fluctuations (Suding et al. 2005). However, despite their widespread use, the foundational assumptions of functional groups are rarely tested.

Functional group models postulate that responses to similar environmental conditions and constraints have driven convergent evolution across phylogenetic lineages, resulting in trait syndromes (Bontemps et al. 2017; Grime 1974; Raffard et al. 2017; Tjoelker et al. 2005) that ecologists can leverage into meaningful functional form groups (Adler et al. 2014; Resetarits and Chalcraft 2007). These groups rely on two assumptions that are rarely tested. The first assumption is that shared traits correspond to some ecological role, process, or function (Resetarits and Chalcraft 2007). The second assumption is that functional groups based on these traits can successfully group species so that intergroup variation meaningfully outweighs intragroup variation (Littler and Littler 1980; Resetarits and Chalcraft 2007; Rosenfeld 2002; Shipley et al. 2016). Thus, species in different groups should be functionally distinct while species within a functional group should be functionally redundant. Functionally redundant

species are those that fulfil similar functional roles, such that within group loss of species will have minimal effect on ecosystem processes (Resetarits and Chalcraft 2007; Rosindell et al. 2012; Sullivan and Zedler 1999). However, evidence from various systems indicates that species' responses to ecological drivers can be highly variable, suggesting that functional similarity may be limited within functional groups (Anderegg 2015; Jaksic et al. 1996; Luck et al. 2013; Sullivan and Zedler 1999). Existing evidence of the validity of these assumptions is primarily from indirect tests (Bellwood et al. 2003; Carey et al. 2013; Chang et al. 2016; Padilla and Allen 2000), with only a handful of studies implicitly evaluating functional group model assumptions (Anderegg 2015; Fong and Fong 2014; Mauffrey et al. 2020; Phillips et al. 1997; Resetarits and Chalcraft 2007; Sullivan and Zedler 1999). Therefore, systematic tests of within group species' trait similarity and ecological function are needed before functional group models can be used to effectively predict species' functional roles and responses to environmental forces.

In this paper, we empirically evaluate the second assumption—that functional groups based on shared traits are successfully grouping species so that intergroup variation meaningfully outweighs intragroup variation—for the Functional Group Model (FGM), a commonly used framework for marine macroalgae. Originally developed by Littler and Littler in the 1980s (Littler and Littler 1980; Littler et al. 1983a; Littler et al. 1983b; Littler and Littler 1984; for a similar model, see Steneck and Dethier 1994) this model has been widely used since (e.g., Fong and Fong, 2014; Gaspar et al. 2017; Hanisak et al. 1990; Lobban and Harrison 1994). The FGM is based on the concept that algal morphology has been shaped over time via similar ecological drivers that forced convergent evolution of specific morphologies (and morphological traits) across diverse taxa. Based on different algal morphologies, in the Littler and Littler (1980) FGM

algal species are divided into 6 functional groups ranked with increasing morphological complexity as sheetlike, filamentous, coarsely branched, thick and leathery, jointed calcareous, and crustose (Table 1-1; Fig. 1-1). We directly test if the model is successful in placing species into these groups based on traits assumed to correlate with ecological function.

To our knowledge, only one study has comprehensively tested the assumptions and predictions of the FGM, though with different traits and at smaller spatial scales than those presented in this study (Mauffrey et al. 2020). Two studies have provided partial tests of the FGM (for direct testing in two FGs see Fong and Fong 2013; for indirect testing see Padilla and Allen 2000), with a third study conducted by Phillips et al. (1997) partially testing assumptions of a similar algal functional group model proposed by Steneck and Dethier (1994). In these four tests, species' responses were highly variable within functional groups and not as predicted by the FGM, violating the FGM assumptions. It is clear that more thorough and direct testing of FGM assumptions and predictions is needed before conclusions can be drawn on the usefulness of these models. Our study is the first to directly test FGM assumptions across both tropical and temperate marine systems by comparing toughness, tensile strength, and growth responses within and between functional groups as well as whether responses align with FGM predictions.

Materials and Methods

Model predictions

The FGM offers several measurable predictions of traits that are indicative of ecosystem function and species' response to environmental drivers. We focus on the FGM predictions of toughness (weight to penetrate), tensile strength (weight to break), and growth (change in weight) (Fig. 1-1). These traits are assumed to be a measure of species' resistance to herbivory, resistance to physical disturbance, and recovery from disturbance/role in ecological succession,

respectively, as different strategy types (for review of terrestrial plant strategies, see Westoby et al. 2002). These strategies can be in turn be related to ecological functions such as productivity and food chain support (Littler and Littler 1980). The FGM model predicts that toughness and tensile strength increase with morphological complexity, while growth is the opposite (Fig. 1-1). Therefore, morphologically complex species should be more resistant to herbivory and disturbance and last in the line of succession while morphologically simple species are predicted to be involved in early successional stages, and vulnerable to herbivory and physical disturbance (Littler et al. 1983b).

Study system

We tested the assumptions of the FGM using 33 total species and five functional groups from both tropical and temperate locales. We collected tropical species from a fringing coral reef lagoon. These systems are generally characterized by low productivity (Borer et al. 2013; Huston and Wolverton 2009), lower physical disturbance, and high herbivory pressure (Floeter et al. 2005; Vergés et al. 2014). Temperate species were collected from intertidal and subtidal reefs, which are generally characterized by higher productivity (Borer et al. 2013; Huston and Wolverton 2009), higher physical disturbance (Littler and Littler 1984), and lower herbivory pressure (Floeter et al. 2005; Vergés et al. 2014). As the FGM is utilized in a variety of habitats in temperate and tropical systems that vary in these environmental contexts, we collected species from different site types in both locales to test assumptions in a variety of systems.

Algal collection

Many algal species exhibit complex life cycles, where different generations can vary in morphology, ploidy, and sex (Thornber 2006; for life cycle types of collected algae, see Table 1-2). While little is known regarding how responses to ecological drivers vary between generations,

there is some evidence these differences may be profound (Krueger-Hadfield 2020; Lubchenco and Cubit 1980; Martinez and Santelices 1998; Thornber 2006). Thus, we have identified what generation we collected, where possible, in Table 1-2.

Thirteen species of tropical algae representing five functional groups were haphazardly collected between January 21 and February 14, 2018 via snorkel from a common site at approximately 2-3-m depth in the patch reef zone of a fringing reef in Cook's Bay in Mo'orea, French Polynesia (Table 1-2, Fig. 1-2B). Collected algal species included *Dictyota bartayresiana*, *Padina boryana*, *Ulva intestinalis*, *Ulva lactuca* (sheetlike), *Caulerpa serrulata*, *Spyridia filamentosa* (filamentous), *Amansia rhodantha*, *Acanthophora spicifera* (coarsely branched), putatively *Gracilaria parvispora* (hereafter *Gracilaria parvispora*), *Sargassum pacificum, Turbinaria ornata* (thick and leathery), *Galaxaura fasciculata,* and *Halimeda opuntia* (jointed calcareous). For the purposes of this study, only whole, macroscopic thalli (a term defined as the body form of an alga) that were attached to the benthos and appeared healthy were collected. Approximately 20 thalli were collected per species for toughness and tensile experiments while approximately 15 thalli were collected per species for growth experiments (see below). Algae were immediately transferred to an outdoor flow-through water table. Using ambient seawater, thalli were cleaned of sediment and other organisms and processed within 24 hours of initial collection.

Twenty species of temperate algae representing four functional groups were collected between April 15 and August 1, 2018 at three sites throughout central and southern California, United States (Table 1-2, Fig. 1-2A). Collected species included *Pyropia perforata, Dictyopteris undulata, Zonaria farlowii, Dictyota binghamiae, Dictyota coriacea* (sheetlike), *Endocladia muricata*, *Mastocarpus papillata*, *Prionitis sternbergii, Laurencia pacifica*, *Pterocladiella*

capillacea, Plocamium pacificum, Colpomenia sinuosa (coarsely branched), *Egregia menziessi*, *Stephanocystis doica*, *Sargassum horneri*, *Sargassum palmeri*, *Silvetia compressa*, *Stephanocystis osmundaceae* (thick and leathery), *Bossiella orbigniana*, and *Calliarthron tuberculosum* (jointed calcareous). Species were collected from intertidal sites in Cambria and Palos Verdes, immediately placed in coolers filled with seawater, and transported back to the University of California, Los Angeles where they were kept in indoor aquaria. Species from Santa Catalina Island were collected from a subtidal site at approximately 2-3-m depth via snorkel and immediately transported back to the University of Southern California Wrigley Institute of Environmental Science (WIES) where they were placed in outdoor flow-through water tables with ambient seawater. Replication, algal cleaning, and algal processing were performed as above.

Thallus toughness

To test the prediction that thallus toughness of species within functional groups was similar and toughness between groups increases from the simplest to the most complex algal thalli, we chose 10 whole thalli of each species. As many complex algal species exhibit apical growth, toughness was tested on blades or tissue from the middle of each thallus, where applicable, to prevent testing younger, potentially weaker, areas. To measure thallus toughness, we secured each subsample below a penetrometer so that the needle of the penetrometer rested on the thallus surface. We added weight until the penetrometer just pierced the thallus surface. This process was repeated for 10 thalli of each species.

Thallus tensile strength

To test the same predictions as above, but for thallus tensile strength, we selected 10 thalli of each species. To control for the very different algal morphologies, we used the whole

algal thallus for each species, from the apex to the base. The basal end of each thalli was secured to a spring scale while just below the apical end was pulled until the thallus broke. The force (weight) required to break the thallus was used as a measure of tensile strength. Data were not used if thalli broke near where the thallus was secured to the spring scale, or where the thallus was held near the apical end. This process was repeated for each of the 10 replicate thalli per species.

Relative growth

To test model predictions for relative growth of tropical species, we conducted field experiments from January 25-February 4, 2018 using six species, with two in each of three functional groups (Table 1-2). Algae were spun in a salad spinner for one minute and wet-weighed into eight replicate 1-g (*A. spicifera* and *A. rhodantha*) or 3-g (*S. pacificum*, *G. fasciculata*, *H. opuntia*) subsamples by trimming whole thalli into appropriate weights, taking care to avoid removing apical meristems. Subsample weights varied by species due to different volume to mass ratios for each species (Mantyka and Bellwood 2007). Thus, in order to achieve similar subsample volumes among focal species, subsample weights had to be increased for more dense (*S. pacificum*) and calcifying algae (*G. fasciculata* and *H. opuntia*). As *T. ornata* is sensitive to trimming, eight replicate individuals of similar size (2.79±0.41SE-g, reproductively mature) were collected and weighed without normalizing to a standard initial weight.

We secured each replicate to the bottom of fully-enclosed, cylindrical cages (12-cm diameter x 10-cm height) constructed of hardware cloth with 1-cm openings that have been shown to have few cage artefacts and to limit herbivory in previous experiments (e.g., Fong et al. 2006; Smith et al. 2010). Cages were randomly attached to rope with at least 0.5-m spacing between replicates and secured to the benthos. Algae in cages were secured in an upright growth

position and ropes were secured to the benthos with coral rubble at ~2-m depth on the same fringing reef as collection. Cages were cleaned of fouling every other day and recovered after 10 days when algae were spun and wet-weighed. Percent change in biomass was calculated as [(final weight-initial weight)/initial weight]*100 and then expressed on a per day basis.

To test the same predictions for relative growth of temperate algae, we used five species, with two in sheetlike, one in coarsely branched, and two in thick and leathery functional groups as they were abundant in the collection site near Santa Catalina Island, California. Algal thalli were spun in a salad spinner for one minute and wet weighed into eight replicate 1-g (*P. capillacea*) or 2-g (*D. undulata, Z. farlowii, S. doica,* and *S. palmeri*) subsamples. As before, subsample weights were adjusted to roughly match volumes. Cages were deployed from July 10-July 20, 2018, as above in ~2-m depth in a sheltered cove just west of WIES (same site as collection) and cleaned every other day. All cages were removed after 10 days, and algae spun and wet-weighed. Per cent change in biomass per day was calculated as above.

Analysis

As environmental conditions are markedly different between temperate and tropical regions (see *Study system* section for overview) and species were collected from each region at different points in time, we analyzed the temperate and tropical species separately. For each response variable, species means were calculated as the average response (weight to penetrate, weight to break, % change in biomass) over all replicates. To compare responses among functional groups for each variable, species' means were used to calculate functional group means. Transformations were applied where necessary to meet the assumptions of parametric statistics. If the data still did not meet parametric assumptions following transformation, nonparametric statistics were utilized (described below).

To compare species means within and between functional groups for the response variables of thallus toughness, tensile strength, and growth, data for measures from individual thalli that met assumptions for parametric statistics were analyzed with a nested ANOVA, with functional group as a fixed factor and species nested within functional group. Data that did not meet parametric assumptions were analyzed with a nested PERMANOVA, with functional group as a fixed factor and species nested within functional group. As there was only one species in the coarsely branched group for the temperate growth experiment, this group was omitted from nested analyses.

Significant nested analyses were followed by 1-factor ANOVAs for parametric data or 1-factor Kruskal-Wallis tests for nonparametric data to separately compare functional group and species means. For pairwise comparisons, significant ANOVAs were followed by a Tukey HSD post-hoc test and significant Kruskal-Wallis tests were followed by Wilcoxon post-hoc tests. P-values were adjusted with Bonferroni's correction for multiple comparisons. All analyses were conducted using base functions in R Statistical Software (R Core Team 2017), except for PERMANOVAs, which were conducted using the "vegan" package for R (Oksanen et al. 2019).

Results

Thallus toughness

For tropical functional groups, there were significant differences in thallus toughness across most groups, a pattern that partially meets the assumptions of the FGM (Fig. 1-3A; ANOVA, $F(4, 125) = 327.61$, $p < 0.001$; Appendix 1, Table 1-S1A; for box plots of all results, see Appendix 1, Figs. 1-S1-6). Moreover, there was an overall pattern of increasing toughness with functional form complexity as predicted by the FGM. However, these differences were not significant between two (filamentous and coarsely branched) of the five functional groups tested.

There were also significant differences in thallus toughness with increasing complexity among temperate functional groups (Fig. 1-3B; ANOVA, $F(3,196) = 165.75$, $p < 0.001$; Appendix 1, Table 1-S1A) while these differences were significant for all four functional groups tested, members of the filamentous group were not tested in the temperate comparison.

There were significant differences in thallus toughness between and within functional groups (Table 1-3A) as well as among the 13 tropical species tested (ANOVA, $F(12,117) = 321.3$, $p < 0.001$; Appendix 1, Table 1-S1A). Further, there was an overall pattern of increasing thallus toughness with increasing complexity that aligned with FGM predictions (Fig. 1-3C). However, there was also considerable variability within some groups, with significant differences among species in two (sheetlike and filamentous) of the five groups tested. Further, in three cases, species in different functional groups were statistically more similar to each other than species in the same group. For example, mean toughness for *P. boryana* (sp. #3 in sheetlike) was closer to *C. serrulata* (sp. #5 in filamentous) than other species in its own functional group. In addition, mean values for *S. filamentosa* (sp. #6 in filamentous) and *A. rhodantha* (sp. #7 in coarsely branched) were almost identical in thallus toughness, but *S. filamentosa* was statistically different from the other member in the filamentous group.

Similarly, there were significant differences between and within functional groups (Table 1-3A) and among the 20 temperate species tested (Kruskal-Wallis, $H(19) = 188.76$, $p < 0.001$; Appendix 1, Table 1-S2A), with an overall pattern of increasing thallus toughness with increasing functional form complexity as predicted by the FGM (Fig. 1-3D). Post-hocs revealed substantial variability between species in the same functional group, with significant differences in thallus toughness among species in all of the functional groups tested. Further, in one case, species in different functional groups were statistically similar while significantly different from

species in their own functional group. *S. horneri* (sp. #29 in thick and leathery) was statistically similar in thallus toughness to species in the coarsely branched and sheetlike functional groups but different from all other members of its group, even a congener.

Thallus tensile strength

Comparing thallus tensile strength across tropical functional groups revealed significant differences (ANOVA, $F(4,12) = 13.43$, $p < 0.001$; Appendix 1, Table 1-S1B). In contrast to thallus toughness, however, the pattern did not support FGM predictions of increasing tensile strength with thallus complexity (Fig. 1-4A). Further, post-hoc analyses indicated similarities between four pairs (sheetlike-filamentous, sheetlike-coarsely branched, filamentous-coarsely branched, filamentous-jointed calcareous, coarsely branched-jointed calcareous) of the five functional groups tested. The thick and leathery group exhibited the greatest (and statistically different) tensile strength despite not being the most complex functional form.

Similarly, there were significant differences in tensile strength between temperate functional groups (ANOVA, $F(3,196) = 53.7$, $p < 0.001$; Appendix 1, Table 1-S1B), but the data did not align with FGM model predictions for tensile strength (Fig. 1-4B). Further, three pairs (sheetlike-jointed calcareous, thick and leathery-jointed calcareous) of the four functional groups were statistically similar, as indicated by post-hoc analyses. Similar to tropical functional groups, the temperate thick and leathery functional group had the greatest tensile strength despite not being the most morphologically complex.

For the tropical species tested, there were significant differences in tensile strength between and within functional groups (Table 1-3B) as well as among species (ANOVA, $F(12,104) = 46.47$, $p < 0.001$; Appendix 1, Table 1-S1B). However, the overall pattern predicted by the FGM of increasing strength with complexity was not observed (Fig. 1-4C). Additionally,

tensile strength varied substantially within the same functional group, with differences among species in four (sheetlike, filamentous, coarsely branched, thick and leathery) of the five functional groups tested. Further, species were statistically more similar to species in different functional groups than their own in four cases. For example, *C. serrulata* (sp. #5 in filamentous) was significantly different from a congener in tensile strength but similar to *U. lactuca* (sp. #4 in sheetlike), *P. boryana* (sp. #2 in sheetlike), and *A. rhodantha* (sp. #7 in coarsely branched). Similarly, *G. parvispora* (sp. #9 in thick and leathery) is statistically different from a congener in its own group but similar to at least seven species in different functional groups.

Similar to the tropical species, there were significant differences in tensile strength between and within functional groups (Table 1-3B) and among species (Kruskal-Wallis, $H(19) = 192.07$, $p < 0.001$; Appendix 1, Table 1-S2B), but the overall pattern predicted by the FGM was not observed (Fig. 1-4D). Further, there were significant differences among species in the same functional group in all of the groups tested. Additionally, species were statistically more similar to species in a different functional group than species in their own group in five cases. For example, *D. undulata* (sp. #15 in sheetlike) is statistically different from every other species in the sheetlike functional group, but similar to *S. palmeri* (sp. #31 in thick and leathery) and *C. tuberculosum* (sp. #33 in jointed calcareous). Additionally, *B. orbigniana* (sp. #32 in jointed calcareous) is significantly different from a congener in the same group but similar to at least four species in different functional groups.

Relative Growth

Comparing tropical functional group means for relative growth revealed significant differences (ANOVA, $F(2,45) = 17.75$, $p < 0.001$; Appendix 1, Table 1-S1C), though the FGM prediction of decreasing relative growth with increasing thallus complexity was only partially

supported (Fig. 1-5A). Although the least complex alga in the coarsely branched group exhibited the fastest mean growth, there were no differences between the other two (thick and leathery-jointed calcareous) functional groups tested. Similarly, significant differences in relative growth were detected among temperate functional groups (ANOVA, $F(2, 37) = 6.46$, $p < 0.001$; Appendix 1, Table 1-S1C), but there was no support for the FGM predictions, as growth was highest in the group with intermediate complexity (Fig. 1-5B). Additionally, growth was similar between the two functional groups that were most different in structural complexity (sheetlike-thick and leathery).

For tropical species tested, there were significant differences in relative growth among species (ANOVA, $F(5,42) = 56.26$, $p < 0.001$; Appendix 1, Table 1-S1C) as well as between and within functional groups (Table 1-3C). However, FGM predictions were not met (Fig. 1-5C). Additionally, there was substantial variability between species in the same functional group, with significant differences between species in the three functional groups tested. Further, in five cases, species in different functional groups were statistically more similar to each other than species in the same functional group. For example, *A. rhodantha* (sp. #7 in coarsely branched) and *G. fasciculata* (sp. #12 in jointed calcareous) were statistically similar to each other in relative growth but different from species in their respective functional groups. A similar pattern is apparent between *T. ornata* (sp. #11 in thick and leathery) and *H. opuntia* (sp. #13 in jointed calcareous). Additionally, while *A. spicifera* (sp. #8 in coarsely branched) exhibited the greatest growth and was significantly different than all species tested, *A. rhodantha,* also in the coarsely branched group, was not different in growth when compared to more complex species. Thus, while the overall growth of the coarsely branched functional group aligns with FGM predictions

(least complex, fastest growth), *A. spicifera* contributed disproportionately to the functional group mean and masked the slower growth of *A. rhodantha*.

We found no significant difference in growth between temperate functional groups, but significant differences within functional groups (Table 1-3C) as well as between species (ANOVA, $F(4, 35) = 7.08$, $p < 0.01$; Appendix 1, Table 1-S1C). The lack of a difference between functional groups was likely due to excluding the coarsely branched group (single member is *P. capillacea*) from the analysis (see *Analysis* section). Further, overall FGM predictions for relative growth were not supported for temperate species (Fig. 1-5D). Rather, there was variability within groups, with differences only detected in the sheetlike group. Additionally, in one case, species were more similar to species in a different functional group than the same functional group. *D. undulata* and *Z. farlowii* (spp. #15 and #18, respectively, both sheetlike) were significantly different from in each other in growth, but not different from species in different functional groups.

Discussion

Current functional groups for marine macroalgae are fundamentally flawed because they fail to meet the underlying assumption that groups cluster species into ecologically meaningful, discrete groups. In both temperate and tropical systems, intragroup variability exceeded intergroup variability, and in many cases species responses overlapped between groups, resulting in seemingly arbitrary groups, at least for the traits measured in this study. While our study is the first to directly refute the underlying assumptions of the FGM across a wide range of functional groups in both temperate and tropical systems, others have found significant variability within functional groups, regardless of the criteria used to generate such groups. Examples across ecosystems and organisms include functional groups based on morphology (Carey et al. 2013–

mollusks; Resetarits and Chalcraft 2007– fish), foraging patterns (Jaksic et al. 1996–birds and mammals; Chang et al. 2016– annelids), physiology (Anderegg 2015– terrestrial plants), and life history traits (Sullivan and Zedler 1999– estuarine plants). Further, studies on macroalgal functional groups have also found significant variability within groups (Phillips et al. 1997; Padilla and Allen 2000; Fong and Fong 2014; Mauffrey et al. 2020), though these studies are geographically limited and focused on different traits than in this study. Thus, conclusions of previous research align with our results, where functional groups did not successfully group species based on traits assumed to relate to morphology due to significant variation in responses between species (including congeners) within the same functional group. This implication has profound effects on the usefulness of these models in any system in generating predictions of responses to environmental drivers and their ability to predict ecological functions. Below we explore two possible repercussions of these effects.

First, use of flawed functional groups could lead to inaccurate predictions of species responses to environmental drivers. For example, based on the FGM, the sheetlike functional group should be most vulnerable to disturbance because of low tensile strength, whereas the jointed calcareous group should be the opposite. However, species in these two groups overlapped in tensile strength, implying that use of functional groups may mask these important similarities and lead to inaccurate predictions of which groups will be most affected by disturbance. Others have arrived at similar conclusions where functional groups did not predict responses to herbivory (Fong and Fong 2014– marine macroalgae), disturbance (Anderegg 2015– terrestrial plants; Carey et al. 2013– mollusks; Fong and Fong 2014, Phillips et al. 1997– marine macroalgae), and competition (Chang et al. 2016– annelids). The inability of functional groups to predict responses to environmental drivers has critical repercussions if using these

groups to draw conclusions of community assembly and dominance (Fong and Fong 2014; McLaren and Turkington 2010; Phillips et al. 1997). For example, in a high-energy, wave swept environment (i.e., heavy disturbance), our results indicate sheetlike growth forms could be as abundant as jointed-calcareous groups, which is not what the FGM predicts. Therefore, based on our study, the FGM should not be used as a predictive tool. Further, our results imply tests of the underlying assumptions of functional group models used in other ecosystems are critical to inform their usefulness.

Second, use of flawed functional groups fundamentally limits our characterization of ecosystem functioning by misattributing function to species. For example, if species in the same functional group are assumed to share traits, but they do not, then the similar downstream functions the species are also expected to perform may be lacking when they are assumed to be fully functional. In our study, the FGM's inability to cluster species with similar thallus toughness, an anti-herbivory trait, consequently impacts the ability of these groups to accurately predict a species' role in food chain support. More specifically, herbivorous fishes thought to specialize on filamentous algae may not consume *S. filamentosa*, as our results indicate this species is significantly tougher than other species in the filamentous group. Therefore, this specialist herbivore may be resource limited, or even lacking, on reefs where *S. filamentosa* is abundant, a misalignment with predictions based on the FGM. Studies across a broad range of systems provide similar implications for food chain support (Resetarits and Chalcraft 2007– fish) as well as guild structure (Jaksic et al. 1996– birds and mammals) and productivity (Mauffrey et al. 2020– marine macroalgae; Sullivan and Zedler 1999– estuarine plants), where functional redundancy was limited within the groups utilized. These findings, in combination with our study, caution against assuming that species within functional groups can functionally replace

one another if lost, and that use of functional groups could ultimately lead to mismanagement of ecosystems if prioritizing groups assumed to perform a particular function.

Overall, our results suggest a different conceptual framework may be required to adequately understand algal strategies in response to ecological drivers and the subsequent impact on ecosystem function. One possibility is adopting a trait-based approach for marine macroalgae. This framework was originally developed for terrestrial vegetation (Chapin 1993; Eviner and Chapin 2003; Grime 1974; Wright et al. 2004; McGill et al. 2006; Voille et al. 2007) in order to understand mechanisms of community assembly and ecosystem functioning, but has been increasingly applied to other taxa such as marine phytoplankton (Edwards et al. 2013; Litchman and Klausmeier 2008) and terrestrial fauna (García-Llamas et al. 2019). There have been some promising recent efforts in this direction for marine macroalgae (Cappelatti et al. 2019; Jänes et al., 2017; Mauffrey et al., 2020; Stelling-Wood et al. 2019), with functional traits successfully predicting in macroalgal productivity (Jänes et al. 2017) and associated community structure (Stelling-Wood et al. 2019), as well as providing stronger links with macroalgal strategies and functions (Cappelatti et al. 2019; Mauffrey et al. 2020). However, more work is needed to understand which traits are most informative for macroalgal eco-physiology and function. Trait-based approaches employ post-hoc groups of species based on measured similarities in traits (Litchman and Klausmeier 2008– phytoplankton; Suding et al. 2008– terrestrial plants), responses to environmental conditions (Cornwell and Ackerly 2010– terrestrial plants), and/or influence on ecosystem function (Cornwell et al. 2008–terrestrial plants). Further, under trait-based approaches, groups may differ when different traits, responses, or functions are considered over space and time (Padilla and Allen 2009; Murray et al. 2014). As many algal species exhibit complex life cycles with separate free-living phases that can differ in

morphology, physiology, ploidy, and sex, trait-based approaches may be a useful method for exploring how these important differences contribute to variations in trait-space (Ellis et al. 2017; Krueger-Hadfield 2020; Thornber 2006). We argue adopting a trait-based approach for marine macroalgae will facilitate higher resolution of the diversity of species' responses to environmental drivers as well as more accurate predictions for ecosystem functioning and algal community assembly.

Tables

Table 1-1. Adapted from Littler and Littler (1984). Macroalgal functional groups, with their corresponding external and internal morphology as well as texture. Morphological complexity increases from top to bottom, with the sheetlike group as the least complex and the crustose group as the most complex.

Functional group	**External morphology**	**Internal morphology**	**Texture**
Sheetlike	Thin, tubular, foliose	Uncorticated, one to several cell layers thick	Soft
Filamentous	Delicately branched	Can be slightly corticated, one to several cell layers thick	Soft
Coarsely branched	Coarsely branched, upright	Corticated, > one cell layer thick	Fleshy, wiry
Thick and leathery	Thick blades and branches	Heavily corticated and highly differentiated, > one cell layer thick	Leathery, rubbery
Jointed calcareous	Articulated, upright	Calcified genicula ("segments"), flexible intergenicula ("joints"), > one cell layer thick	Stony
Crustose	Prostrate, epilithic crusts	Calcified or uncalcified, > one cell layer thick	Stony or fleshy, depending on calcification

Table 1-2. Species used during study with their designated functional group, species # (used in figures), the type of life cycle they exhibit, the generation and ploidy of collected thalli (if known), the site and habitat where they were collected, and the experiments in which they were used during this study.

Collection Site	Habitat	Functional group	#	Species	Life cycle type	Generation ID	Experiments
Cook's Bay, Mo'orea 17°29'20.0"S 149°49'31.3"W	Subtidal	Sheetlike	1	*Dictyota bartayresiana*	Haplodiplontic	Unknown	Toughness, tensile
		Sheetlike	2	*Padina boryana*	Haplodiplontic	Unknown	Toughness, tensile
		Sheetlike	3	*Ulva intestinalis*	Haplodiplontic	Unknown	Toughness, tensile
		Sheetlike	4	*Ulva lactuca*	Haplodiplontic	Unknown	Toughness, tensile
		Filamentous	5	*Caulerpa serrulata*	Diplontic	2N gametophyte	Toughness, tensile
		Filamentous	6	*Spyridia filamentosa*	Triphasic	Unknown	Toughness, tensile
		Coarsely branched	7	*Amansia rhodantha*	Triphasic	Unknown	Toughness, tensile, growth
		Coarsely branched	8	*Acanthophora spicifera*	Triphasic	Unknown	Toughness, tensile, growth
		Thick and leathery	9	*Gracilaria parvispora*	Triphasic	1N gametophyte	Toughness, tensile
		Thick and leathery	10	*Sargassum pacificum*	Diplontic	2N gametophyte	Toughness, tensile, growth
		Thick and leathery	11	*Turbinaria ornata*	Diplontic	2N gametophyte	Toughness, tensile, growth
		Jointed calcareous	12	*Galaxaura fasciculata*	Triphasic	1N gametophyte	Toughness, tensile, growth
		Jointed calcareous	13	*Halimeda opuntia*	Diplontic	2N gametophyte	Toughness, tensile, growth
Cambria, California 35°32'52.4"N 121°05'53.0"W	Intertidal	Sheetlike	17	*Pyropia perforata*	Prototriphasic	1N gametophyte	Toughness, tensile
		Coarsely branched	20	*Endocladia muricata*	Triphasic	Unknown	Toughness, tensile
		Coarsely branched	22	*Mastocarpus papillata*	Triphasic	1N gametophyte	Toughness, tensile
		Coarsely branched	25	*Prionitis sternbergiii*	Triphasic	Unknown	Toughness, tensile
		Jointed calcareous	32	*Bossiella orbigniana*	Triphasic	Unknown	Toughness, tensile
		Jointed calcareous	33	*Calliarthron tuberculosum*	Triphasic	Unknown	Toughness, tensile
Santa Catalina Island, California 33°26'40.4"N 118°29'19.2"W	Subtidal	Sheetlike	15	*Dictyopteris undulata*	Haplodiplontic	Unknown	Toughness, tensile, growth
		Sheetlike	18	*Zonaria farlowii*	Haplodiplontic	Unknown	Toughness, tensile, growth
		Coarsely branched	21	*Laurencia pacifica*	Triphasic	Unknown	Toughness, tensile
		Coarsely branched	23	*Pterocladiella capillacea*	Triphasic	Unknown	Toughness, tensile, growth
		Coarsely branched	24	*Plocamium pacificum*	Triphasic	Unknown	Toughness, tensile
		Thick and leathery	26	*Egregia menzeissi*	Haplodiplontic	2N sporophyte	Toughness, tensile
		Thick and leathery	27	*Stephanocystis doica*	Diplontic	2N gametophyte	Toughness, tensile, growth
		Thick and leathery	29	*Sargassum horneri*	Diplontic	2N gametophyte	Toughness, tensile
		Thick and leathery	31	*Sargassum palmeri*	Diplontic	2N gametophyte	Toughness, tensile, growth
Palos Verdes, California 33°47'38.4"N 118°24'27.7"W	Intertidal	Sheetlike	14	*Dictyota binghamiae*	Haplodiplontic	Unknown	Toughness, tensile
		Sheetlike	16	*Dictyota coriacea*	Haplodiplontic	Unknown	Toughness, tensile
		Coarsely branched	19	*Colpomenia sinuosa*	Haplodiplontic	1N gametophyte	Toughness, tensile
		Thick and leathery	28	*Silvetia compressa*	Diplontic	2N gametophyte	Toughness, tensile
		Thick and leathery	30	*Stephanocystis osmundaceae*	Diplontic	2N gametophyte	Toughness, tensile

Table 1-3. Statistical results of nested PERMANOVA or ANOVA (dependent on data meeting ANOVA assumptions, test used denoted in far-left column), with algal species nested within algal functional group. Tests conducted for thallus toughness, thallus tensile strength, and relative growth for tropical and temperate algal species. *P*-values lower than Bonferroni's corrected alpha are statistically significant (denoted in bold).

	Source of Variation	*Df*	*SS*	*MS*	*F*	*P*
A.	**Toughness**					
PERMANOVA	Tropical					
	Functional Group	4	64783	16196	506.90	**<0.001**
	Species[Functional Group]	8	1472	184	5.76	**<0.001**
	Residuals	117	3738	32		
	Temperate					
	Functional Group	3	411666	137222	2700.3	**<0.001**
	Species[Functional Group]	16	75223	4701	95.52	**<0.001**
	Residuals	180	9147	51		
B.	**Tensile**					
PERMANOVA	Tropical					
	Functional Group	4	15760984	3940246	64.60	**<0.001**
	Species[Functional Group]	8	16699419	2087427	34.22	**<0.001**
	Residuals	117	7136685	60997		
	Temperate					
	Functional Group	3	9206793	3068931	821.84	**<0.001**
	Species[Functional Group]	16	16461428	1028839	275.52	**<0.001**
	Residuals	180	672162	3734		
C.	**Growth**					
PERM-ANOVA	Tropical					
	Functional Group	2	125191	62595	111.43	**<0.001**
	Species[Functional Group]	3	136095	45365	80.76	**<0.001**
	Residuals	42	23593	562		
ANOVA	Temperate					
	Functional Group	1	0.00000004	0.00000004	0.01	0.92
	Species[Functional Group]	2	0.00004164	0.00002082	5.78	**0.01**
	Residuals	28	0.0001008	0.000003601		

Figure captions

Fig. 1-1. Predictions of the Littler and Littler (1980) Functional Group Model (FGM) for macroalgae. The model predicts that thallus toughness and thallus tensile strength increase with morphological complexity as you move from the simple, sheetlike functional group (left) to the most complex, crustose functional group (right). These predictions are opposite for growth rate. These performance traits are assumed to correlate with ecosystem functions (right), where thallus toughness is a metric of resistance to herbivory, thallus tensile strength is a metric of resistance to disturbance, and growth rate is a metric of recovery from disturbance and role in succession.

Fig. 1-2. Maps of study locations and collection sites (yellow circles). Top panel shows world map with study regions, with yellow square A highlighting California study region and yellow square B highlighting Mo'orea, French Polynesia study region. Collection sites in California (panel A, bottom) include Cambria, Palos Verdes, and Santa Catalina Island (from north to south), whereas collection sites in Mo'orea, French Polynesia (panel B, bottom) include Cook's Bay.

Fig. 1-3. Thallus toughness by functional group (left panels A and B) and species (right panels C and D), with tropical algae in the top row (panels A and C) and temperate algae in the bottom row (panels B and D). Individual bars represent weight to penetrate (g) (mean ± SE), colors represent functional group designations. For species numbers on x-axis, refer to Table 1-2. Note difference in scales.

Fig. 1-4. Thallus tensile strength by functional group (left panels A and B) and species (right panels C and D), with tropical algae in the top row (panels A and C) and temperate algae in the bottom row (panels B and D). Individual bars represent weight to break (g) (mean ± SE), colors represent functional group designations. For species numbers on x-axis, refer to Table 1-2. Note difference in scales.

Fig. 1-5. Relative growth by functional group (left panels A and B) and species (right panels C and D), with tropical algae in the top row (panels A and C) and temperate algae in the bottom row (panels B and D). Individual bars represent growth (% change in weight (g) day^{-1}) (mean ± SE), colors represent functional group designations. For species numbers on x-axis, refer to Table 1-2. Note difference in scales.

Figures

Fig. 1-1

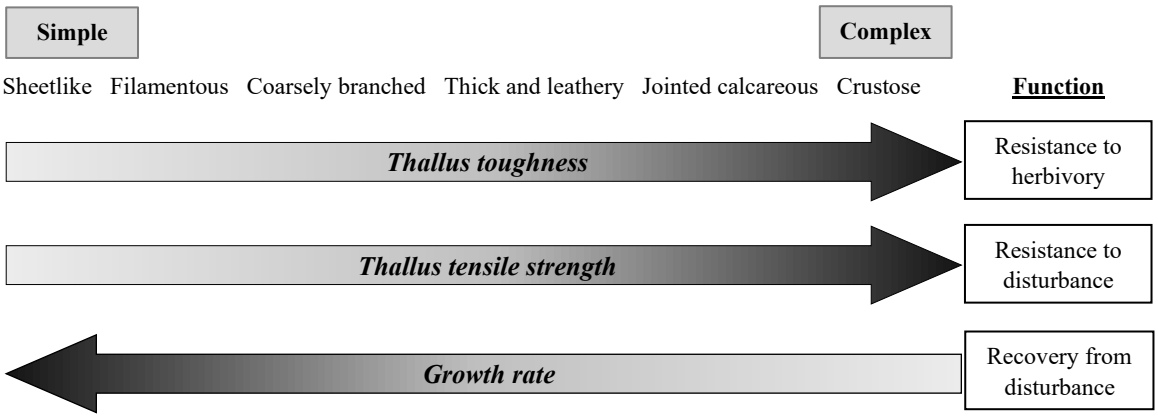

Fig. 1-2

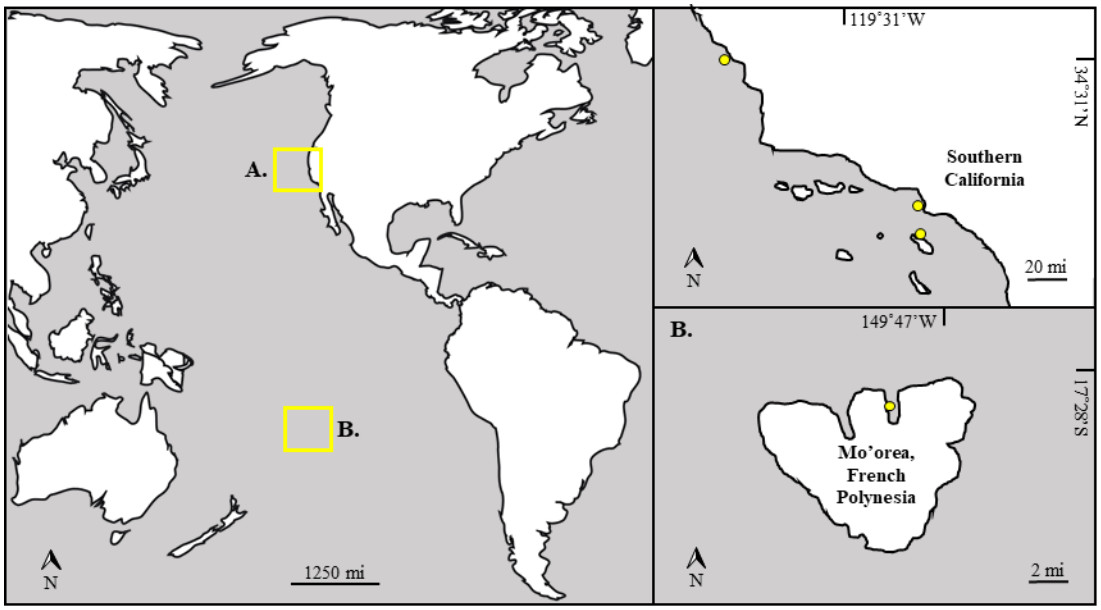

Fig. 1-3

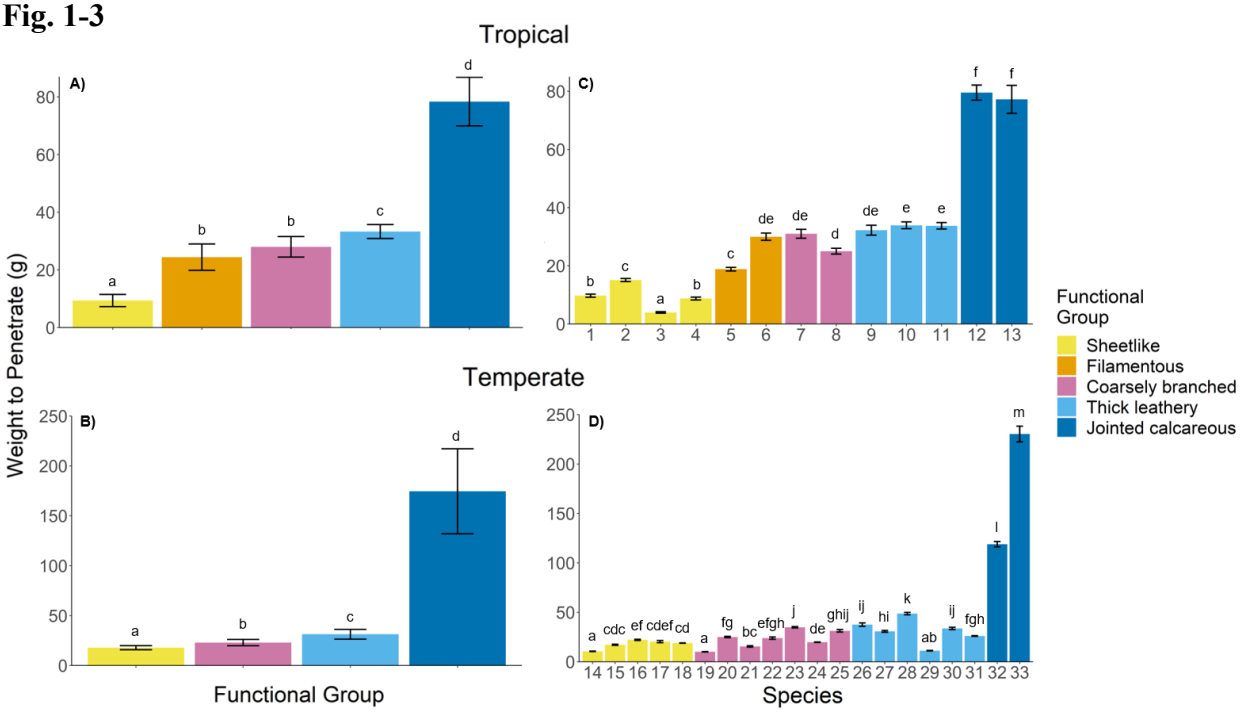
Tropical
Temperate
A)
B)
C)
D)
Weight to Penetrate (g)
Functional Group
Species
Functional Group
Sheetlike
Filamentous
Coarsely branched
Thick leathery
Jointed calcareous

Fig. 1-4

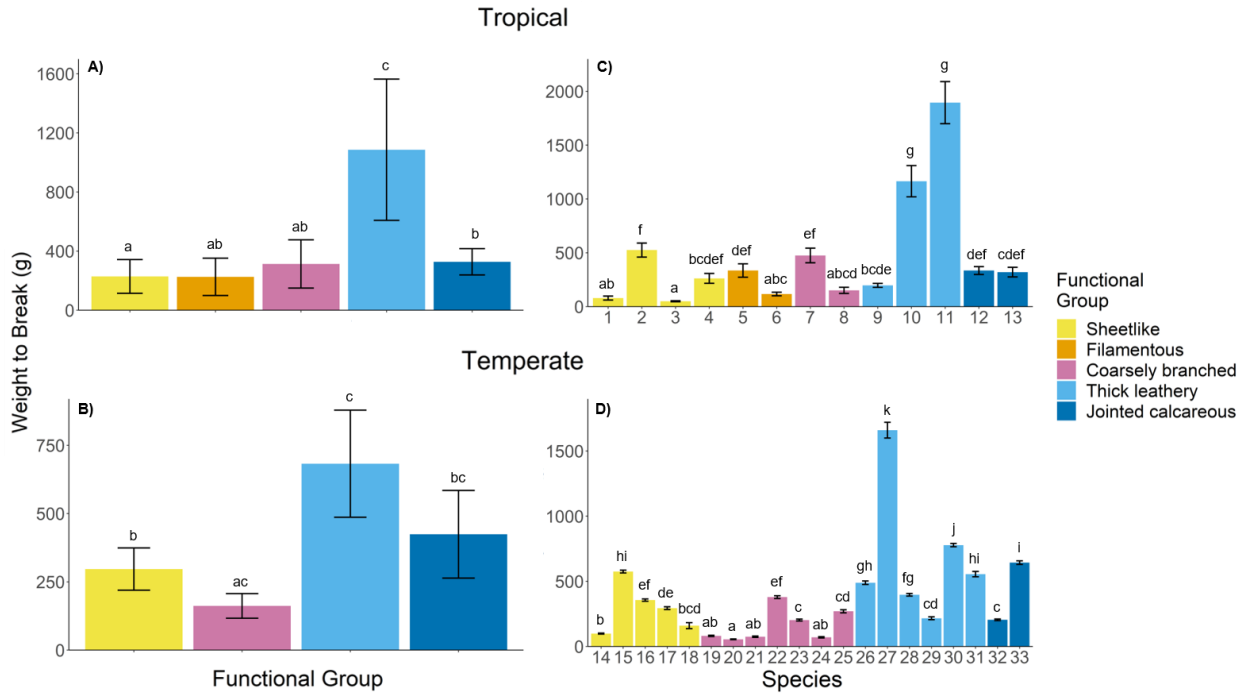
Tropical
Temperate
A)
B)
C)
D)
Weight to Break (g)
Functional Group
Species
Functional Group
Sheetlike
Filamentous
Coarsely branched
Thick leathery
Jointed calcareous

Fig. 1-5

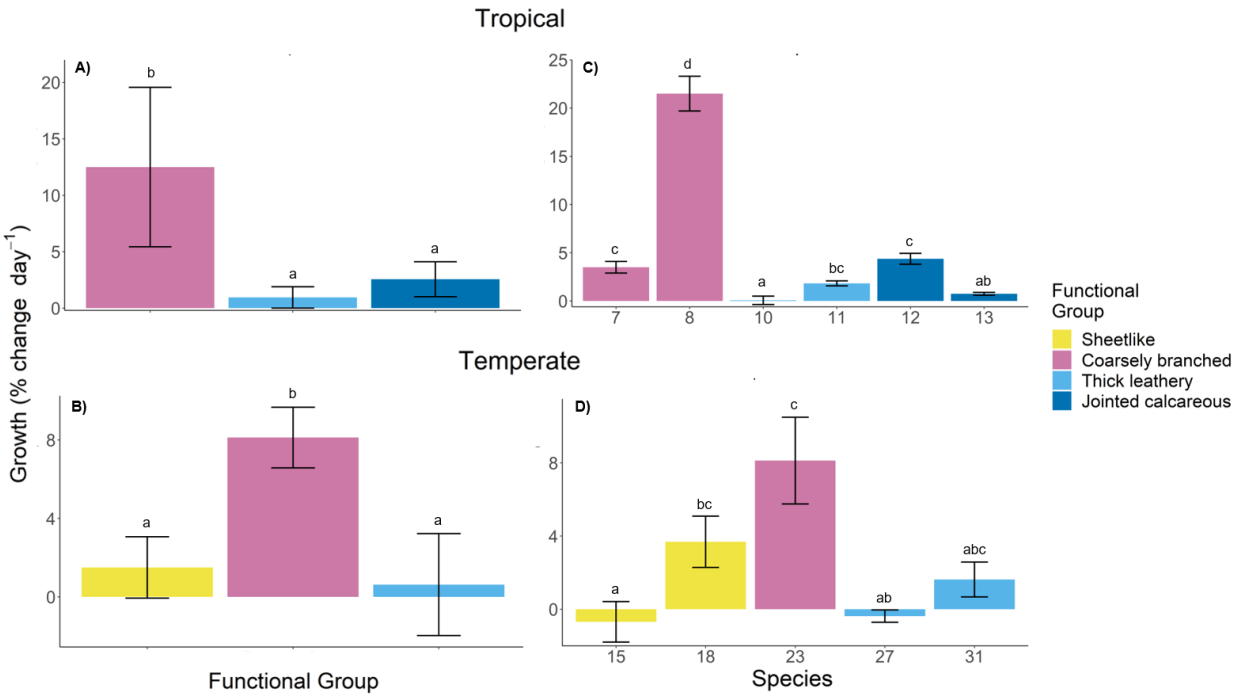

References

Adler, P.B., Salguero-Gómez, R., Compagnoni, A., Hsu, J.S., Ray-Mukherjee, J., Mbeau-Ache, C., and Franco, M. 2014. Functional traits explain variation in plant life history strategies. *Proceeding of the National Academy of Sciences* 111(2): 740-745. doi: 10.1073/pnas.1315179111

Anderegg, W.R.L. 2015. Spatial and temporal variation in plant hydraulic traits and their relevance for climate change impacts on vegetation. *New Phytologist* 205: 1008-1014. doi: 10.1111/nph.12907

Balata, D., Piazzi, L., and Rindi, F. 2011. Testing a new classification of morphological functional groups of marine macroalgae for the detection of responses to stress. *Marine Biology* 158: 2459-2469. doi: 10.1007/s00227-011-1747-y

Bellwood, D.R., Hoey, A.S., and Choat, H. 2003. Limited functional redundancy in high diversity systems: resilience and ecosystem function on coral reefs. *Ecology Letters* 6: 281-285. doi:10.1046/j.1461-0248.2003.00432.x

Bellwood, D.R., Streit, R.P., Brandl, S.J., and Tebbett, S.B. 2019. The meaning of the term

'function' in ecology: A coral reef perspective. *Functional Ecology* 33: 948-961. doi: 10.1111/1365-2435.13265

Blaum, N., Mosner, E., Schwager, M., and Jeltsch, F. 2011. How functional is functional? Ecological groupings in terrestrial animal ecology: Towards an animal functional type approach. *Biodiversity and Conservation* 20: 2333-2345. doi: 10.1007/s10531-011-9995-1

Blondel, J. 2003. Guilds or functional groups: Does it matter? *Oikos* 100: 223-231.

Bontemps, A., Davi, H., Lefèvre, F., Rozenberg, P., and Oddou-Muratorio, S. 2017. How do functional traits syndromes covary with growth and reproductive performance in a water-stressed population of *Fagus sylvatica*? *Oikos* 126: 1472-1483. doi: 10.1111/oik.04156

Borer, E.T., Bracken, M.E.S., Seabloom, E.W., Smith, J.E., Cebrian, J., Cleland, E.E., Elser, J.J., …Ngai, J.T. 2013. Global biogeography of autotroph chemistry: is isolation a driving force? *Oikos* 122: 1121-1130. doi: 10.1111/j.1600-0706.2013.00465.x

Boulangeat, I., Philippe, P., Abdulhak, S., Douzet, R., Garraud, L., Lavergne, S., Lavorel, S., …Thuiller, W. 2012. Improving plant functional groups for dynamic models of biodiversity: At the crossroads between functional and community ecology. *Global Change Biology* 18: 3464-3475. doi: 10.1111/j.1365-2486.2012.02783.x

Cappelatti, L., Mauffrey, A.R.L., and Griffin, J.N. 2019. Applying continuous functional traits to large brown macroalgae: variation across tidal emersion and wave exposure gradients. *Marine Biology* 166: 145. doi: 10.1007/s00227-019-3574-5

Carey, N., Galkin, A., Henriksson, P., Richards, J.G., and Sigwart, J.D. 2013. Variation in oxygen consumption among 'living fossils' (Mollusca: Polyplacophora). *Journal of the Marine Biological Association of the United Kingdom* 93(1): 197-207. doi: 10.1017/S0025315412000653

Chang, C., Szlavecz, K., Filley, T., Buyer, J.S., Bernard, M.J., and Pitz, S.L. 2016. Belowground competition among invading detritivores. *Ecology* 97(1): 160-170. doi: 10.1890/15-0551.1

Chapin, F.S. I. 1993. Functional role of growth forms in ecosystem and global processes. In J.R. Ehleringer, and C.B. Field (Eds). *Scaling physiological processes: leaf to globe* (pp. 287-312). San Diego, CA: Academic Press.

Cheal, A.J., MacNeil, M.A., Cripps, E., Emslie, M.J., Jonker, M., Schaffelke, B., and Sweatman, H. 2010. Coral-macroalgal phase shifts or reef resilience: links with diversity and functional roles of herbivorous fishes on the Great Barrier Reef. *Coral Reefs* 29: 1005-1015. doi: 10.1007/s00338-010-0661-y

Cleland, E.E., Chiariello, N.R., Loarie, S.R., Mooney, H.A., and Field, C.B. 2006. Diverse responses of phenology to global changes in a grassland ecosystem. *Proceedings of the*

National Academy of Sciences 103(37): 13740-13744. doi: 10.1073pnas.0600815103

Cornwell, W.K. and Ackerly, D.D. 2010. A link between plant traits and abundance: Evidence from coastal California woody plants. *Journal of Ecology* 98: 814-821. doi: 10.1111/j.1365-2745.2010.01662.x

Cornwell, W.K., Cornelissen, J.H.C., Amatangelo, K., Dorrepaal, E., Eviner, V.T., Godoy, O., …Westoby, M. 2008. Plant species traits are the predominant control on litter decomposition rates within biomes worldwide. *Ecology Letters* 11: 1065-1071. doi: 10.1111/j.1461-0248.2008.01219.x

De Graaf, R.M., Tilghman, N.G., and Anderson, S.H. 1985. Foraging guilds of North American birds. *Environmental Management* 9(6): 493-536.

Edwards, K.F., Klausmeier, C.A., and Litchman, E. 2013. A three-way trade-off maintains functional diversity under variable resource supply. *The American Naturalist* 182(6): 786-800. doi: 10.1086/673532

Eviner, V.T., and Chapin, F.S.III. 2003. Functional matrix: A conceptual framework for predicting multiple plant effects on ecosystem processes. *Annual Review of Ecology, Evolution and Systematics* 34: 455-485. doi: 10.1146/annurev.ecolsys.34.011802.132342

Floeter, S.R., Behrens, M.D., Ferreira, C.E.L., Paddack, M.J., and Horn, M.H. 2005. Geographical gradients of marine herbivorous fishes: patterns and processes. *Marine Biology* 147: 1435-1447. doi: 10.1007/s00227-005-0027-0

Fong, C.R., and Fong, P. 2014. Why species matter: an experimental assessment of assumptions and predictive ability of two functional-group models. *Ecology* 95(8): 2055-2061.

Fong, P., Smith, T.B., and Wartian, M.J. 2006. Epiphytic cyanobacteria maintain shifts to macroalgal dominance on coral reefs following ENSO disturbance. *Ecology* 87: 1162-1168.

García-Llamas, P., Rangel, T.F., Calvo, L., and Suárez-Seoane, S. 2019. Linking species functional traits of terrestrial vertebrates and environmental filters: A case study in temperate mountain systems. *PLoS ONE* 14(2): e0211760. doi: 10.1371/journal.pone.0211760

Gaspar, R., Pereira, L., and Neto, J.M. 2017. Intertidal zonation and latitudinal gradients on macroalgal assemblages: Species, functional groups and thallus approaches. *Ecological Indicators* 81: 90-103. doi: 10.1016/j.ecolind.2017.05.060

Gitay, H., and Nobel, I.R. 1997. What are functional types and how should we seek them? In Smith, T.M., Shugart, H.H., Woodward, F.I. (Eds) *Plant functional types-their relevance to ecosystem properties and global change*. Cambridge, UK: University Press.

Green, A.L., and Bellwood, D.R. 2009. Monitoring functional groups of herbivorous reef

fishes as indicators of coral reef resilience-A practical guide for coral reef managers in the Asia Pacific region. IUCN working group on Climate Change and Coral Reefs. IUCN, Gland, Switzerland. 70 pages.

Grime, J.P. 1974. Vegetation classification by reference to strategies. *Nature* 250: 26-31.

Hanisak, M.D., Littler, M.M., and Littler, D.S. 1990. Application of the functional-form model to the culture of seaweeds. *Hydrobiologia* 204: 73-77. doi:10.1007/BF00040217

Harrison, S.P., Prentice, I.C., Barboni, D., Kohfeld, K.E., Ni, J., and Sutra, J.P. 2010. Ecophysiological and bioclimatic foundations for a global plant functional classification. *Journal of Vegetation Science* 21: 300– 317. doi: 10.1111/j.1654-1103.2009.01144.x

Huston, M.A. and Wolverton, S. 2009. The global distribution of net primary production: resolving the paradox. *Ecological Monographs* 79(3): 343-377.

Jaksic, F.M., Feinsinger, P., and Jimenez, J.E. 1996. Ecological redundancy and long-term dynamics of vertebrate predators in semiarid Chile. *Conservation Biology* 10(1): 252-262.

Jänes, H., Kotta, J., Pärnoja, M., Crowe, T.P., Rindi, F., and Orav-Kotta, H. 2017. Functional traits of marine macrophytes predict primary production. *Functional Ecology* 31: 975-986. doi: 10.1111/1365-2435.12798

Krueger-Hadfield, S.A. 2020. What's ploidy got to do with it? Understanding the evolutionary ecology of macroalgal invasions necessitates incorporating life cycle complexity. *Evolutionary Applications* 13: 486-499. doi: 10.1111/eva.12843

Levine, J.M. 2016. A trail map for trait-based studies. *Nature* 529: 163-164. doi: 10.1038/nature16862

Litchman, E., and Klausmeier, C.A. 2008. Trait-based community ecology of phytoplankton. *Annual Review of Ecology, Evolution, and Systematics* 39: 615-639. doi: 10.1146/annurev.ecolsys.39.110707.173549

Littler, M.M., and Littler, D.S. 1980. The evolution of thallus form and survival strategies in benthic marine macroalgae: Field and laboratory tests of a functional form model. *The American Naturalist* 116(1): 25-44. doi: 10.1086/283610

Littler, M.M., Littler, D.S., and Taylor, P.R. 1983a. Evolutionary strategies in a tropical barrier reef system: functional form groups of marine macroalgae. *Journal of Phycology* 19: 223-231.

Littler, M.M., Taylor, P.R., and Littler, D.S. 1983b. Algal resistance to herbivory on a Caribbean barrier reef. *Coral Reefs* 2: 111-118.

Littler, M.M., and Littler, D.S. 1984. Relationships between macroalgal functional form groups and substrata stability in a subtropical rocky-intertidal system. *Journal of Experimental Marine Biology and Ecology* 74: 13-34. doi: 10.1016/0022-0981(84)90035-2

Lobban, C., and Harrison, P.J. 1994. *Seaweed ecology and physiology* (366 pp). New York, NY:Cambridge University Press.

López-Martínez, J.O., Sanaphre-Villanueva, L., Dupuy, J.M., Hernández-Stefanoni, J.L., Meave, J.A., and Gallardo-Cruz, J.A. 2013. β-Diversity of functional groups of woody plants in a tropical dry forest in Yucatan. *PLoS ONE* 8(9): e0073660. doi: 10.1371/journal.pone.0073660

Lubchenco, J., and Cubit, J. 1980. Heteromorphic life histories of certain marine algae as adaptations to variations in herbivory. *Ecology* 61: 3, 676-687. doi: 10.2307/1937433

Luck, G.W., Carter, A., and Smallbone, L. 2013. Changes in bird functional diversity across multiple land uses: Interpretations of functional redundancy depend on functional group identity. *PLoS ONE* 8(5): e63671. doi:10.1371/journal.pone.0063671

Mantyka, C.S., and Bellwood, D.R. 2007. Direct evaluation of macroalgal removal by herbivorous coral reef fishes. *Coral Reefs* 26: 435-442. doi: 10.1007/s00338-007-0214-1

Martinez, E.A., and Santelices, B. 1998. Selective mortality on haploid and diploid microscopic stages of *Lessiona nigrescens* Bory (Phaeophyta, Laminariales). *Journal of Experimental Marine Biology and Ecology* 229: 219-39. https://doi.org/10.1016/S0022-0981(98)00063-X

Mauffrey, A.R.L., Cappelatti, L., and Griffin, J.N. 2020. Seaweed functional diversity revisited: Confronting traditional groups with quantitative traits. *Journal of Ecology* 00: 1-16. doi: 10.1111/1365-2745.13460

McGill, B.J., Enquist, B.J., Weiher, E., and Westoby, M. 2006. Rebuilding community ecology from functional traits. *Trends in Ecology and Evolution* 21(4): 178-185. doi: 10.1016/j.tree.2006.02.002

McLaren, J.R., and Turkington, R. 2010. Ecosystem properties determined by plant functional group identity. *Journal of Ecology* 98: 459-469. doi: 10.1111/j.1365 2745.2009.01630.x

Murray, F., Douglas, A., and Solan, M. 2014. Species that share traits do not necessarily form distinct and universally applicable functional effect groups. *Marine Ecology Progress Series* 516: 23-34. doi: 10.3354/meps11020

Naeem, S. 2009. Advancing realism in biodiversity research. *Trends in Ecology and Evolution* 23(8): 414-416. doi:10.1016/j.tree.2008.05.003

Oksanen, J., Blanchet, F.G., Friendly, M., Kindt, R., Legendre, P., McGlinn, D., Minchin, P.R.,

…Wagner, H. 2019. vegan: Community Ecology Package. R package version 2.5-4. https://CRAN.R-project.org/package=vegan

Padilla, D.K., and Allen, B.J. 2000. Paradigm lost: reconsidering functional form and group hypotheses in marine ecology. *Journal of Experimental Marine Biology and Ecology* 250: 207-221. doi: 10.1016/S0022-0981(00)00197-0

Phillips, J., Kendrick, G.A., and Lavery, P. 1997. A test of a functional group approach to detecting shifts in macroalgal communities along a disturbance gradient. *Marine Ecology Progress Series* 153: 125-138. doi: 10.3354/meps153125

Pokorny, M.L., Sheley, R.L., Zabinski, C.A., Engel, R.E., Svejcar, T.J., and Borkowski, J.J. 2005. Plant functional group diversity as a mechanism for invasion resistance. *Restoration Ecology* 13(3): 448-459. doi: 10.1111/j.1526-100X.2005.00056.x

Raffard, A., Lecerf, A., Cote, J., Buoro, M., Lassus, R., and Cucherousset, J. 2017. The functional syndrome: linking individual trait variability to ecosystem functioning. *Proceedings of the Royal Society B* 284: 20171893. doi: 10.1098/rspb.2017.1893

R Core Team. 2017. R: A language and environment for statistical computing. R Foundation for Statistical Computing, Vienna, Austria. www.r-project.org.

Resetarits, W.J., and Chalcraft, D.R. 2007. Functional diversity within a morphologically conservative genus of predators: Implications for functional equivalence and redundancy in ecological communities. *Functional Ecology* 21: 793-804. doi: 10.1111/j.1365-2435.2007.01282.x

Reynolds, C.S. 1984. *The ecology of freshwater phytoplankton*. Cambridge, UK: University Press.

Root, R. B. 1967. Niche exploitation pattern of blue-gray gnatcatcher. *Ecological Monographs* 37: 317-334.

Rosenfeld, J.S. 2002. Functional redundancy in ecology and conservation. *Oikos* 98(1) 156-162.

Rosindell, J., Hubbell, S.P., He, F., Harmon, J., and Etiene, R.S. 2012. The case for ecological neutral theory. *Trends in Ecology and Evolution* 27: 203-208. doi: doi.org/10.1038/nature16862

Ryznar, E.R., Fong, P. and Fong, C.R. 2020. Data from: When form does not predict function: empirical evidence violates functional form hypotheses for marine macroalgae. Digital Dryad Repository. https://doi.org/10.5068/D1KM3P

Shipley, B., De Bello, F., Cornelissen, J.H.C., Laliberté, E., Laughlin, D.C., and Reich P.B. 2016. Reinforcing loose foundation stones in trait-based plant ecology. *Oecologia* 180:

923-931. doi: 10.1007/s00442-016-3549-x

Smith, J.E., Hunter, C.L., and Smith, C.M. 2010. The effects of top-down versus bottom-up control benthic coral reef community structure. *Oecologia* 163: 497-507.

Steneck, R.S., and Dethier, M.N. 1994. A functional group approach to the structure of algal-dominated communities. *Oikos* 69: 476-498.

Stelling-Wood, T.P., Gribben, P.E., and Poore, A.G.B. 2020. Habitat variability in an underwater forest: Using a trait-based approach to predict associated communities. *Functional Ecology* 34: 888-898. doi: 10.1111/1365-2435.13523

Suding, K.N., Collins, S.L., Gough, L., Clark, C., Cleland, E.E., Gross, K.L., Milchunas, D.G., and Pennings, S. 2005. Functional- and abundance-based mechanisms explain biodiversity loss due to N fertilization. *Proceedings of the National Academy of Sciences* 102(2): 4387-4392. doi:10.1073pnas.0408648102

Sullivan, G., and Zedler, J.B. 1999. Functional redundancy among tidal marsh halophytes: A test. *Oikos* 84(2): 246-260.

Thomas, H.J.D., Myers-Smith, I.H., Bjorkman, A.D., Elmendorf, S.C., Blok, D., Cornelissen, J.H.C., …van Bodegom, P.M. 2018. Traditional plant functional groups explain variation in economic but not size-related traits across the tundra biome. *Global Ecology and Biogeography* 28: 78-95. doi:10.1111/geb.12783

Thornber, C.S. 2006. Functional properties of the isomorphic biphasic algal life cycle. *Integrative and Comparative Biology* 46(5): 605-614.

Tilman, D. 2001. Functional diversity. In: Levin, SA (ed). *Encyclopedia of biodiversity*. San Diego, CA: Academic Press. 109-120.

Tilman, D., Knops, J., Wedin, D., Reich, P., Ritchie, M., and Siemann, E. 1997. The influence of functional diversity and composition on ecosystem processes. *Science* (277): 1300-1302. doi: 10.1126/science.277.5330.1300

Tjoelker, M.G., Craine, J.M., Wedin, D., Reich, P.B., and Tilman, D. 2005. Linking leaf and root trait syndromes among 39 grassland and savannah species. *New Phytologist* 167: 493-508. doi:10.1111/j.1469-8137.2005.01428.x

Vergés, A., Steinberg, P.D., Hay, M.E., Poor, A.G.B., Campbell, A.H., Ballesteros, E., Heck Jr, K.L., …Wilson, S.K. 2014. The tropicalization of temperate marine ecosystems: Climate-mediated changes in herbivory and community phase shifts. *Proceedings of the Royal Society B* 281: 20140846. doi: http://dx.doi.org/10.1098/rspb.2014.0846

Voille, C., Marie-Laure, N., Vile, D., Kazakou, E., Fortunel, C., Hummel, I., and Garnier, E. 2007. Let the concept of trait be functional! *Oikos* 116: 882-892. doi: 10.1111/j.2007.0030-1299.15559.x

Westoby, M., Falster, D.S., Moles, A.T., Vesk, P.A., and Wright, I.J. 2002. Plant ecological strategies: Some leading dimensions of variation between species. *Annual Review of Ecology and Systematics* 33: 125-149. doi: 10.1146/annurev.ecolsys.33.010802.150452

Wright, I.J., Reich, P.B., Westoby, M., Ackerly, D.D., Baruch, Z., Bongers, F., Cavender-Bares, J., … Villar, R. 2004. The worldwide leaf economics spectrum. *Nature* 428: 821-827.

CHAPTER 2

Disturbance, not herbivory, may facilitate the invasion of a marine algal "passenger" on temperate rocky reefs

Abstract

Sargassum horneri, a brown alga, recently invaded the California coast. Despite its rapid spread, empirical tests that evaluate mechanisms underlying *S. horneri*'s invasion success are lacking. To fill this knowledge gap, we conducted three field experiments on temperate rocky reefs in southern California using growth as a proxy for invasion success. We first tested whether *S. horneri* invasion success differed with herbivory strength and native diversity by conducting a 2-factor experiment that varied site (with different levels of baseline urchin densities and native algal diversity) and urchin access. We found that *S. horneri* growth only differed among urchin access treatments and not sites. We then evaluated whether *S. horneri* could successfully invade established algal canopies as a driver or whether it required open space as a passenger via a 2-factor field experiment that varied *S. horneri* size (small, medium, large) and canopy type (*S. horneri*, *Macrocystis pyrifera*, -canopy). We found that all *S. horneri* sizes grew fastest when canopy was lacking and light was high and slower in both canopy habitats with lower light; overall, small *S. horneri* grew slowest. Finally, we evaluated whether herbivore preference for native species could facilitate *S. horneri*'s invasion by conducting a 2-factor field experiment that varied species (*M. pyrifera*, *S. horneri*) and herbivore access. We found uncaged algae were consumed and caged algae grew, but this was not different between species. Taken together, our results suggest that *S. horneri* is a "passenger" invader that will take advantage of points in time and space where light is plentiful, such as when *M. pyrifera* is removed via disturbance. Further,

our results suggest that herbivory and native algal diversity are likely not key determining factors of the invasion success of *S. horneri*.

Introduction

Invasive species are altering ecosystem structure and functioning globally, yet invasions into marine systems are understudied (Caselle et al. 2017; Dijkstra et al. 2017; Papacostas et al. 2017). Invasive species are defined as species that establish outside of their native range and negatively impact the communities they invade (Inderjit et al. 2006; Williams and Smith 2007). Macroalgae account for 20-30% of all marine invasive species (Schaffelke et al. 2006; Schaffelke and Hewitt 2007; Thomas et al. 2016) and can negatively impact native community biomass (*for review*, *see* Gallardo et al. 2016; Mathieson et al. 2003; Trowbridge 2001; Williams and Grosholz 2002), functioning (Chisholm and Moulin 2003; Dumay et al. 2002a; Ferrer et al. 1997; Pederson et al. 2005), structure (Balata et al. 2004; Sánchez and Fernández 2005; York et al. 2006) and biodiversity (Piazzi et al. 2001; Stæer et al. 2000; Schmidt and Scheibling 2006). Despite their negative impacts, mechanisms that determine the success or failure of marine algal invasions are poorly understood (Inderjit et al. 2006; Papacostas et al. 2017; Williams and Smith 2007). Marine invasions are predicted to increase with continued globalization and shifts in ocean climate (Cohen and Carlton 1998; Godwin 2003; Grosholz 2002; Kaluza et al. 2010; Seebens et al. 2013; Stachowicz et al. 2002), highlighting the need to understand factors facilitating algal invasions.

One conceptual model, where invading species are categorized as “passengers” vs. “drivers,” may provide a useful framework for studying the mechanisms underpinning success of invasive marine algae. Originally developed by MacDougall and Turkington (2005), this model defines “drivers” as species that successfully invade a community through direct interactions

with native species and subsequently modify the recipient community through their success (South and Thomsen 2016). In contrast, "passengers" require environmental change that disproportionately limits or removes native species and releases previously unavailable resources in order to successfully invade. Once invaded, passengers can also modify the recipient community. Therefore, "drivers" are predicted to cause ecosystem change whereas "passengers" take advantage of it (MacDougall and Turkington 2005; South and Thomsen 2016).

One mechanism by which invasive species can drive ecosystem change is through exploitative competition for limiting resources, while passengers are considered competitively inferior. For marine macroalgae, light, space, and nutrients are primary resources determining growth and survival (Carpenter 1990; Sousa 1979) and competitive dominance is achieved through superior exploitation of these resources (MacDougall and Turkington 2005; Seabloom et al. 2003). Traits that facilitate resource exploitation for macroalgae can be morphological (e.g., height) and/or physiological (e.g., rapid growth) (Vaz-Pinto et al. 2014). Invaders are more likely to be successful "drivers" if these traits facilitate greater resource acquisition than native competitors. In contrast, passengers proliferate when disturbances remove dominant species, facilitating colonization of newly opened space. (Connell and Slayter 1997; Elton 1958; MacDougall and Turkington 2005; Minchinton and Bertness 2003; Moyle 1986). In marine systems, disturbances such as intense wave-action associated with storms and large-scale climatic events can remove competitively superior native algae, and studies have shown that some invasive algae are only able to colonize following disturbance (Ambrose and Nelson 1982; Bulleri et al. 2010; Scheibling and Gagnon 2006; Thompson and Schiel 2012; Valentine and Johnson 2003). However, despite its importance for understanding invasion success, experimental tests exploring the role of competitive superiority and facilitation by disturbance in

the driver-passenger framework are rare for marine macroalgal invasions (South and Thomsen 2016; Williams and Smith 2007).

Resistance to herbivory is another mechanism that may facilitate the invasion success of both drivers and passengers. Herbivore resistance can occur because invasive species possess novel defenses that make them unpalatable (Callaway and Ridenour 2004; Cappuccino and Carpenter 2005) or native consumers fail to recognize newcomers as a potential food source (Keane and Crawley 2002). In both cases, native macroalgae may be preferentially consumed, reducing the strength of competition between invasive and native algae and facilitating invasion success as a result (Pulzatto et al. 2018; Vermeij et al. 2009). Herbivore resistance as an invasion mechanism is generally supported for marine macroalgae. A review of 407 algal introductions (Williams and Smith 2007) found that although introduced algae were consumed, native species were largely preferred by generalist herbivores. Further, others have found that invasive algae are only consumed when associated with native species (Noé et al. 2018) or when native species are absent (Sumi and Scheibling 2005), or that the intensity of herbivory was not strong enough to control invader spread despite consumption by herbivores (Britton-Simmons 2004; Chavanich and Harris 2004; Conklin and Smith 2005; Vermeij et al. 2009). For example, sea urchins were not capable of controlling the rapid growth of the annual invasive alga, *Undaria pinnatifida*, and facilitated its spread through consumption of native species (Edgar et al. 2004; Valentine and Johnson 2003). While evaluations of herbivore resistance by macroalgal invaders are common, results may depend on herbivory intensity and whether native species are available. Therefore, further tests are needed to understand the role of herbivores in promoting invasion success, particularly for recent and/or understudied macroalgal invasions.

Native community diversity is considered a primary driver of community resistance to invasion by both drivers and passengers (Britton-Simmons 2006; Elton 1958). It is hypothesized that diverse communities reduce the chance of successful invasion because resources are more completely utilized, limiting the number of open niches that a passenger can exploit. Further, the probability of encountering a competitively superior species is higher in more diverse communities, limiting the chance a driver will be successful (Clark and Johnston 2011; Elton 1958; Stachowicz et al. 1999). Some have argued that functional diversity and the composition of native assemblages may serve as better indicators of biotic resistance than taxonomic diversity by taking into account how different species uniquely limit resources and invasion success due to differences in traits and functional roles (Arenas et al. 2006; Britton-Simmons 2006; Caselle et al. 2017; Clark et al. 2004; Dukes 2001; Vaz-Pinto et al. 2012; Villéger et al. 2008; Reed and Foster 1984). For example, canopy-forming macroalgae are capable of significantly reducing the amount of light reaching the benthos and the shading effect of different canopies is species-specific (Clark et al. 2004). While the relationship between native diversity and community resistance to invasion is widely documented in other systems (Davis et al. 2000; Stachowicz et al. 2007; Vaz-Pinto et al. 2012), there is variable support for this relationship in marine invasions (Arenas et al 2006; Dunstan and Johnson 2004; Fridley et al. 2007; Papacostas et al. 2017) and tests of community invasibility by marine macroalgae are rare (Williams and Smith 2007). Therefore, greater understanding of whether native diversity enhances biotic resistance to marine macroalgal invasions is needed.

California has experienced multiple marine algal invasions within the last 30 years (Britton-Simmons 2004; Miller et al. 2011), with the invasion of *Sargassum horneri* as one of the most recent and least understood. Native to east Asia, *S. horneri* first appeared in southern

California in 2003 and has since spread throughout the region and into Baja California, Mexico (Kaplanis et al. 2016; Marks et al. 2015). *S. horneri* exhibits high fecundity, rapid growth, tolerance of a wide range of environmental conditions, and an annual life-history (Kaplanis et al. 2016; Marks et al. 2015), which are characteristics that may facilitate rapid proliferation and resource exploitation following a disturbance as a "passenger". However, there have been very few investigations of mechanisms facilitating the success of *S. horneri*, despite documented negative impacts (Ginther and Steele 2018; Srednick and Steele 2019; Sullaway and Edwards 2020) and its invasion into critical habitats such as giant kelp (*Macrocystis pyrifera*) forests. Some studies suggest that *S. horneri* may be a passenger taking advantage of open niches by observing differences in peak seasonal biomass and depth distributions of *S. horneri* compared to native species (e.g., Marks et al. 2020a). Further, Caselle et al. (2017) found that low diversity sites (urchin barrens) as well as high diversity sites with an established native algal assemblage were resistant to *S. horneri* invasion; however, native diversity in this study was calculated across multiple trophic levels rather than just macroalgae. To date, conclusions regarding *S. horneri*'s invasion mechanisms and community invasibility have been correlational (Caselle et al. 2017; Marks et al. 2020a), stressing the need to empirically evaluate whether *S. horneri* is able to invade as a driver or requires ecosystem change as a passenger.

There is ambiguous evidence to support herbivore resistance as an invasion mechanism for *S. horneri*. Some have found herbivores preferentially consume native species over *S. horneri* (Marks et al. 2020a), suggesting that herbivore avoidance of *S. horneri* may facilitate its success. Others have concluded that herbivore resistance does not explain the success of *S. horneri* because herbivores had no clear preference for native algae compared to *S. horneri* (Kaplanis et al. 2020) or congeners (Pederson et al. 2016). Finally, Caselle et al. (2017) hypothesized that

areas with high levels of herbivory may be resistant to *S. horneri* invasion. Based on current evidence, it is unclear whether herbivores facilitate the invasion success of *S. horneri* by disproportionately consuming native species or whether herbivores enhance community resistance to invasion above certain densities. Taken together, these studies motivate further investigation into the role of herbivore resistance in the invasion of *S. horneri*.

We evaluated whether *S. horneri* is a driver or passenger invader by empirically investigating how interactions with native species and herbivory influence its success. Specifically, we evaluated three questions: 1) Does *S. horneri*'s invasion success (measured as growth) differ between sites that vary in baseline native algal diversity and urchin herbivory? 2) How does canopy-forming algae influence where *S. horneri* can invade? and 3) Do herbivores prefer to consume native *M. pyrifera* over *S. horneri*?

Methods

2.1. Overview

We conducted three field experiments to evaluate whether *S. horneri* is a driver or passenger invader on temperate rocky reefs in southern California, using growth as a proxy for invasion success (Mächler and Altermatt 2012; van Kleunen et al. 2010). More specifically, we first tested whether *S. horneri* invasion success differed with herbivory strength and native algal diversity by conducting a 2-factor field experiment that varied site (with different levels of baseline urchin densities and native algal diversity) and urchin access. We then evaluated whether *S. horneri* could successfully invade established algal canopies as a driver or whether it required open space as a passenger via a 2-factor field experiment that varied *S. horneri* size (small, medium, large) and canopy type (*S. horneri*, *M. pyrifera*, -canopy). Finally, we evaluated whether herbivore preference for native species could facilitate *S. horneri*'s invasion by

conducting a 2-factor field experiment that varied species (*M. pyrifera*, *S. horneri*) and herbivore access.

2.2. Study system

All research was conducted on the leeward side of Santa Catalina Island, California, USA (Fig. 2-1; 33°26'40.8"N 118°29'41.2"W). Catalina rocky reefs are generally characterized by a combination of cobble, boulder, and bedrock substrate interspersed with sand and shell debris (Marks et al. 2020a). Native algal cover varies by area and species, with some areas characterized by a mixed community of abundant small (<0.5m) understory native species (i.e., *Dictyota spp.*, *Dictyopteris undulata*, *Zonaria farlowii,* and foliose red algae), larger (~>0.5m) native understory species (i.e., *Stephanocystis osmundaceae, Sargassum palmeri, Ecklonia arborea*), and native canopy-forming *M. pyrifera* whereas other areas are dominated by crustose coralline red algae (CCA) and relatively devoid of non-calcareous understory species (Marks et al. 2020a; Sullaway and Edwards 2020).

Dominant invertebrate herbivores on Catalina rocky reefs include several species of snail and the black sea urchin (*Centrostephanus coronatus*) (Marks et al. 2020a). *C. coronatus* shelters in rocky crevasses during the day and forages at night within a radius of approximately 1m (Nelson and Vance 1979). Herbivorous fishes around Catalina include opaleye (*Girella nigricans*) and halfmoon (*Medialuna californiensis*) (Bredvik et al. 2011), though temperate herbivorous fishes have been shown generally to have weak top-down effects on algal communities compared to invertebrate herbivores (Barry and Ehret 1993). Therefore, fish were not surveyed in this study.

2.3. Evaluating the effects of urchin herbivory and site on S. horneri

To evaluate differences in the strength of herbivory across sites with varying algal diversity and natural urchin densities, we conducted a 2-factor field experiment. The first factor was urchin herbivory and the second was site.

2.3.1. Site selection and characterization

Four sites were chosen that were observed (and verified, see below) to have relatively high or low levels of native algal diversity. These sites were also observed (and verified, see below) to naturally vary in baseline urchin densities. All sites were just west of the University of Southern California Wrigley Institute for Environmental Studies (WIES), ranged from 8-9m in depth, and were less than 750m apart (sites 1-4, Fig. 2-1) to minimize the potential for confounding environmental factors. Sites included Isthmus Point (Site #1; 33°26'45.0"N 118°29'51.8"W), Isthmus Reef (Site #2; 33°26'54.9"N 118°29'29.0"W), Chalk Cliffs (Site #3; 33°26'39.4"N 118°29'22.6"W), and Campground (Site #4; 33°26'36.0"N 118°29'28.1"W).

To quantify native algal diversity at each site, surveys were conducted between July 16-18, 2018 following protocols adapted from the Partnership for Interdisciplinary Studies of Coastal Oceans (PISCO et al. 2011). To assess algal diversity and percent cover at each site, 45 intersecting points within 10 $1m^2$ quadrats were surveyed at randomly-selected points along each of two 30m transects laid parallel to shore along an 8m depth contour. We modified PISCO protocols by grouping algae into division (Rhodophyta, Ochrophyta, Chlorophyta). At the time of these surveys and field experiment (see below), canopy-forming *M. pyrifera* was absent in all of these study sites. We also recorded relief and substrate type (see Appendix 2 for methods).

Mean percent algal cover per m^2 was calculated by averaging percent cover by division for each quadrat for each site (n=20, N=80). Native algal diversity by algal division was calculated using the equation for the Shannon-Weiner Diversity Index, $H' = - [\sum P_i \ln P_i]$, where

P_i was the proportion of each algal division, *i*, in each quadrat and ln P_i is the natural logarithm of this proportion. Finally, mean percent cover per m^2 of CCA was calculated as above as it is structurally distinct from other algal groups. The proportion of relief type at each site and mean cover of substrate categories were also calculated (see Appendix 2).

To assess urchin density at each site, 2m x 30m band surveys were conducted along the same transects used for the algal surveys (n = 2, N = 8). Divers surveyed a 1m area on both sides of the transect for urchins, searching in crevasses and beneath algae for cryptic individuals. All urchins within each band were counted and identified to species. Urchin density was normalized to per m^2, calculated by dividing the total number of urchins in each band by the number of m^2 in the band transect ($60m^2$).

2.3.1.1. Statistical analysis for site characterization

All site characterization data were evaluated for normality and homogeneity of variances. Urchin density met parametric assumptions untransformed while native algal diversity and CCA percent cover were x^2 and $x^{1/2}$, respectively, to meet assumptions. These data were analyzed via a 1-factor ANOVA and significant ANOVA tests were followed by a Tukey HSD post-hoc. As the percent cover of algal divisions were not independent (i.e., cover of Rhodophyta was likely influenced by the cover of Ochrophyta within a quadrat) and no transformations helped native algal division percent cover by site meet parametric assumptions, we analyzed these data using a 1-factor PERMANOVA. Significant PERMANOVAs were followed by Pillai post-hoc analysis. For analysis of inanimate cover data, see Appendix 2. All analyses here and hereafter were conducted using base functions in R Statistical Software (R Core Team 2017), except for PERMANOVAs, which were conducted using the "vegan" package for the main analysis (Oksanen et al. 2019) and the "RVAideMemoire" package for post-hocs in R (Hervé 2020).

2.3.2. Experimental design

To empirically evaluate the effects of urchin herbivory (+/- barriers) and site (with varying levels of diversity and urchin densities) on *S. horneri* growth, transplant experiments were conducted at each site between July 25-August 8, 2018. Only small non-reproductive sizes (≤5cm; Marks et al. 2018) of *S. horneri* were utilized in the study. We used this size to minimize the risk of unintentionally spreading the invader (Marks et al. 2018) and because survival and growth of small, vulnerable stages can be an indicator of overall population growth (North et al. 1986) and invasion success. We collected twenty whole thalli (≤5cm) that appeared healthy with intact stipes, blades, and holdfasts and lacking pnuematocysts. *S. horneri* thalli were collected from each site at approximately 8m depth, transported immediately to WIES, transferred to an outdoor, flow-through water table, and cleaned of sediment and other organisms using ambient seawater from the WIES flow through system. Algae were spun in a salad spinner for one minute and wet weighed.

To restrict access by urchins, we secured half of the replicate thalli from each site in an upright growth position to the bottom of cylindrical urchin barriers (15cm diameter x 15cm height). Barriers were constructed of hardware cloth with 1cm openings that have been shown to have few artifacts (e.g., Fong et al. 2006, Smith et al. 2010). Barrier tops were open with a 5cm outward angled overhanging edge while barrier bottoms were completely closed. This open-topped barrier design with an overhanging edge has been shown to exclude sea urchins but allow other types of herbivory to occur (Carpenter 1986), allowing us to specifically evaluate the effects of urchin herbivory pressure. The other half of the replicate thalli from each site was open to all herbivory with no barriers. The protected (+barrier) and unprotected (-barrier) replicates were randomly attached to rope (+barrier replicates were attached by securing the barriers to

rope, -barrier replicates were directly attached to rope) and secured to the benthos at approximately 8m depth in the same location as collection at each site. There was at least 0.5m between replicates. Barriers were cleaned of fouling every other day. All replicates were recovered after 14 days then spun and wet-weighed. *S. horneri* is a fast-growing alga (4.46% day^{-1} maximum relative growth for adult blade weight; Choi et al. 2008), suggesting that differences in growth due to our treatments should be detectable over a 14-day period. Percent change in biomass was calculated as [(final weight-initial weight)/initial weight]*100 and then expressed on a per day basis. Mean percent change in biomass day^{-1} was calculated over all replicates by urchin barrier treatment for each site.

2.3.2.1. Statistical analysis

Experimental data met parametric assumptions of normality and heterogeneity of variance. To compare mean percent change in biomass day^{-1} by site and barrier treatment, the data was analyzed via a 2-factor ANOVA.

2.4. Evaluating the effects of canopy-forming algae and herbivory on different sizes of S. horneri

2.4.1. Site selection

We selected three canopy types at the northwestern side of Bird Rock (Site #5, Fig. 2-1; 33°27'05.3"N 118°29'17.3"W) that were characterized as either 1) dominated by adult *M. pyrifera* ("*M. pyrifera*"), 2) dominated by large (>50cm) *S. horneri* ("*S. horneri*"), or 3) devoid of canopy-forming algae ("-canopy"). The -canopy habitat was not an urchin barren and was characterized by sparse cover of small understory algal species and CCA on bedrock. These canopy types were directly adjacent to each other in an approximately $10m^2$ in area and occupied a depth range of 10-11m.

2.4.2. Transplant experiment with S. horneri

To evaluate how canopies formed by *M. pyrifera* and *S. horneri* influence the growth of different size classes of *S. horneri*, we conducted a 2-factor field experiment with canopy type and *S. horneri* size as factors between January 26-February 8, 2019. We collected 30 small (<10cm; 7.44±0.3 SE cm), 30 medium (10-50cm; 27.54±1.81 SE cm), and 30 large (51-150cm; 83.8±5.22 SE cm) thalli of *S. horneri* from the site dominated by large *S. horneri*. No individuals had reproductive structures. All thalli were transported back to WIES and wet-weighed as above. One thallus of each size was attached to each of 10 paracord lines that functioned as blocks. Each size was present in each block and spaced approximately 0.5m apart, but the order of the sizes within the block was random. All experimental units were open to herbivory. Lines were secured to the benthos as above at approximately 10m depth in each canopy type. Two Onset light and temperature dataloggers (UA-002-64 HOBO Waterproof Temperature/Light Pendant Data Logger) were deployed at the holdfast level in each canopy type and set to record light (lux) in ten second intervals. All HOBO loggers and thalli were recovered after fourteen days and thalli were spun and wet-weighed. Mean percent change in biomass day^{-1} was calculated as above by size in each canopy type. Light data for HOBO loggers were limited to daylight hours between 10:00-16:30 and then averaged over the experimental time period for each canopy type.

2.4.2.1. Statistical analysis for transplant experiment with S. horneri

Data met normality and homogeneity of variance assumptions for parametric statistics. To test whether *S. horneri* mean percent change in biomass day^{-1} was different among *S. horneri* sizes and canopy types, we performed a 2-factor ANOVA. Significant ANOVAs were followed by a Tukey HSD post-hoc analysis. Further, we conducted linear regressions for each size to test for relationships between light (lux) and percent change in biomass day^{-1}.

2.4.3. Herbivory experiment with S. horneri *and* M. pyrifera

To assess how herbivory may impact the growth of *S. horneri* and *M. pyrifera*, we conducted a 2-factor field experiment in the -canopy type at Bird Rock between July 20-August 2, 2019, with access to herbivores as one factor and species as the second factor.

We collected twenty thalli of both small *S. horneri* (≤5cm) and blade-stage *M. pyrifera* (<30cm) within the experimental site, spun and weighed all thalli as above, and photographed each thallus using an Olympus Tough TG-4 camera. To restrict access by all macro herbivores (> 1cm), we secured half of the replicates of each species in an upright growth position to the bottom of fully enclosed cylindrical cages (12cm diameter x 10cm height) constructed of hardware cloth with 1cm openings. The other half of the replicates for each species was not caged therefore open to all herbivores. The caged and uncaged replicates were randomly attached to rope and secured to the benthos at approximately 10m depth in the same location as collection. Cages were at least 0.5m apart and were cleaned of fouling every other day as above.

All replicates were recovered after 14 days and spun, wet-weighed, and photographed. Percent change in biomass per day was calculated as above, and mean percent change in biomass day^{-1} was calculated over all replicates by caging treatment for each species. Percent change in surface area of each thallus was calculated from "before" and "after" photographs using the image analysis and processing software, ImageJ (Schneider et al. 2012) and expressed on a per day basis. Mean percent change in surface area (cm^2 day^{-1}) was calculated over all replicates by caging treatment for each species.

2.4.3.1. Statistical analyses for herbivory experiment

Percent change in biomass was $x^{1/3}$ transformed to meet parametric assumptions whereas percent change in surface area met parametric assumptions untransformed. To test for differences in mean percent change in biomass and percent change in surface area between

caging treatments and species (*M. pyrifera* and *S. horneri*), we performed a 2-factor ANOVA for each response.

Results

3.1. Evaluating the effects of urchin herbivory and site on S. horneri

3.1.1. Site characterizations

Native algal diversity by division was significantly different among sites (Table 2-1A; Fig. 2-2A). Sites +D-U (high diversity, low urchins) and +D+U (high diversity, high urchins) generally had higher algal diversity than the other two sites. Although there was some overlap in diversity between -D+U (low diversity, high urchins) and +D+U sites, this was likely associated with their higher variances. Percent cover of algal divisions was significantly different among sites (Table 2-1B; Fig. 2-2B), with all pairs of sites varying significantly from each other except for sites with urchins (-D+U and +D+U). Percent cover of algae in the division Ochrophyta was highest in the sites without urchins (-D-U (low diversity, low urchins) and +D-U), while percent cover of algae in Rhodophyta was either not different (-D+U) or higher (+D+U) than cover of Ochrophyta in sites with urchins. Sites were generally characterized by low inanimate percent cover and medium relief (see Appendix 2).

Urchin density was significantly different among sites (Table 2-1C; Fig. 2-2C). Post-hocs confirmed that sites chosen a priori to be high urchin density sites (-D+U and +D+U) had higher urchin densities than the other two sites. *C. coronatus* was the primary urchin species in our sites. Finally, CCA percent cover was significantly different among sites (Table 2-1D; Fig. 2-2D). Generally, CCA percent cover was highest in sites with the highest urchin densities (-D+U and +D+U), though the two sites with low urchin densities were statistically different with CCA percent cover higher in the site that also had higher diversity (+D-U).

3.1.2. Experimental results

There was a significant difference in percent change in biomass day^{-1} between treatments with and without urchin barriers (Table 2-1E; Fig. 2-2E). *S. horneri* grew or remained the same when protected from urchins, and lost biomass when open to herbivores. Percent change in biomass was not significantly different among sites (i.e., baseline levels of diversity or urchins), nor was there an interaction between factors.

3.2. Evaluating the effects of canopy-forming algae and herbivory on different sizes of S. horneri

3.2.1. Canopy effects on S. horneri

There were significant differences in percent change in biomass among *S. horneri* sizes and canopy types with no interaction (Table 2-2A; Fig. 2-3A). Overall, small *S. horneri* grew the least and large *S. horneri* grew the most. Further, there was no growth of *S. horneri* for any size class under *M. pyrifera* canopy. Under *S. horneri* canopy, only large *S. horneri* appeared to grow, although none of the means differed among size classes in either *M. pyrifera* or *S. horneri* canopy types. All sizes grew the fastest in the habitat lacking algal canopy. Overall biomass nearly doubled from initial biomass over 14 days in the -canopy habitat. There was a significant relationship between light and percent change in biomass for small (p<0.05), medium (p<0.001), and large (p<0.001) *S. horneri* size (Fig. 2-3B). Light explained the least amount of variation in percent change in biomass for small *S. horneri* (r^2=0.15), the most variation for medium *S. horneri* (r^2=0.58), and an intermediate amount of the variation in percent change in biomass for large *S. horneri* (r^2=0.44).

3.2.2. Herbivory experiment with S. horneri *and* M. pyrifera

Percent change in biomass was significantly different between caging treatments but not between species (Table 2-2B; Fig. 2-5A). Overall, caged algae grew and uncaged algae remained

the same or lost biomass. While *S. horneri* tended to grow faster than *M. pyrifera* overall, this trend was not significant. Similarly, percent change in surface area was significantly different between caging treatments (Table 2-2C; Fig. 2-5B) but not between species. In general, caged algae increased in surface area and uncaged algae decreased in surface area.

Discussion

We found that *S. horneri* is a "passenger" of environmental change and not a "driver" of its own invasion success, as *S. horneri* grew faster in our study when the native canopy-forming *M. pyrifera* was absent and slower when *M. pyrifera* canopy was present. To our knowledge, our study is the first to experimentally test this hypothesis, although others have hypothesized that success of *S. horneri* depends on exploitation of open niches rather than competitive superiority (Caselle et al. 2017; Marks et al. 2020a; Sullaway and Edwards 2020). Disturbance is one process that removes dominant canopy-forming macroalgae, releasing previously unavailable resources such as space and light (Connell and Slayter 1997; Elton 1958; Minchinton and Bertness 2003; Moyle 1986) that "passengers" may then exploit. Our study followed a prolonged heatwave and extreme El Niño Southern Oscillation in 2014-2016 that led to declines in *M. pyrifera* canopy throughout much of southern California (Cavanaugh et al. 2019; Edwards 2019; Reed et al. 2016). *S. horneri* rapidly increased following this period (Marks et al. 2017), fueling speculation that this invader exploited disturbance-driven changes in the ecosystem as a "passenger" (Sullaway and Edwards 2020). *M. pyrifera* forests are naturally highly variable (Reed et al. 2016) and experience frequent disturbances, potentially making this system more vulnerable to the widespread and rapid proliferation of invasive passengers such as *S. horneri*. More broadly, others have found opportunistic "passengers" increased following declines in canopy-forming algae due to disturbances like severe storms (Foster 1982b) and experimental

removal (South and Thomsen 2016; Valentine and Johnson 2003). As disturbances are predicted to increase in duration and intensity with global change (Carnell and Keough 2020; DiLorenzo et al. 2010; Doney et al. 2012; Smale et al. 2019), our results imply that *S. horneri* will also increase in prevalence if these disturbances disproportionately impact native species such as *M. pyrifera*.

One mechanism that may support the success of *S. horneri* as a passenger is alleviation of light limitation. We found shading by larger-canopy forming algae reduced the amount of light reaching the benthos. Whether the canopy was dominated by *M. pyrifera* or conspecifics, *S. horneri* grew slower in low-light habitats. Further, overall larger thalli of *S. horneri* grew faster than smaller thalli, perhaps due to greater access to light. While evidence across *S. horneri*'s native and invasive range suggests it can grow in a variety of light levels and depths (Choi et al. 2008; Aguilar-Rosas et al. 2007; Yoshida 1983), it has been suggested that light (and space) limitation is likely determining the distribution of *S. horneri* (Caselle et al. 2017; Marks et al. 2020a) and congeners (Thomsen et al. 2006). In our experiment, space limitation is unlikely to explain the difference in growth among different *S. horneri* sizes, as all sizes were simultaneously placed under the same algal canopies and therefore influenced by the same spatial limitations; one caveat is that smaller thalli may need less space than larger thalli. Similar conclusions have been made for the invasive congener, *S. muticum*, where Vaz-Pinto et al. (2012) found that light, not space, significantly impacted recruitment and colonization. Additionally, slow growth of *S. horneri* in low-light stands of conspecific large adults indicates that self-shading may serve as a density-dependence mechanism, as has been previously suggested for this species (Marks et al. 2017), *S. muticum* (Andrew and Viejo 1998; Arenas and Fernández 2000), and other marine macrophytes (Dean et al. 1989; Reed 1990; Schiel 1985;

Schiel and Choat 1980). Taken together, this evidence demonstrates that *S. horneri* may take advantage of points in time and space where light levels are high, such as following loss of the *M. pyrifera* canopy due to winter swell events in southern California (Dayton and Tegner 1984) or during the senescence period in its own annual life cycle, to increase in prevalence and spread.

Our study does not implicate herbivory as a critical force driving invasion success, as herbivores neither avoided the invader nor disproportionately targeted native species. In our study, herbivores effectively removed *S. horneri* across sites that differed in baseline herbivory and algal community structure. Further, small thalli of both *M. pyrifera* and *S. horneri* grew when caged and were consumed when open to herbivory; although herbivores seemed to consume *M. pyrifera* more than *S. horneri*, this difference was not significant. This result contrasts with Marks et al. (2020a) who found that the dominant urchin in our study strongly preferred native kelps (*M. pyrifera* and *E. arborea*) over *S. horneri*. These contrasting results could be due to our study utilizing smaller *S. horneri* thalli (1.36±0.24 SE g: herbivory experiment; 0.82±0.07 SE g: urchin herbivory and site experiment), whereas Marks et al. (2020a) used larger *S. horneri* thalli (7.64±0.34 SE g; Marks et al. 2020b) which may have a partial refuge from herbivory. Davis (2018) found that consumption of the tropical macroalga, *Turbinaria ornata*, decreased as thallus size increased, concluding that alga >2cm may have a refuge from herbivory. More broadly, many primary producers decrease in palatability with age due to factors such as increased toughness and chemical defenses (Briggs et al. 2018; Cronin and Hay 1996). In addition to size, another possible explanation for why *S. horneri* is a successful invader despite being palatable could be that herbivory is not strong enough to control rapid *S. horneri* spread, as has been found for other algal invaders (Britton-Simmons 2004; Chavanich and Harris 2004; Conklin and Smith 2004; Vermeij et al. 2009). Taken together, herbivores may

be able to control small *S. horneri,* particularly if native algae such as *M. pyrifera* are not available, but the strength of this control is likely not enough to limit *S. horneri* spread.

Contrary to our hypothesis, native algal diversity did not seem to determine where *S. horneri* could grow and succeed, at least in our sites on Catalina. In our experiment evaluating the effects of urchin herbivory and site on *S. horneri* growth, growth only differed between caging treatments despite native algal diversity varying among sites. Similar conclusions have been reached for *S. horneri*'s congener invader, *S. muticum*, where shading exerted by the native community was the strongest predictor of invasion success (i.e., settlement, recruitment, survival), regardless of whether the native algal community exhibited high or low species diversity (Vaz-Pinto et al. 2012). It is possible that overall native algal diversity across all of our sites was too low to significantly influence growth. Sites used by Caselle et al. (2017) exhibited pre-invasion (2010-2012) native algal diversity by division levels ranging from ~0.6-0.8 (SBC Marine Biodiversity Observation Network) whereas diversity in our sites ranged from ~0.4-0.6. Further, large canopy-forming foundational algae such as *M. pyrifera* that were abundant in the more diverse sites in Caselle et al (2017) were lacking from our sites during this experiment. Lack of these foundational species may have disproportionately influenced biotic resistance to invasion beyond that captured with diversity measures, as kelp forests generally support greater numbers of predators that consume herbivores, therefore facilitating increased native algal diversity (Caselle et al. 2017; Eriksson et al. 2006; Schiel and Foster 2015). Alternatively, while diversity varied among our sites, it is possible that functional diversity did not differ leading to similar *S. horneri* growth patterns across sites. In this case, functional diversity may be a better indicator of invasion resistance by taking into account how resources are limited by the native

community due to differences in traits, functions, and species identity (Arenas et al. 2006; Dukes 2001; Shea and Chesson 2002).

Understanding mechanisms that facilitate the success of marine invasions is increasingly important as the frequency of marine invasions is projected to rise (Cohen and Carlton 1998; Grosholz 2002; Seebens et al. 2013; Stachowicz et al. 2002). We found that *S. horneri* likely takes advantage of disturbance to the native community as a passenger and herbivory does not provide a strong explanation for invasion success. As disturbances are expected to increase in frequency and intensity with global change (DiLorenzo et al. 2010; Doney et al. 2012; Smale et al. 2019; Carnell and Keough 2020), our results imply that impacted areas may be hotspots for future *S. horneri* spread.

Tables

Table 2-1. Statistical results of ANOVA or PERMANOVA (dependent on data meeting ANOVA assumptions, test used denoted in far-left column). Tests conducted for native algal diversity (A), native algal composition by division (B), urchin density (C), crustose coralline algae (CCA) (D), and percent change in biomass (E). *P*-values lower than alpha=0.05 are statistically significant (denoted in bold).

	Source of Variation	*Df*	*SS*	*MS*	*F*	*P*
A.	**Algal diversity**					
ANOVA	Site	3	0.58	0.19	8.56	**<0.001**
	Residuals	75	1.7	0.02		
B.	**Algal composition**					
PERM-ANOVA	Site	3	4.64	1.55	23.01	**<0.001**
	Residuals	75	5.04	0.07		
C.	**Urchin density**					
ANOVA	Site	3	4.81	1.6	30.11	**<0.01**
	Residuals	4	0.21	0.05		
D.	**CCA**					
ANOVA	Site	3	81.6	27.2	15.58	**<0.001**
	Residuals	72	125.7	1.75		
E.	**Change in biomass**					
ANOVA	Site	3	31.4	10.4	0.56	0.65
	Caged/uncaged	1	563.8	563.8	29.93	**<0.001**
	Site*Caged/uncaged	3	94.9	31.6	1.68	0.18
	Residuals	66	1243.4	18.8		

Table 2-2. Statistical results of ANOVA tests conducted for *Sargassum horneri* change in biomass (A), change in biomass by species and caging treatment (B), and change in surface area by species and caging treatment (C). *P*-values lower than alpha=0.05 are statistically significant (denoted in bold).

	Source of Variation	*Df*	*SS*	*MS*	*F*	*P*
A.	***S. horneri* change in biomass**					
ANOVA	Canopy type	2	508.4	254.18	25.75	**<0.001**
	Stage	2	167.9	83.95	8.51	**<0.001**
	Canopy type*Stage	4	30.1	7.52	0.76	0.55
	Residuals	81	799.5	9.87		
B.	**Change in biomass (herbivory)**					
ANOVA	Species	1	0.0004	0.0004	3.17	0.08
	Caged/uncaged	1	0.0013	0.0013	10.07	**<0.01**
	Species*Caged/uncaged	1	0.0001	0.0001	1.03	0.32
	Residuals	35	0.0045	0.0001		
C.	**Change in surface area (herbivory)**					
ANOVA	Species	1	9.77	9.77	1.45	0.24
	Caged/uncaged	1	30.31	30.31	4.51	**<0.05**
	Species*Caged/uncaged	1	4.74	4.74	0.71	0.41
	Residuals	36	241.92	6.72		

Figure captions

Fig. 2-1. Map displaying study location and sites. Top panel displays general study region in southern California. Bottom panel displays the specific study location and sites around Santa Catalina Island, with sites numbered as follows: 1=Isthmus Point, 2=Isthmus Reef, 3=Chalk Cliffs, 4=Campground, and 5=Bird Rock. The star in the bottom panel denotes the University of Southern California's Wrigley Institute for Environmental Studies (WIES).

Fig. 2-2. Results from site surveys (panels A-D) and an experiment evaluating the effect of site and urchin herbivory on *Sargassum horneri* (panel E). +/- D indicates sites with high or low diversity, respectively, and +/-U indicates sites with high or low urchin densities, respectively. Displays native algal diversity by site (panel A; mean H' m^{-2} ± SE), native algal composition by division and site (panel B; mean % cover m^{-2} ± SE; patterned bars=Rhodophyta, solid bars=Ochrophyta), urchin density by site (panel C; mean number m^{-2} ± SE), crustose coralline algae (CCA) percent cover by site (panel D; mean ± SE), and percent change in biomass of *Sargassum horneri* by site and caging treatment (panel E; mean ± SE; patterned bars=caged replicates, solid bars=uncaged replicates). Bars with different lowercase letters in panels A, B (sites), C, and D are significantly different.

Fig. 2-3. Results from an experiment evaluating the effects of canopy-forming algae on *Sargassum horneri*. Displays *Sargassum horneri* percent change in biomass (g day^{-1}) by canopy type (panel A; mean ± SE; colors represent different *S. horneri* sizes), *S. horneri* percent change

in biomass (g day^{-1}) in relation to light levels (lux) in each canopy type (panel B; colors represent different *S. horneri* sizes, shapes represent different canopy types). Bars with different lowercase letters in panel A are significantly different.

Fig. 2-4. Results from an experiment evaluating the effects of herbivory on *Sargassum horneri* and *Macrocystis pyrifera*. Displays percent change in biomass (panel A) and surface area (panel B) for *M. pyrifera* (purple) and *S. horneri* (dark blue), with hashed bars representing caged replicates and solid bars representing uncaged replicates open to herbivory. Individual bars represent percent change in biomass (g day^{-1}) (mean ± SE) in panel A and percent change in surface area (cm^2 day^{-1}) (mean ± SE).

Figures

Fig. 2-1

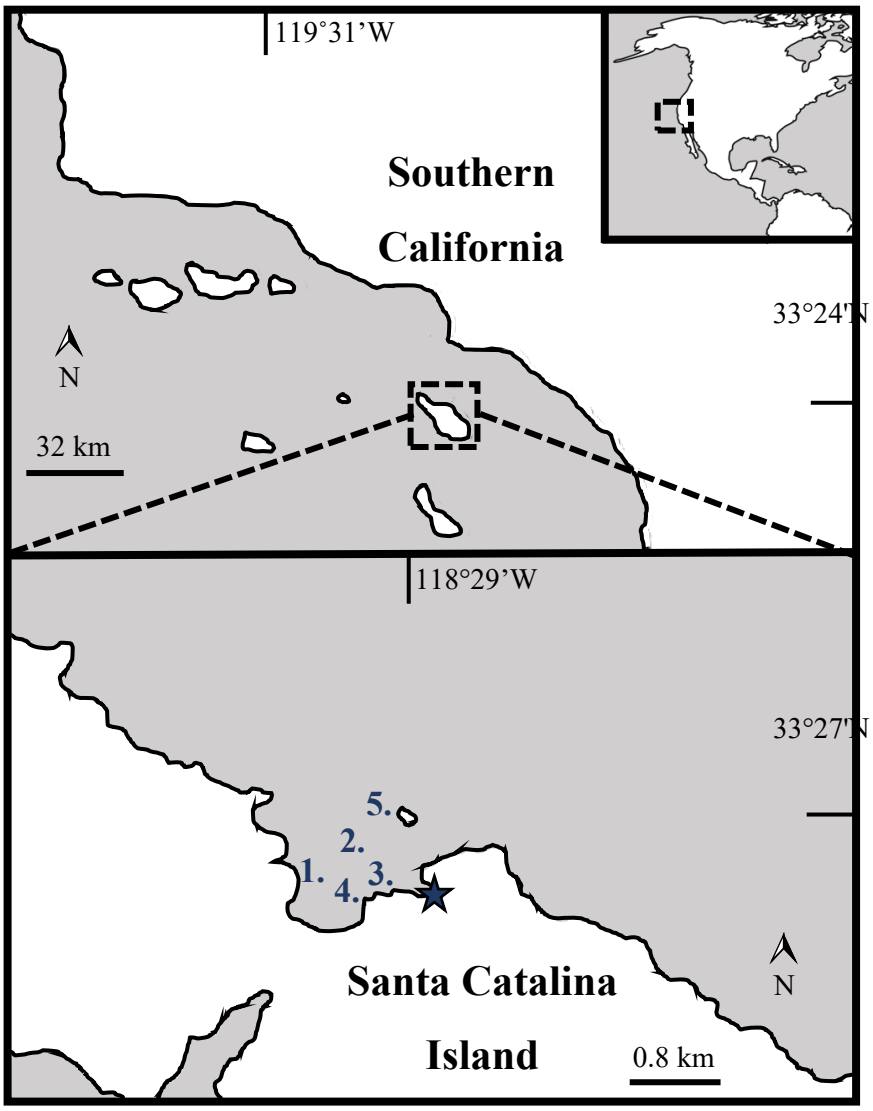

Fig. 2-2

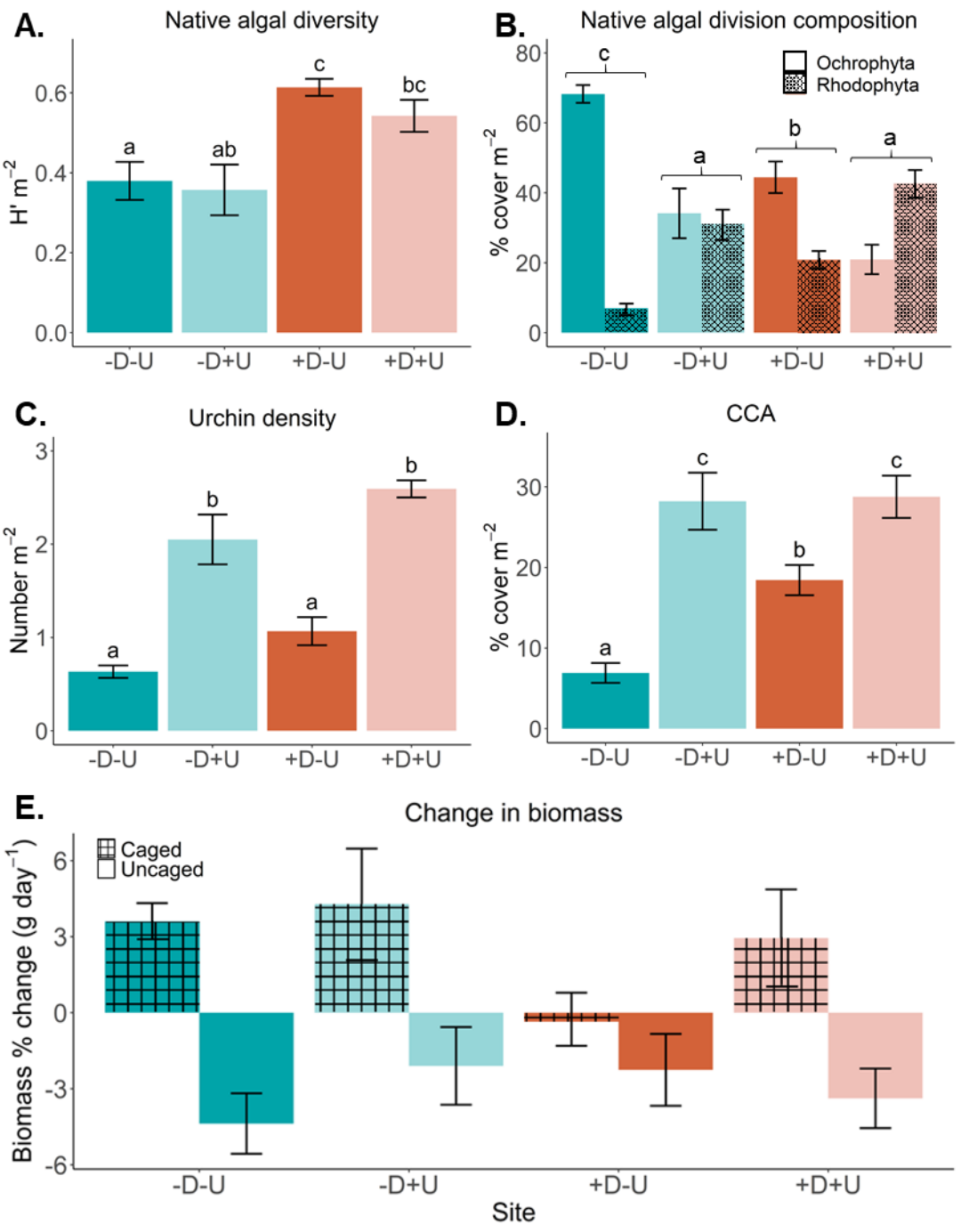
A.
Native algal diversity
H' m^{-2}
0.0
0.2
0.4
0.6
a
ab
c
bc
-D-U
-D+U
+D-U
+D+U
B.
Native algal division composition
% cover m^{-2}
0
20
40
60
80
Ochrophyta
Rhodophyta
c
a
b
a
C.
Urchin density
Number m^{-2}
0
1
2
3
a
b
a
b
D.
CCA
% cover m^{-2}
0
10
20
30
a
c
b
c
E.
Change in biomass
Biomass % change (g day^{-1})
-6
-3
0
3
6
Caged
Uncaged
Site

Fig. 2-3

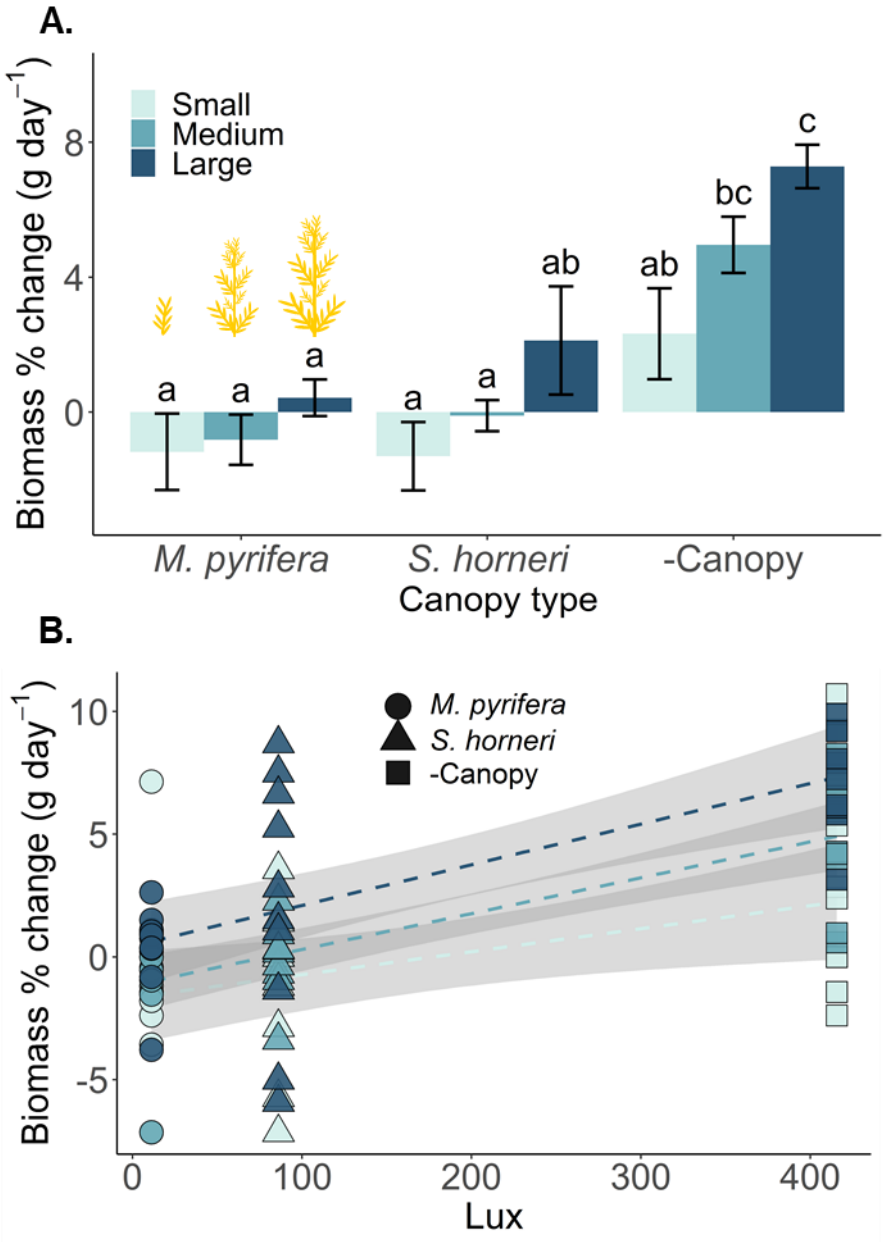
A.
Small
Medium
Large
Biomass % change (g day^{-1})
8
4
0
a
a
a
a
ab
ab
bc
c
M. pyrifera
S. horneri
-Canopy
Canopy type
B.
M. pyrifera
S. horneri
-Canopy
Biomass % change (g day^{-1})
10
5
0
-5
0
100
200
300
400
Lux

Fig. 2-4

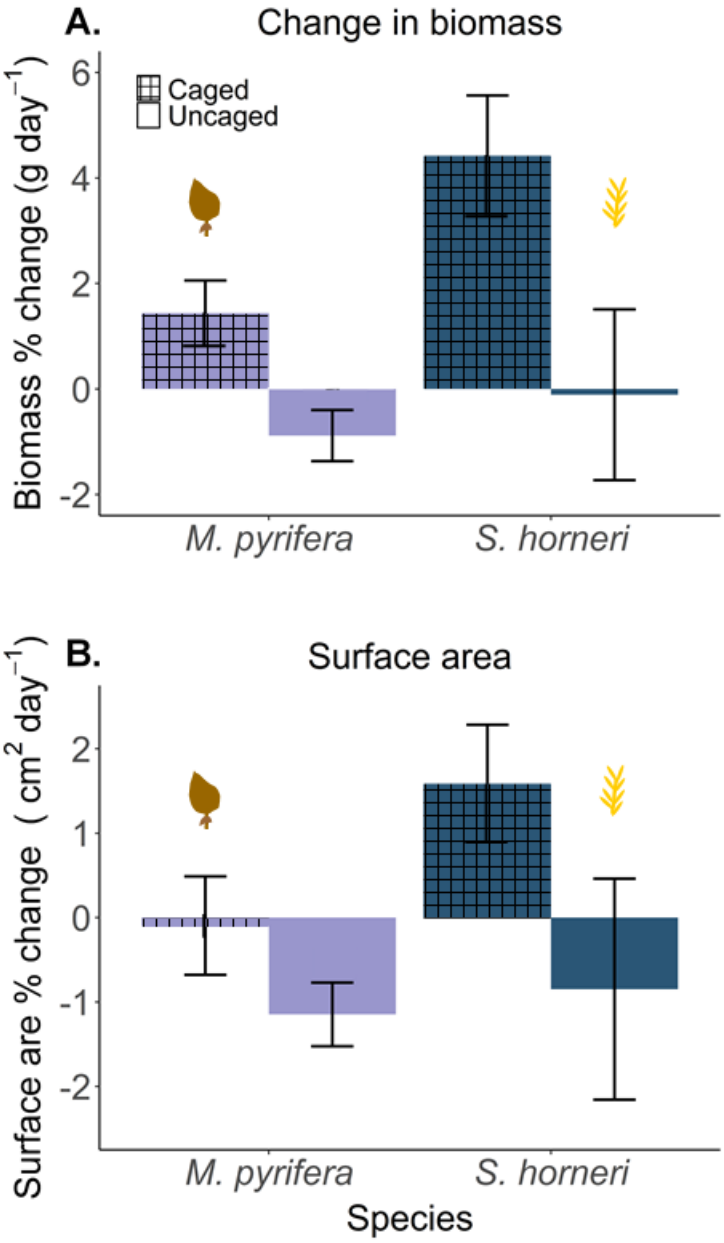
A.
Change in biomass
Caged
Uncaged
Biomass % change (g day^{-1})
6
4
2
0
-2
M. pyrifera
S. horneri
B.
Surface area
Surface are % change (cm^2 day^{-1})
2
1
0
-1
-2
M. pyrifera
S. horneri
Species

References

Aguilar-Rosas, L.E., Aguilar-Rosas, R., Kawai, H., Uwai, S., and Valenzuela-Espinoza, E. 2007. New record of *Sargasssum filicinum* Harvey (Fucales, Phaeophyceae) in the Pacific Coast of Mexico. *Algae* 22: 17-21. doi: 10.4490/ALGAE.2007.22.1.017

Ambrose, R.F. and Nelson, B.V. 1982. Inhibition of giant kelp recruitment by an introduced brown alga. *Botanica Marina* 25: 265-267. doi: 10.1515/botm.1982.25.6.265

Andrew, N.L., and Viejo, R.M. 1998. Ecological limits to the invasion of *Sargassum muticum* in northern Spain. *Aquatic Botany* 60: 251-263. doi: 10.1016/S0304-3770(97)00088-0

Arenas, F., and Fernández, C. 2000. Size structure and dynamics in a population of *Sargassum muticum* (Phaeophyceae). *Journal of Phycology* 36: 1012-1020. doi: 10.1046/j.1529-8817.2000.99235.x

Arenas, F., Sánchez, I., Hawkins, S.J., and Jenkins, S.R. 2006. The invasibility of marine algal assemblages: Role of functional diversity and identity. *Ecology* 87: 2851-61. doi: 10.1890/0012-9658(2006)87[2851:TIOMAA]2.0.CO;2

Balata, D., Piazzi, L., and Cinelli, F. 2004. A comparison among assemblages in areas invaded by *Caulerpa taxifolia* and *C. racemosa* on a subtidal Mediterranean rocky bottom. *Marine Ecology* 25:1–13. doi: 10.1111/j.1439-0485.2004.00013.x

Barry, J.P., and Ehret, M.J. 1993. Diet, food preference, and algal availability for fishes and crabs on intertidal reef communities in southern California. *Environmental Biology of Fishes* 37: 75-95.

Bredvik, J.J., Boerger, C., and Allen, L.G. 2011. Age and growth of two herbivorous, kelp forest fishes, the Opaleye *(Girella nigricans*) and Halfmoon (*Medialuna californiensis*). *Bulletin of the Southern California Academy of Science* 110(1): 25-34. doi: 10.3160/0038-3872-110.1.25

Briggs, C.J., Adam, T.C., Holbrook, S.J., and Schmitt, R.J. 2018. Macroalgae size refuge from herbivory promotes alternative stable states on coral reefs. *PLoS ONE* 13(9): e0202273. doi: 10.1371/journal.pone.0202273

Britton-Simmons, K.H. 2004. Direct and indirect effects of the introduced alga *Sargassum muticum* on benthic, subtidal communities of Washington State, USA. *Marine Ecology Progress Series* 27: 61-78. doi: 10.3354/meps277061

Britton-Simmons, K.H. 2006. Functional group diversity, resource preemption and the genesis of invasion resistance in a community of marine algae. *Oikos* 113: 395-401. doi: 10.1111/j.2006.0030-1299.14203.x

Bulleri, F., Balata, D., Bertocci, I., Tamburello, L., and Benedetti-Cecchi, L. 2010. The seaweed *Caulerpa racemosa* on Mediterranean rocky reefs: from passenger to driver of ecological change. *Ecology* 91: 2205-2212. doi: 10.1890/09-1857.1

Callaway, R.M., and Ridenour, W.M. 2004. Novel weapons: invasive success and the evolution of increased competitive ability. *Frontiers in Ecology and the Environment* 2(8): 436-443. doi: 10.1890/1540-9295(2004)002[0436:NWISAT]2.0.CO;2

Cappuccino, N., and Carpenter, D. 2005. Invasive exotic plants suffer less herbivory than non-invasive exotic plants. *Biology Letters* 1:435–438. doi: 10.1098/rsbl.2005.0341

Carnell, P.E., and Keough, M.J. 2020. More severe disturbance regimes drive the shift of a kelp forest to a sea urchin barren in south-eastern Australia. *Scientific Reports* 10: 11272. doi: 10.1038/s41598-020-67962-y

Carpenter, R.C. 1986. Partitioning herbivory and its effects on coral reef algal communities. *Ecological Monographs* 56:345–363. doi: 10.2307/1942551

Carpenter, R.C. 1990. Mass mortality of *Diadema antillarum*: Long-term effects on sea urchin population dynamics and coral reef algal communities. *Marine Biology* 104: 67 -77.

Caselle, J.E., Davis, K., and Marks, L.M. 2017. Marine management affects the invasion success of a non-native species in a temperate reef system in California, USA. *Ecology Letters* 21:43-53. doi: 10.1111/ele.12869

Cavanaugh, K.C., Reed, D.C., Bell, T.W. Castorani, M.C.N., and Beas-Luna, R. 2019. Spatial variability in the resistance and resilience of giant kelp in Southern and Baja California to a multiyear heatwave. *Frontiers in Marine Science* 6: 413. doi: 10.3389/fmars.2019.00413

Chavanich S., and Harris L.G. 2004. Impact of the non-native macroalga *Codium fragile* (Sur.) Hariot ssp. *tomentosoides* (van Goor) Silva on the native snail *Lacuna vincta* (Montagu, 1803) in the Gulf of Maine. *Veliger* 47:85–90.

Chisholm, J.R.M. and Moulin, P. 2003. Stimulation of nitrogen fixation in refractory organic sediments by *Caulerpa taxifolia*. *Limnology and Oceanography* 48:787–94. doi: 10.4319/lo.2003.48.2.0787

Choi, H.G., Lee, K.H., Yoo, H.I., Kang, P.J., Kim, Y.S., and Nam, K.W. 2008. Physiological differences in the growth of *Sargassum horneri* between germling and adult stages. *Journal of Applied Phycology* 20: 729-735. doi: 10.1007/s10811-007-9281-5

Clark, G.F., and Johnston, E.L. 2011. Temporal change in the diversity-invasibility relationship in the presence of a disturbance regime. *Ecology Letters* 14: 52-57. doi: 10.1111/j.1461-0248.2010.01550.x

Clark, R.P., Edwards, M.S., and Foster, M.S. 2004. Effects of shade from multiple kelp canopies on an understory algal assemblage. *Marine Ecology Progress Series* 267: 107-119. doi: 10.3354/meps267107

Cohen, A.N., and Carlton, J.T. 1998. Accelerating invasion rate in a highly invaded estuary. *Science* 279 (5350): 555-558. doi: 10.1126/science.279.5350.555

Conklin, E.J., and Smith, J.E. 2005. Abundance and spread of the invasive red algae, *Kappaphycus* spp. In Kane'ohe Bay, Hawai'i and an experimental assessment of management options. *Biological Invasions* 7: 1029-1039. doi: 10.1007/s10530-004-3125-x

Connell, J.H. and Slayter, R.O. 1977. Mechanisms of succession in natural communities and their role in community stability and organization. *The American Naturalist* 111(982): 1119–1144.

Cronin, G., and Hay, M.E. 1996. Chemical defenses, protein content, and susceptibility to herbivory of diploid vs. haploid stages of the isomorphic brown alga *Dictyota ciliolate* (Phaeophyta). *Botanica Marina* 39: 395-399. doi: 10.1515/botm.1996.39.1-6.395

Davis, M.A., Grime, D.J.P., and Thompson, K. 2000. Fluctuating resources in plant communities: a general theory of invasibility. *Journal of Ecology* 88: 528-534. doi: 10.1046/j.1365-2745.2000.00473.x

Davis, S.L. 2018. Associational refuge facilitates phase shifts to macroalgae in a coral reef ecosystem. *Ecosphere* 9(5): 2272. doi: 10.1002/ecs2.2272

Dayton, P.K., and Tegner, M.J. 1984. Catastrophic storms, El Niño and patch stability in a southern California kelp community. *Science* 224: 283-285. doi: 10.1126/science.224.4646.283

Dean, T.A., Thies, K., and Lagos, S.L. 1989. Survival of juvenile giant kelp: the effects of demographic factors, competitors, and grazers. *Ecology* 70: 483-495. doi: 10.2307/1937552

Dijkstra, J.A., Harris, L.G., Mello, K., Litterer, A., Wells, C., and Ware, C. 2017. Invasive seaweeds transform habitat structure and increase biodiversity of associated species. *Journal of Ecology* 106(6): 1668-1678. doi: 10.1111/1365-2745.12775

DiLorenzo, E., Cobb, K.M., Furtado, J.C., Schneider, N., Anderson, B.T., Bracco, A., Alexander, M.A., and Vimont, D.J. 2010.Central North Pacific El Niño and decadal climate change in the North Pacific Ocean. *Nature Geoscience* 3: 762-765. doi: :10.1038/NGEO984

Doney, S.C., Ruckelshaus, M., Duffy, J.E., Barry, J.P., Chan, F., English, C.A., Galindo, H.M., … Talley, L.D. 2012. Climate change impacts on marine ecosystems. *Annual*

Review of Marine Science 4: 11-37. doi: 10.1146/annurev-marine-041911-111611

Dukes, J.S. 2001. Biodiversity and invasibility in grassland microcosms. *Oecologia* 126: 563-568. doi: 10.1007/s004420000549

Dumay, O., Fernandez, C., and Pergent, G. 2002a. Primary production and vegetative cycle in *Posidonia oceanica* when in competition with the green algae *Caulerpa taxifolia* and *Caulerpa racemosa*. *Journal of the Marine Biological Association of the United Kingdom* 82:379–87. doi: 10.1017/S0025315402005611

Dunstan, P.K., and Johnson, C.R. 2004. Invasion rates increase with species richness in a marine epibenthic community by two mechanisms. *Oecologia* 138: 285-292. doi: 10.1007/s00442-003-1400-7

Edgar, G.J., Barrett, N.S., Morton, A.J., and Samson, C.R. 2004. Effects of algal canopy clearance on plant, fish, and macroinvertebrate communities on eastern Tasmanian reefs. *Journal of Experimental Marine Biology and Ecology* 312: 67-87. doi: 10.1016/j.jembe.2004.06.005

Edwards, M.S. 2019. Comparing the impacts of four ENSO events on giant kelp (*Macrocystis pyrifera*) in the northeast Pacific Ocean. *Algae* 34(2): 141-151. doi: 10.4490/algae.2019.34.5.4

Elton, C.S. 1958. The ecology of invasions. Methuen, New York. pp. 181.

Eriksson, B.K., Rubach, A., and Hillebrand, H. 2006. Biotic habitat complexity controls species diversity and nutrient effects on net biomass production. *Ecology* 87(1): 246-254. doi: 10.1890/05-0090

Ferrer, E., Garreta, A.G., and Ribera, M.A. 1997. Effect of *Caulerpa taxifolia* on the productivity of two Mediterranean macrophytes. Marine Ecology Progress Series 149:279–87. doi: 10.3354/MEPS149279

Fong, P., Smith, T.B., and Wartian, M.J. (2006). Epiphytic cyanobacteria maintain shifts to macroalgal dominance on coral reefs following ENSO disturbance. *Ecology* 87: 1162-1168. doi: 10.1890/0012-9658(2006)87[1162:ECMSTM]2.0.CO;2

Foster, M.S. 1982b. The regulation of macroalgal associations in kelp forests. In: Srivastava L (ed) Synthetic and degradative processes in marine macrophytes. Walter de Gruyter, Berlin.

Fridley, J., Stachowicz, J., Naeem, S., Sax, D., Seabloom, E., Smith, M., Stohlgren, T.J… Von Holle, B. 2007. The invasion paradox: Reconciling pattern and process in species invasions. *Ecology* 88(1): 3-17. doi: 10.1890/0012-9658(2007)88[3:TIPRPA]2.0.CO;2

Gallardo, B., Clavero, M., Sánchez, M.I., and Vilá, M. 2016. Global ecological impacts of

invasive species in aquatic systems. *Global Change Biology* 22: 151-163. doi: 10.1111/gcb.13004

Ginther, S.C., and Steele, M.A. 2018. Limited recruitment of an ecologically and economically important fish, *Paralabrax clathratus*, to an invasive alga. *Marine Ecology Progress Series* 602: 213-224. doi: 10.3354/meps12673

Godwin, L.S. 2003. Hull fouling of maritime vessels as a pathway for marine species invasions to the Hawaiian Islands. *Biofouling* 19(S1): 123-131. doi: 10.1080/0892701031000061750

Grosholz, E.D. 2002. Ecological and evolutionary consequences of coastal invasions. *Trends in Ecology and Evolution* 17: 22-27. doi: 10.1016/S0169-5347(01)02358-8

Hervé, M. 2020. RVAideMemoire: Testing and Plotting Procedures for Biostatistics. R package version 0.9-78. https://CRAN.R-project.org/package=RVAideMemoire

Inderjit, D.C., Ranelletti, M., and Kaushik, S. 2006. Invasive marine algae: an ecological perspective. *The Botanical Review* 72(2): 153–178.

Kaluza, P., Kolzsch, A., Gastner, M.T., and Blasius, B. 2010. The complex network of global cargo ship movements. *Journal of the Royal Society Interface* 7: 1093-1103. doi: 10.1098/rsif.2009.0495

Kaplanis, N.J., Harris, J.L, and Smith, J.E. 2016. Distribution patterns of the non-native seaweeds *Sargassum horneri* (Turner) C. Agardh and *Undaria pinnatifida* (Harvey) Suringar on the San Diego and Pacific coast of North America. *Aquatic Invasions* 11(2): 111-124. doi: 10.3391/ai.2016.11.2.01

Kaplanis, N.J., Harris, J.L., and Smith, J.E. 2020. A cross-genus comparison of grazing pressure by two native marine herbivores on native, non-native naturalized, and non-native invasive *Sargassum* macroalgae. *Helgoland Marine Research* 74:9. doi:10.1186/s10152-020-00541-w

Keane, R. M., and Crawley, M. J. 2002. Exotic plant invasions and the enemy release hypothesis. *Trends in Ecology and Evolution* 17: 164–170. doi: 10.1016/S0169-5347(02)02499-0

MacDougall, A.S., and Turkington, R. 2005. Are invasive species the drivers or passengers of change in degraded ecosystems? *Ecology* 86: 42-55. doi:10.1890/04-0669

Mächler, E., and Altermatt, F. 2012. Interactions of species traits and environmental disturbance predicts invasion success of aquatic microorganisms. *PLoS ONE* 7(9): e45400. doi: 10.1371/journal.pone.0045400

Marks, L.M., Reed, D.C. and Holbrook, S.J. 2018. Life history traits of the invasive seaweed

Sargassum horneri at Santa Catalina Island, California. *Aquatic Invasions* 13(3): 339-350. doi: 10.3391/ai.2018.13.3.03

Marks, L.M., Reed, D.C., and Holbrook, S.J. 2020a. Niche complementarity and resistance to grazing promote the invasion success of *Sargassum horneri* in North America. *Diversity* 12(2): 54. doi: 10.3390/d12020054

Marks L., Reed, D., and Holbrook, S. SBC LTER: REEF: Data to support ″Niche Complementarity and resistance to grazing promote the invasion success of Sargassum horneri in North America″. Environ. Data Initiat, 2020; doi:10.6073/pasta/2c2237bb3cee86e7c6d9488e8ce2795d.

Marks, L.M., Reed, D.C., and Obaza, A.K. 2017. Assessment of control methods for the invasive seaweed *Sargassum horneri* in California, USA. *Management of Biological Invasions* 8(2): 205–213. doi: 10.3391/mbi.2017.8.2.08

Marks, L.M., Salinas-Ruiz, P., Reed, D.C., Holbrook, S.J., Culver, C.S., Engle, J.M., Kushner, D.J., Caselle, J.E., Freiwald, J., Williams, J.P., Smith, J.R., Aguilar-Rosas, L.E., and Kaplanis, N.J. 2015. Range expansion of a non-native, invasive macroalga *Sargassum horneri* (Turner) C. Agardh, 1820 in the eastern Pacific. *BioInvasions Records* 4(4): 243–248. doi: 10.3391/bir.2015.4.4.02

Mathieson, A. C., Dawes, C.J., Harris, L.G., and Hehre, E.J. 2003. Expansion of the Asiatic green alga *Codium fragile* ssp. *tomentosoides* in the Gulf of Maine. *Rhodora* 105: 1-53.

Miller, K.A., Aguilar-Rosas, L.E., and Pedroche, F.F. 2011. A review of non-native seaweeds from California, USA and Baja California, Mexico (Reseña de algas marinas no nativas de California, EUA y Baja California, México). *Hidrobiológica* 21: 365-379.

Minchinton, T.E.,and Bertness, M.D. 2003. Disturbance-mediated competition and the spread of *Phragmites australis* in a coastal marsh. *Ecological Applications* 13: 1400–1416. doi: 10.1890/02-5136

Moyle, P.B. 1986. Fish introductions into North America: patterns and ecological impact., In: Mooney HA et al. Ecology of Biological Invasions of North America and Hawaii, Springer-Verlag, New York.

Nelson, B.V., and Vance, R.R. 1979. Diel foraging patterns of the sea urchin *Centrostephanus coronatus* as a predator avoidance strategy. *Marine Biology* 51: 251-258. doi: 10.1007/BF00386805

Noé, S., Badalamenti, F., Bonaviri, C., Musco, L., Fernández, T.V., Vizzini, S., and Gianguzza, P. 2018. Food selection of a generalist herbivore exposed to native and alien seaweeds. *Marine Pollution Bulletin* 129(2): 469-473. doi: 10.1016/j.marpolbul.2017.10.015

North, W.J., Jackson, G.A., and Manley, S.L. 1986. *Macrocystis* and its environment, knowns and unknowns. *Aquatic Botany* 26: 9-26. doi: 10.1016/0304-3770(86)90003-3

Oksanen, J., Blanchet, F.G., Friendly, M., Kindt, R., Legendre, P., McGlinn, D., Minchin, P.R.,…Wagner, H. 2019. vegan: Community Ecology Package. R package version 2.5-4. https://CRAN.R-project.org/package=vegan

Papacostas, K.J., Rielly-Carroll, E.W., Georgian, S.E., Long, D.J., Princiotta, S.D., Quattrini, A.M., Reuter, K.E., and Freestone, A.L. 2017. Biological mechanisms of marine invasions. *Marine Ecology Progress Series* 565: 251-268. doi: 10.3354/meps12001

Pederson, M.F., Johnsen, K.L., Halle, L.L., Karling, N.D., and Salo, T. 2016 Enemy release an unlikely explanation for the invasive potential of the brown alga *Sargassum muticum*: experimental results, literature review, and meta-analysis. *Marine Biology* 163: 197. doi: 10.1007/s00227-016-2968-x

Pedersen, M.F., Stæhr, P.A., Wernberg, T., and Thomsen, M.S. 2005. Biomass dynamics of exotic *Sargassum muticum* and native *Halidrys siliquosa* in Limfjorden, Denmark—Implications of species replacements on turnover rates. *Aquatic Botany* 83:31–47. doi: 10.1016/j.aquabot.2005.05.004

Piazzi, L., Ceccherelli, G., and Cinelli, F. 2001. Threat to macroalgal diversity: effects of the introduced green alga *Caulerpa racemosa* in the Mediterranean. *Marine Ecology Progress Series* 210:149–59. doi: 10.3354/meps210149

PISCO, Carr, M., and Caselle, J. 2011. Pisco: Subtidal: Community surveys.

Pulzatto, M.M., Lolis, L.A., Louback-Franco, N., Mormul, R.P. 2018. Herbivory on freshwater macrophytes from the perspective of biological invasions: A systematic review. *Aquatic Ecology* 52: 297-309. doi: 10.1007/s10452-018-9664-5

R Core Team. 2017. R: A language and environment for statistical computing. R Foundation for Statistical Computing, Vienna, Austria. www.r-project.org.

Reed, D.C. 1990. An experimental evaluation of density dependence in a subtidal algal population. *Ecology* 71: 2286-2296. doi: 10.2307/1938639

Reed, D. C., and Foster, M. S. 1984. The effects of canopy shadings on algal recruitment and growth in a giant kelp forest. *Ecology* 65(3): 937-948. doi: 10.2307/1938066

Reed, D.C., Washburn, L., Rassweiler, A., Miller, R., Bell, T., and Harrer, S. 2016. Extreme warming challenges sentinel status of kelp forests as indicators of climate change. *Nature Communications* 7: 13747. doi: 10.1038/ncomms13757

Sánchez, I., and Fernández, C. 2005. Impact of the invasive seaweed *Sargassum muticum* (Phaeophyta) on an intertidal macroalgal assemblage. *Journal of Phycology* 41: 923-30.

doi: 10.1111/j.1529-8817.2005.00120.x

Shea, K., and Chesson, P. 2002. Community ecology theory as a framework for biological invasions. *Trends in Ecology and Evolution* 17(4): 170-176. doi: 10.1016/S0169-5347(02)02495-3

SBC Marine Biodiversity Observation Network, Miller, R.J., Rassweiler, A.R., Caselle, J., Kushner, D., … O'Brien, M. 2020. Santa Barbara Channel Marine BON: Nearshore kelp forest integrated benthic cover, 1980-ongoing. doi: 10.6073/pasta/f4615e14bd95ebbee6696b3ed540b2f0

Schaffelke, B. and Hewitt, C.L. 2007. Impacts of introduced seaweeds. *Botanica Marina* 50: 397–417. doi: 10.1515/BOT.2007.044

Schaffelke B., Smith, J.E., and Hewitt, C.L. 2006. Introduced macroalgae- a growing concern. Journal of Applied Phycology 18:529-41. doi: 10.1007/s10811-006-9074-2

Scheibling, R.E., and Gagnon, P. 2006. Competitive interactions between the invasive green alga *Codium fragile* ssp. *Tomentosoides* and native canopy-forming seaweeds in Novia Scotia (Canada). *Marine Ecology Progress Series* 325: 1-14. doi: 10.3354/meps325001

Schiel, D.R. 1985. Growth, survival, and reproduction of two species of marine algae at different densities in natural stands. *Journal of Ecology* 73: 199-217. doi: 10.2307/2259778

Schiel, D.R., and Choat, J.H. 1980. Effects of density on monospecific stands of marine algae. *Nature* 285: 324-326. doi: 10.1038/285324a0

Schiel, D.R., and Foster, M.S. 2015. *The biology and ecology of giant kelp forests.* University of California Press.

Schmidt, A.L., and Scheibling, R.E. 2006. A comparison of epifauna and epiphytes on native kelps (*Laminaria* species) and an invasive alga (*Codium fragile ssp tomentosoides*) in Nova Scotia, Canada. *Botanica Marina* 49:315–30. doi: 10.1515/BOT.2006.039

Schneider, C. A., Rasband, W. S., and Eliceiri, K. W. 2012. NIH Image to ImageJ: 25 years of image analysis. *Nature methods* 9(7): 671-675 PMID 22930834

Seabloom, E.W., Harpole, W.S., Reichman, O.J., and Tilman, D. 2003. Invasion, competitive dominance, and resource use by exotic and native California grassland species. *Proceedings of the National Academy of Sciences* 100(23): 13384-13389. doi: 10.1073/pnas.1835728100

Seebens, H., Gastner, M.T., and Blasius, B. 2013. The risk of marine bioinvasion caused by global shipping. *Ecology Letters* 16: 782-790. doi: 10.1111/ele.12111

Smale, D.A., Wernberg, T., Oliver, E.C.J., Thomsen, M., Harvey, B.P., Straub, S.C., and Burrows, M.T. 2019. Marine heatwaves threaten global biodiversity and the provision of ecosystem services. *Nature Climate Change* 9: 306-12. doi: 10.1038/s41558-019-0412-1

Smith, J.E., Hunter, C.L., and Smith, C.M. (2010). The effects of top-down versus bottom-up control benthic coral reef community structure. Oecologia, 163, 497-507. doi: 10.1007/s00442-009-1546-z

Sousa, W. P. 1979. Experimental investigation of disturbance and ecological succession in a rocky intertidal algal community. *Ecological Monographs* 49: 227–254. doi: 10.2307/1942484

South, P.M., and Thomsen, M.S. 2016. The ecological role of invading *Undaria pinnatifida*: an experimental test of the driver-passenger models. *Marine Biology* 163: 175. doi: 10.1007/s00227-016-2948-1

Srednick, G.S., and Steele, M.A. 2019. Macroalgal height is more important than species identity in driving differences in the distribution and behavior of fishes. *Marine Ecology Progress Series* 613: 139-149. doi: 10.3354/meps12898

Stachowicz, J.J., Bruno, J.F., Duffy, J.E. 2007. Understanding the effects of marine biodiversity on communities and ecosystems. *Annual Reviews of Ecology, Evolution, and Systematics* 38: 739-766. doi: 10.1146/annurev.ecols ys.38.09120 6.09565 9

Stachowicz, J.J., Terwin, J.R., Whitlatch, R.B., and Osman, R.W. 2002. Linking climate change and biological invasions: Ocean warming facilitates nonindigenous species invasions. *Proceedings of the National Academy of Sciences* 99: 15497-15500. doi: 10.1073/pnas.242437499

Stachowicz, J.J., Whitlatch, R.B., and Osman, R.W. 1999. Species diversity and invasion resistance in a marine ecosystem. *Science* 286: 1577-1579. doi: 10.1126/science.286.5444.1577

Stæhr, P.A., Pedersen, M.F., Thomsen, M.S., Wernberg, T., and Krause-Jensen, D. 2000. Invasion of *Sargassum muticum* in Limfjorden (Denmark) and its possible impact on the indigenous macroalgal community. *Marine Ecology Progress Series* 207:79–88. doi: 10.3354/meps207079

Sullaway, G., and Edwards, M. 2020. Impacts of the non-native alga, *Sargassum horneri*, on benthic community production in a California kelp forest. *Marine Ecology Progress Series* 637: 45-57. doi: 10.3354/meps13231

Sumi, C.B.T., and Scheibling, R.E. 2005. Role of grazing by sea urchins *Strongylocentrotus droebachiensis* in regulating the invasive alga *Codium fragile spp. tomentosoides* in Nova Scotia. *Marine Ecology Progress Series* 292:203–212. doi: 10.3354/meps292203

Thompson, G.A., and Schiel, D.R. 2012. Resistance and facilitation by native algal communities on the invasion success of *Undaria pinnatifida*. *Marine Ecology Progress Series* 468: 95-105. doi: 10.3354/meps09995

Thomsen, M.S., Wernberg, T., Stær, P.A., and Pederson, M.F. 2006. Spatio-temporal distribution patterns of the invasive macroalga *Sargassum muticum* within a Danish *Sargassum*-bed. *Helgoland Marine Research* 60: 50-58. doi: 10.1007/s10152-005-0016-1

Trowbridge C.D. 2001. Coexistence of introduced and native congeneric algae: *Codium fragile* and *Codium fragile* spp. *tomentosoides* on Irish rocky intertidal shores. *Journal of the Marine Biological Association of the United Kingdom* 81: 931–937. doi: 10.1017/S0025315401004854

Valentine, J.P., and Johnson, C.R. 2003. Establishment of the introduced kelp *Undaria pinnatifida* in Tasmania depends on disturbance to native algal assemblages. *Journal of Experimental Marine Biology and Ecology* 295: 63-90. doi: 10.1016/S0022-0981(03)00272-7

Van Kleunen, M., Weber, E., and Fischer, M. 2010. A meta-analysis of trait differences between invasive and non-invasive plant species. *Ecology Letters* 13: 235-245. doi: 10.1111/j.1461-0248.2009.01418.x

Vaz-Pinto, F., Martínez, B., Olabarria, C., and Arenas, F. 2014. Neighborhood competition in coexisting species: The native *Cystoseira humilis* vs. the invasive *Sargassum muticum*. *Journal of Experimental Marine Biology and Ecology* 454: 32-41. doi: 10.1016/j.jembe.2014.02.001

Vaz-Pinto, F., Olabarria, C., and Arenas, F. 2012. Propagule pressure and functional diversity: interactive effects on a macroalgal invasion process. *Marine Ecology Progress Series* 471: 51-60. doi: 10.3354/meps10024

Vermeij, M.J.A., Smith, T.B., Dailer, M.L., and Smith, C.M. 2009. Release from native herbivores facilitates the persistence of invasive marine algae: a biogeographical comparison of the relative contribution of nutrients and herbivory to invasion success. *Biological Invasions* 11: 1463-1474. doi: 10.1007/s10530-008-9354-7

Villéger, S., Mason, N.W.H., and Mouillot, D. 2008. New multidimensional functional diversity indices for a multifaceted framework in functional ecology. *Ecology* 89: 2290-2301. doi: 10.1890/07-1206.1

Williams, S.L. and Grosholz, E.D. 2002. Preliminary reports from the *Caulerpa taxifolia* invasion in southern California. *Marine Ecology Progress Series* 233: 307–310

Williams, S.L. and Smith, J.E. 2007. A Global Review of the Distribution, Taxonomy, and Impacts of Introduced Seaweeds. *Annual Review of Ecology, Evolution, and Systematics* 38(1): 327–359. doi: 10.1146/annurev.ecolsys.38.091206.095543

York, P.H., Booth, D.J., Glasby, T.M., and Pease, B.C. 2006. Fish assemblages in habitats dominated by *Caulerpa taxifolia* and native seagrasses in south-eastern Australia. *Marine Ecology Progress Series* 312:223–34. doi: 10.3354/meps312223

Yoshida, T. 1983. Japanese species of *Sargassum* subgenus *Bactrophycus* (Phaeophyta, Fucales). *Journal of the Faculty of Science Hokkaido University Series V (Botany)* 13: 99-246.

CHAPTER 3

A simulation model demonstrates life history and abiotic factors mediate competition between a perennial foundational alga, giant kelp, and an annual invasive alga

Abstract

Species invasions cause a cascade of impacts, including losses of biodiversity, ecosystem functioning, and services. Invasions that replace foundation species, such as kelp (*Macrocystis pyrifera)*, are particularly concerning as declines of these critical foundation species can result in widespread community loss. *Sargassum horneri* is an annual marine macroalga that invaded Californian coastal habitats, including perennial kelp forests, beginning in 2003. However, little is known about factors facilitating *S. horneri*'s invasion success, such as whether abiotic drivers influence population dynamics or how the invasive may be interacting with native kelp. To address these gaps, we developed stage-structured population models for kelp and *S. horneri* driven by light and temperature, and then combined these models to evaluate species interactions. To calibrate our single-species models, we compared model predictions to empirical field data and found predictions aligned closely with observed dynamics. To evaluate the role of intra- vs. interspecific interactions in invasion success, we compared predictions of the combined and single-species models. We found that the population structure of both species was strongly influenced by intraspecific and interspecific competition for light, with larger stages limiting recruitment. Further, when species initially coexisted as dense populations, kelp drove *S. horneri* to local extinction while *S. horneri* influenced the timing and intensity of kelp recruitment. Finally, to evaluate if each species could "invade" mature stands of the opposite species, we simulated recruitment at different levels of interspecific competition and assessed population trajectories. *S. horneri* could not invade kelp forests during peak recruitment months, but

persisted longer when invasion preceded periods with minimal densities of large kelp. In contrast, kelp can recolonize only when large *S. horneri* stages were sparse and competition for light was low, but then could drive *S. horneri* to local extinction. Our results suggest that light, temperature, and intraspecific competition structure *S. horneri* populations. Further, kelp and *S. horneri* interactions are controlled by their life histories, with kelp dominance and reestablishment facilitated by continuous reproduction and perennial persistence, and *S. horneri* invasion success and resistance to kelp reestablishment limited by seasonal reproduction and annual senescence. Taken together, our results imply that invasion of *S. horneri* is dependent on disturbances that remove the dominant kelp.

Introduction

Invasive species are a leading cause of global loss of biodiversity as well as ecosystem functioning and associated services, motivating much research into invasion causes and consequences (e.g., Hooper et al. 2005; Inderjit et al. 2006; Katsanevakis et al. 2014; Simberloff et al. 2013; Tait et al. 2015). However, marine invasions, particularly marine algal invasions, are understudied (Chan and Briski 2017; Inderjit et al. 2006; Papacostas et al. 2017; Williams and Smith 2007), despite evidence that algal invaders can impact native community structure (Balata et al. 2004; Sánchez and Fernández 2005), biomass (Mathieson et al. 2003; Trowbridge 2001), and functioning (Chisholm and Moulin 2003; Dumay et al. 2002a). Invasions into marine systems have accelerated over the last few decades (Bax et al. 2003; Rilov and Crooks 2009) and are predicted to continue increasing with global change (Grosholz 2002; Seebens et al. 2013; Stachowicz et al. 2002). Therefore, there is an urgent need to identify mechanisms facilitating invasion success and resistance, as well as to understand the resilience of native ecosystems.

Modeling approaches can provide a powerful tool to advance our understanding of algal invasion mechanisms, as empirical studies are rare and those that do exist have several limitations. Studies investigating invasion mechanisms for marine algae tend to be limited in scope, for example, by only focusing on short-term invasion trajectories (Britton-Simmons and Abbott 2008), "case-studies" of the occurrence and spread of one species (Valentine and Johnson 2007), or one aspect of the invasion process (e.g., establishment vs. persistence) (Melbourne et al. 2007). Such studies are also limited by ethical considerations, as activities such as experimentally simulating invasion or manipulating the native community to assess biotic resistance may not be permitted (California Code of Regulations), and if they are, may cause more harm than good (Kettenring and Adams 2011). Modeling approaches help bypass some of these limitations by allowing the simultaneous investigation of species invasions across multiple interacting factors, time scales, and scenarios. For example, use of a field-parameterized model enabled longer-term explorations of establishment and spread of the invasive alga, *Sargassum muticum*, compared to shorter-term field experiments (Britton-Simmons and Abbott 2008). Further, model results revealed different long-term effects of disturbance on invasion success that would have been missed if the researchers only focused on short-term experimental patterns. Here we use stage-structured population models to evaluate factors influencing invasive establishment and persistence as well as native resistance and recovery over long timescales.

Intra- and interspecific competition are major structuring forces for algal populations (*for reviews*, *see* Edwards and Connell 2012, Olson and Lubchenco 1990) and strong determinants of invasive success (Vaz-Pinto et al. 2014) that are often mediated by size-structured access to resources. Although space and nutrients are important for marine algae, light is considered the primary limiting resource for algal growth, survival, and reproduction (Arenas et al. 2002;

Edwards and Connell 2012; Steneck et al. 2002). Access to light can be facilitated by morphological traits such as thallus size, height, and/or overall biomass, as well as physiological traits such as rapid growth to a large size (Carpenter 1990; Edwards and Connell 2012; Olson and Lubchenco 1990; Paine 1990; Vaz-Pinto et al. 2014). Within algal populations, self-thinning that occurs as thalli increase in density and/or size and light becomes limited has been found to be an important density-dependent process (Andrew and Viejo 1998; Creed et al. 1998; Reed and Foster 1984). Between populations, algal species with traits that allow them to access more light and reduce its availability to competitors will likely dominate. Therefore, the probability of invasion success may be greater if the algal invaders are able to exploit light more completely and efficiently than native species via size-related traits.

Differences in life history traits, such as longevity and reproduction, can also determine the outcome of competition by mediating resource acquisition strategies (Bonsall et al. 2004; Lancaster 2016) and these differences can vary greatly among algal species. For example, annual species are generally short-lived as they die-back every year, guaranteeing that held resources will be released during the senescent period (Corbin and D'Antonio 2004). This contrasts with perennial species that can persist and potentially dominate for multiple years (Olson and Lubchenco 1990). Further, the ability to reproduce year-round allows a species to take advantage of times when resources are plentiful and the probability of survival is high, whereas species with seasonal reproduction may not be able to do so, consequently constraining their ability to establish (Friedman 2020; Reed 1996). Therefore, the strength of competition may vary between interacting invasive and native algal populations with different life history strategies depending on which stages are present and how resources are being utilized, thereby influencing temporal outcomes of invasive success and biotic resistance.

One of the most recent and least understood invasions in California is of the brown alga, *Sargassum horneri*. Native to east Asia, *S. horneri* was first detected in southern California in 2003 and has since spread throughout the region and into Baja California, Mexico (Kaplanis et al. 2016; Marks et al. 2015). *S. horneri* exhibits many "invasive" traits (Valentine and Johnson 2007), including high fecundity, rapid growth, wide environmental tolerance, self-fertilization, and long-range dispersal via gas-bladders (Choi et al. 2003; Kaplanis et al. 2016; Marks et al. 2015). Further, *S. horneri* displays an obligate annual life history (Marks et al. 2018), with patterns of growth and maturation correlated with light and temperature in its native range (Choi et al. 2007; Choi et al. 2020; Mikami et al. 2006; Yoshida et al. 2001). In southern California, small stages prevalent in summer rapidly grow into larger, mature thalli in fall and winter that can reach up to 3m in height (Marks et al. 2018). Reproduction occurs in spring followed by senescence and recruitment (Marks et al. 2018; Marks et al. 2020a). The few studies that exist of *S. horneri* interactions with native species speculate that *S. horneri* requires open niches to invade due to competitive inferiority (Caselle et al. 2017; Marks et al. 2020a; Sullaway and Edwards 2020). However, once established, *S. horneri* can form dense monocultures with shaded understories that may potentially outcompete smaller native species for light. Therefore, developing a model that incorporates *S. horneri* seasonality and population structure as well as interactions with native species may deepen our understanding of drivers of invasion success and resistance.

Some habitats historically dominated by the brown alga, *Macrocystis pyrifera*, or giant kelp, have become heavily invaded by *S. horneri*. *M. pyrifera* is a well-studied coastal foundation species that supports diverse species assemblages through the complex "forest" it creates (Ambrose and Nelson 1982; Dayton and Parnell 1992; Gaitán-Espitia et al. 2014; Steneck

et al. 2002). *M. pyrifera* can rapidly grow up to 40m in height and form a dense surface canopy that can reduce bottom light availability by up to 99% (Foster 1975; Gerard 1984a). This light reduction generally limits the recruitment and survival of understory algae, including conspecifics, to areas where the canopy has been cleared (Clark et al. 2004; Reed and Foster 1984; Schiel and Foster 2015). Further, *M. pyrifera* populations may persist for multiple years via a perennial life history and year-round reproduction. Based on these traits, it has been assumed that *M. pyrifera* is the competitive dominant once established (Edwards and Connell 2012; Olson and Lubchenco 1990). However, *M. pyrifera* requires ample light, high nutrients, and cool temperatures to recruit, grow, and survive (Deysher and Dean 1986; Reed et al. 2016), and deviations from optimal conditions can impact *M. pyrifera* population structure. For example, a seminal *M. pyrifera* stage-structured model illustrated that seasonal temperatures and intraspecific competition for light dictated recruitment and subsequent population structure (Burgman and Gerard 1990). Despite significant overlap in resource requirements, whether interactions between *S. horneri* and *M. pyrifera* influence the long-term invasion success of *S. horneri* and recovery of *M. pyrifera* has yet to be investigated.

We developed stage-structured population models to evaluate how abiotic drivers and size-structured competition for light influence the population dynamics and persistence of *S. horneri* and *M. pyrifera*. Specifically, we investigated three questions: 1) Can a model that incorporates relationships between abiotic drivers (temperature and light) and *S. horneri* demographic processes (growth, survival, and reproduction) predict field population dynamics? 2) How do intra- vs. interspecific interactions govern the dynamics of *S. horneri* and *M. pyrifera* population structure where these species co-occur? and 3) Can each species "invade" mature stands of the opposite species?

Methods

To address these questions, we developed population-level matrix models for each species that incorporate intraspecific interactions and environmental drivers. Our single-species *M. pyrifera* model was based on a previous stage-structured model of *M. pyrifera* (Burgman and Gerard 1990). The single-species *S. horneri* model was developed *de novo* but with a similar structure as the single-species *M. pyrifera* model. We then tested the predictions of the single-species models by comparing them to the data used to build each model. To model interspecific interactions, we combined the single-species matrix models and compared the output for the combined model to the single-species models. Finally, we ran several simulations to evaluate the invasion success of *S. horneri* into an established *M. pyrifera* forest, and the recovery potential of *M. pyrifera* into an existing dense stand of *S. horneri*.

Single-species population models (intraspecific interactions): Overall approach

We utilized a matrix population model framework originally developed by Leslie (1945) to project population changes over time. Each population is stage-structured by height (and biomass for *S. horneri*), with each stage representing a state variable. Simulations are deterministic and in discrete time with a monthly timestep. All simulations were run using R Statistical Software (R Core Team 2017). We made two central assumptions in developing these models: 1) light is the limiting resource, and 2) space is not limiting. Thus, we included a function that reduces the amount of available light at the sea floor as each population increases in height and density, but did not explicitly incorporate space into the model. We also did not explicitly partition out the effects of herbivory or other species-species interactions, but these effects are incorporated implicitly in the transition and survival parameters for each species, as

parameters were estimated from field data in southern California (Burgman and Gerard 1990; SBC LTER et al. 2018).

Single-species population models (intraspecific interactions): Model adaptation for M. pyrifera

The single-species *M. pyrifera* population model, adapted from Burgman and Gerard (1990), specifies five life-history stages: gametophytes (microscopic), recruit sporophytes (<2cm), blade-stage sporophytes (2-100cm), subadult sporophytes (100cm-10m), and adult sporophytes (>10m; ≥5 canopy fronds) (Fig. 3-1A). The original model includes five size subclasses within each immature sporophyte stage (recruit, blade-stage, subadult) that we did not include in our model for simplicity. Adult sporophytes are divided into five subclasses, with the subclasses 5-9 distinguished as having 5-9 canopy fronds, respectively, that are used to calculate canopy density. Therefore, the single-species *M. pyrifera* model is comprised of nine stages (state variables). *M. pyrifera* exhibits a perennial life cycle where individuals are capable of persisting for multiple years (Ladah and Zertuche-González 2007). In the model we assumed that adults are the only stage capable of reproducing and that reproduction can occur throughout the year if particular criteria are met (see below; Burgman and Gerard 1990; Anderson and North 1967; Reed et al. 1988). Therefore, all stages of *M. pyrifera* may co-occur at any given point in time.

The state of the population at time *t* is represented by the population vector, *N(t)*, which includes the monthly densities (# individuals m^{-2}) of each life history stage (Fig. 3-1B). The stage densities in the next month are calculated by multiplying the population at time *t* by the transition matrix, *M*, as in Eq. 1:

$$N(t+1) = MN(t) \quad (1)$$

Monthly mean survival probabilities for recruit sporophytes, blade-stage sporophytes, and subadult sporophytes (X_{P22}, X_{P33}, X_{P44}, respectively) are constants (Table 3-1), while adult survival probabilities (X_{P55}) fluctuate monthly (Fig. 3-2A) (Burgman and Gerard 1990) but are consistent across adult subclasses. As the adult spore production rate, b_p, is difficult to estimate in the field (Burgman and Gerard 1990), the mean density of female gametophytes is specified as an extrinsic input each month (Fig. 3-2B). Adult survival and gametophyte density were adapted from Burgman and Gerard (1990), who parameterized their model from data collected in a southern California kelp population (Dean et al. 1989; Anderson and North 1966; Anderson and North 1967; Reed et al. 1988).

Growth (G_{ji}), or the probability that an individual in one stage (*i)* will survive and transition to the next stage (*j*) each month, depends on monthly mean values of light reaching each stage (see below) and on temperature at the sea floor, or 'bottom temperature'. The transition between the gametophyte and recruit sporophyte stage (G_{P21}) represents recruitment, or the addition of individual sporophyte thalli to the population, and is defined as the number of gametes produced by female gametophytes that are fertilized and develop into recruit sporophytes (Burgman and Gerard 1990). In the model, recruitment occurs only during "recruitment windows", or periods where bottom temperatures are ≤16.3˚C and bottom light levels are ≥0.7 mol photons $m^{-2}d^{-1}$) (Table 3-1, Eq. 2) as empirically determined *in situ* by Deysher and Dean (1986). Outside of these recruitment windows, G_{P21}=0.

Transitions between immature sporophyte stages (recruit, blade-stage, subadult) in relation to light were empirically determined *in situ* by Dean and Jacobsen (1984) and fitted with von Bertalanffy growth equations (Table 3-1, Eq. 3-4). The maximum potential growth rate ($Gmax_i$) is a function of the median thallus size (S_i) for each stage *i*. The realized growth rate

(G_{ji}) is a function of $Gmax_i$, the immature sporophyte growth coefficient (k), the growth-compensation light level (C_i), which is the level of light at which zero growth occurs for each stage, and the amount of available light reaching each stage (L_{Ri}). C_i and k are specified as constants for all immature stages but are modified along with $Gmax_i$ under various bottom temperature scenarios (Table 3-1, Eq. 5). Thus, as bottom temperature increases in the model, immature sporophytes generally require more light for growth and growth slows overall as specified by Dean and Jacobsen (1984).

Finally, adult growth from one subclass to the next (A_{Pij}) occurs via the accumulation or loss of canopy fronds (fronds reaching the surface) in relation to surface temperature (Table 3-1, Eq. 6-7), as specified by Burgman and Gerard (1990). Adult growth assumes a fixed rate of frond growth, but frond loss increases with increasing surface temperature and density of canopy fronds. Adult sporophytes are divided into five subclasses, numbered 5-9 because they have 5-9 canopy fronds, respectively. The total number of canopy fronds m^{-2} (D) is calculated by multiplying the number of canopy fronds for each adult subclass by the density of individuals in that subclass and summing the products (Table 3-1, Eq. 8).

Because transition probabilities cannot exceed 1, growth parameters were interpreted as rates and converted to probabilities equal to $1\text{-}e^{-G}$. However, the gametophyte stage is capable of producing more than one zygote (Reed et al. 1991) so the transition from gametophyte to the recruit sporophyte stage (G_{P21}) was not transformed in this way.

Intraspecific competition for light is incorporated into the model (Fig. 3-3A) by calculating the shading parameter, or the proportion of light (P_{Li}) that remains available after passing through stage i. For immature sporophytes (recruit, blade-stage, and subadult), P_{Li} is a function of the density of individuals in that stage (N_i) and the median size (S_i) of that stage

(Table 3-1, Eq. 9). For adult sporophytes, P_{Li} is a function of canopy density, D (Table 3-1, Eq. 10). To calculate the amount of available light reaching each stage (L_{Ri}), the total amount of available bottom light (L) (Fig. 3-2C) is multiplied by the shading parameter (P_{Li}) of larger stages and stages of the same size (Table 3-1, Eq. 11). Thus, the total amount of available bottom light decays as *M. pyrifera* gets larger (with more canopy fronds) and/or more abundant, with the smallest size classes receiving the least amount of light (Fig. 3-3A).

Single-species population models (intraspecific interactions): Model development for S. horneri

The single-species model for *S. horneri* utilizes a similar structure as for *M. pyrifera*, but modified for *S. horneri*'s life history (Fig. 3-1C). Adapted from height and biomass data collected by SBC LTER et al. (2018) (see Appendix 3-S1 for methods), we classified five stages: 1) recruits (≤5cm), 2) immature (5-280cm; lacking receptacles), 3) stage I adult (5-280cm; receptacles present, lacking embryos), 4) stage II adult (5-300cm; with embryo-bearing receptacles), and 5) senescent (5-220cm). We did not include a gametophyte stage for *S. horneri* because it exhibits a diplontic life cycle whereas *M. pyrifera* exhibits a haplodiplontic life cycle that alternates between multicellular gametophyte and sporophyte stages. These stages serve as state variables in the matrix model (Fig. 3-1D), where stage densities in the next month are calculated with M and the population vector ($N(t)$) using Eq. 1 above. While the immature stage, stage I adults, and stage II adults generally fall within the same height range, each stage has higher biomass than the previous (SBC LTER et al. 2018), which influences the shading coefficient that each stage exerts (see below).

Differences between the life histories of *S. horneri* and *M. pyrifera* required several modifications to our modeling approach. *S. horneri* exhibits a highly seasonal, annual life cycle (Marks et al. 2018; Choi et al. 2020; Ang and De Wreede 1990) where certain stages and life-

history events (e.g., reproduction, senescence, recruitment) only occur during certain months. Specifically, Ang and De Wreede (1990) generalize the life history of *Sargassum* into three 4-month phases: 1) fast growth (FG), 2) reproduction, senescence, recruitment (RSR), and 3) slow growth (SG) (Table 3-2; for more details, see Appendix 3-S2). They then utilize field data that they divided into these phases to parameterize a stage-structured model for a congener. This resulted in six 2-month transition matrices per year with two matrices per every 4-month phase (FG, RSR, SG). We followed this method by defining FG, RSR, and SG phases for *S. horneri* and estimating different growth (G_{ji}), survival (X_{ii}), and recruitment (b_S) parameters (Fig. 3-1D) for two matrices for each of these phases using field data.

To parameterize the matrix *M* (Fig. 3-1D) using field data collected by SBC LTER et al. (2018), we calculated mean monthly stage densities across all sites and years (Table 3-2). As data were lacking for July, August, October, and November, we plotted monthly data and interpolated between known values to estimate data for missing months. We then divided the data into three 4-month FG, RSR, and SG phases (as in Ang and De Wreede (1990); Table 3-2). As in the prior study (Ang and De Wreede 1990), 2-month periods fit field data better than the coarser subdivision of four months, so we used 2-month periods (two per FG, RSR, and SG phase) to estimate six 2-month transition matrices per year. To do so, we utilized the quadratic programming method as described by Wood et al. (1997) and Caswell (2001, section 6.2.2.) to estimate transition probabilities with unique values of G_{ji}, X_{ii}, and b_S from these data for each of the six matrices (see Appendix 3-S2 for details).

To follow parallel construction with the single-species *M. pyrifera* model, we then used growth values estimated via quadratic programming to establish growth thresholds with temperature and light. For temperature, we plotted monthly values of G_{ji} estimated via quadratic

programming for immature (G_{S32}) and stage I (G_{S43}) adult *S. horneri* and monthly mean bottom temperature values from Fig. 3-2D (values collected within the depth and regional range of the *S. horneri* field data) (Fig. 3-4A, B). Then, we determined temperature intervals where growth was similar and established generalized temperature/growth thresholds (Table 3-3, Eq. 13-14), adjusting some values estimated via quadratic programming to produce output that better fit the field data. Growth between the recruit and immature stages (G_{S21}) showed no consistent correlation with temperature (See Appendix 3-S3), therefore we used adjusted G_{S21} values from quadratic programming to achieve single-species and combined model outputs (see below) that align with observations in the field (Bell et al., unpublished data). G_{S21} values cycle yearly according to Fig. 3-4C. Further, the transition between stage II adults and the senescent stage is more likely due to decay following reproduction (Marks et al. 2018) than abiotic factors, so we set G_{S54} to cycle consistently throughout the year based on estimations from quadratic programming (Fig. 3-4C).

To incorporate similar thresholds with light as in the single-species *M. pyrifera* model, we estimated the growth-compensation light level (C_i) for each *S. horneri* stage using linear regression equations (see Appendix 3-S4) derived from field data in southern California by calculating the light level at which growth ceased (y=0). Therefore, if the light reaching each *S. horneri* stage was at or below that stage's growth-compensation light level, then G_{ji}=0 (Table 3-2, eq. 12-14). Finally, monthly survival probabilities for all stages (X_{S11}, X_{S22}, X_{S33}, X_{S44}, X_{S55}) and recruitment (b_s) were estimated via quadratic programming, and cycle consistently throughout the year (Fig. 3-4C, D, respectively).

We incorporated intraspecific competition for light in the single-species *S. horneri* model (Fig. 3-3B) using the *M. pyrifera* immature sporophyte shading equation to simulate *S.*

horneri shading. We assumed senescent, decaying stages would not significantly contribute to shading as they wither and lose their blades. Therefore, we did not include this stage in competition for light. Each *S. horneri* stage (recruit, immature, stage I adult, stage II adult) has a shading effect (P_{Li}) that is influenced by the density (N_i) and median size of that stage (S_i) (Table 3-3, Eq. 15-18). Further, we modified the coefficient in each equation to match shading exerted by each stage in the field (Ryznar et al., unpublished data; Marks et al. 2020a). The total amount of available bottom light, L, is reduced via shading from larger stages and stages of the same size.

Single-species population models (intraspecific interactions): Output and calibration

The standard input for the single-species *M. pyrifera* model starts in January and utilizes the same initial conditions specified by Burgman and Gerard (1990) (Table 3-1). Further, parameters governing adult survival, gametophyte density, temperature, and light cycle consistently throughout the year (Fig. 3-2). In the original model, Burgman and Gerard (1990) omit the first two years of simulation to allow dynamics to stabilize before graphing the output. We followed this protocol in our simulations by running the model for 84 months (seven years) but only graphing the output for the last 60 months (five years).

Using base functions and the *ggplot2* package (Wickham 2016) in R, we calculated density m^{-2} over time and plotted these trajectories over five years (years 3-7) for each stage. We also plotted the density of recruit sporophytes to visualize recruitment intensity and frequency in relation to bottom light (mol photons m^{-2} day^{-1}) over time, as recruitment has been shown to be especially important for populations of *M. pyrifera* (Deysher and Dean 1986; Burgman and Gerard 1990). We also identified ‘recruitment windows’, or periods in the model when

environmental conditions were suitable for recruitment, i.e., when bottom light was >0.7 mol photons m^{-2} day^{-1} and bottom temperatures where ≤16.3˚C.

To test whether our single-species *M. pyrifera* model adequately recreated the original model, we compared our deterministic model output with Burgman and Gerard's (1990) deterministic model output for adult and canopy density. We also compared our deterministic model output to their stochastic model output of recruit, blade-stage, subadult, adult sporophyte, and canopy density (see Appendix 3-S5).

The standard input for the single-species *S. horneri* model starts in January and utilizes the mean January densities for each stage from the SBC LTER et al. (2018) data as initial conditions in the model (Table 3-3). Parameters governing survival, recruitment, and the transitions from recruit to immature and stage II adult to senescent cycle consistently throughout the year (Fig. 3-4C, D) along with the same environmental inputs (temperature and light) as in the single-species *M. pyrifera* model (Fig. 3-2C, D). This is reasonable because light and temperature data in the original *M. pyrifera* model were collected in southern California within the depth range of where the *S. horneri* survey data were collected. We ran the model for seven years and plotted stage densities over five years as above.

To assess the goodness-of-fit between the single-species *S. horneri* model and the field data upon which it was built, we compared our model output for all stage densities over time with the mean monthly stage densities from the original field data collected by SBC LTER et al. (2018).

Combined population models (intra- and interspecific interactions): Model development

To evaluate interspecific interactions between *M. pyrifera* and *S. horneri*, we developed an expanded model that combined the single-species *M. pyrifera* and *S. horneri* models above.

Through combining the single-species models, we developed a new transition matrix (M) and population vector ($N(t)$) (Fig. 3-1E) and calculated stage densities in the next month following Eq. 1. We incorporated interspecific competition for light in the same manner as for each single-species model, where the total amount of available light (L) was multiplied by the shading effect (P_{Li}) of larger stages and stages of the same size of the same species and of the opposite species (Fig. 3-3C). In this scenario, *M. pyrifera* adults receive the greatest amount of light because they are the tallest, and *M. pyrifera* recruit sporophytes receive the least as the smallest stage in both populations.

Combined population models (intra- and interspecific interactions): Model output and analysis

Stage densities over time for both species, as well as *M. pyrifera* recruitment, were calculated and plotted as above. To evaluate the effects of combining the model on each population, we compared the model outputs for each single-species model (without interspecific competition) with the combined model outputs (with interspecific competition).

Introduction scenarios: Introduction of S. horneri *into a* M. pyrifera *population*

To evaluate whether *S. horneri* could invade a mature *M. pyrifera* forest, we ran the combined model as above but with all *S. horneri* stages initially set to zero and *M. pyrifera* initial conditions as in Table 3-1, allowing *M. pyrifera* populations to develop as in the single-species model. To simulate a single recruitment event from distant *S. horneri* populations, we seeded *S. horneri* with 100 recruits, about half of the maximum number of recruits observed in the single-species model, in June when *S. horneri* has peak seasonal recruitment. Simulations were run during three *M. pyrifera* population scenarios in June of years 1-3: 1) intermediate adult and canopy frond density, 2) low adult and canopy frond density, and 3) high adult and canopy frond

density. In each scenario, we plotted *S. horneri* and *M. pyrifera* population dynamics for eight years (years 3-10 of simulation) as this is how long it took for population trajectories to resolve.

Introduction scenarios: Introduction of M. pyrifera *into a* S. horneri *population*

To evaluate whether *M. pyrifera* could recolonize a mature *S. horneri* stand, we ran the combined model with all *M. pyrifera* stages initially set to zero and *S. horneri* initial conditions set to those in Table 3-3, allowing *S. horneri* to develop as in the single-species model. To simulate a single recruitment event from distant *M. pyrifera* populations, we then seeded *M. pyrifera* with 500 gametophytes, about half of the maximum number of gametophytes observed in the single-species model. In each simulation, cyclic gametophyte densities (Fig. 3-2B) were reestablished if *M. pyrifera* adults exceeded 0.02 thalli m^{-2}, a threshold that has been observed for *in situ* recruitment adjacent to adult thalli (Anderson and North 1966; Burgman and Gerard 1990). We ran three *S. horneri* population scenarios: 1) low immature density, high adult (both stages) density, 2) intermediate immature density, low adult density, and 3) high immature density, low adult density. In each scenario, we plotted *S. horneri* and *M. pyrifera* population dynamics for eight years. Additionally, to evaluate *M. pyrifera* recolonization success across a broader range of scenarios, we seeded *M. pyrifera* gametophytes every month within a five-year time frame with the potential for reestablishment as above, and recorded the density of large *S. horneri* stages (immature + adult densities), the percent reduction in bottom light by large *S. horneri* stages at the time of invasion ($t_{invasion}$), and the maximum number of *M. pyrifera* adults after ten years ($t_{10years}$).

Results

Single-species population models (intraspecific interactions): Output and calibration

While model inputs of gametophyte densities of *M. pyrifera* had consistent yearly cycles as specified in the original model (Burgman and Gerard 1990), how these individuals moved through the life-history stages was modified by recruitment success and intraspecific competition (Fig. 3-5A). Recruit sporophytes exhibit peaks in population density in September, December, and June every three years, reaching their maximum density at about 50 individuals m^{-2} during winter with smaller density peaks in summer. Recruit density peaks correspond to months when densities of adults and canopy fronds are relatively low, implying a period of low intraspecific competition for light, and these peaks in recruits drive the three-year cycle observed in densities of subsequent stages. Blade sporophytes and subadults reach maximum densities around 1.6 and 1.1 individuals m^{-2} in late summer and early fall, respectively, after peaks in recruit sporophytes. Thus, it takes approximately 8-10 months for recruit sporophytes to transition into the adult stage, with maximum densities around 0.4 individuals m^{-2}. Adults can persist for multiple years, with significant accumulations of adults (peaks in density) occurring in fall and early winter during which adults accumulate more fronds. Finally, the canopy exhibits several peaks within three-year intervals that generally occur in the spring when surface temperatures are low, with canopy reaching a maximum of approximately 8 fronds m^{-2}. The canopy reaches its lowest densities in late summer or early fall when surface temperatures are at their maximum.

Overall, our model reproduced the annual and multi-annual dynamics of adult and canopy densities from the original deterministic model, albeit the magnitudes of the predicted population fluctuations were not identical (Fig. 3-5A, bottom two panels). These mismatches may be due to our lack of the original code used for the model; this code is no longer available (M.A. Burgman, pers. comm.). Due to this, we made some assumptions of model structure, specifically how to incorporate and calculate canopy density as well as how to interpret the

mathematical notation for immature sporophyte growth and temperature. Further, not including five size subclasses for each sporophyte stage may have resulted in a shorter residence time for each stage. Adult densities predicted from our single-species model are lower than observed in the original Burgman and Gerard (1990) deterministic model output. However, the timing of peaks in adult density in both models generally match, although we predicted a peak near the end of the five-year simulation that is not in the original. The maximum canopy density observed in our model is higher than what is observed in the original deterministic model but smaller peaks fall largely within the range of what is observed in the original. The timing of canopy peaks generally corresponds to peaks observed in the original deterministic model despite the single-species model predicting a smaller peak in canopy density in year two not observed in the original. For full model comparison of our deterministic model to the stochastic model in Burgman and Gerard (1990), see Fig. 3-S2.

Recruitment occurs in months when bottom temperatures are low and bottom light is high due to reduced intraspecific competition for light (Fig. 3-6A). Recruitment windows are only observed in years when adult density is <0.1 thalli m^{-2} and they do not form a dense canopy (compare Fig. 3-5A with Fig. 3-6A). Two to three months of recruitment windows occur during recruitment years (years 1, 2, 4 and 5).

The single-species model output for *S. horneri* closely replicated the field data (SBC LTER et al. 2018) upon which it was built (Appendix 3-S6). *S. horneri* single-species model predictions show distinct seasonal cycles of recruitment, growth through the size/stage classes, reproduction, and senescence (Fig. 3-7A). Intraspecific competition for light is seemingly less limiting for recruitment of *S. horneri* than for *M. pyrifera* as *S. horneri* recruits were present year-round. Recruits peak yearly in June at approximately 125 individuals m^{-2} and persist at

lower densities throughout the year. The population reaches its highest density but likely its weakest shading effect in the summer because of the extremely high density of recruits and low density of larger stages. Recruits transition into the immature stage by the fall with peak densities at around 32 individuals m^{-2}. Immature stages transition into stage I adults by March and stage II adults by April, during which population density is at its lowest point at approximately 8 individuals m^{-2}, but exerting the strongest shading effect due to dominance by adult stages. The peak of stage II adults bearing embryos signifies the peak in reproduction. Following reproduction, stage II adults transition into the senescent stage by May.

Combined population models (intra- and interspecific interactions): Model output and analysis

Adding interspecific competition with *S. horneri* changed the temporal patterns and magnitude of *M. pyrifera* recruitment, which propagated through all subsequent stages (Fig. 3-5A, B). With interspecific competition, recruit sporophytes no longer experience large winter peaks and instead only peak in early summer and at lower densities (Fig. 3-5B). Recruit densities were reduced by 61% with interspecific competition, while blade, subadult, adult, and canopy densities were reduced by 13%, 20%, 32%, and 10%, respectively, with competition from *S. horneri*. Further, peaks in adult density occur on two-year intervals instead of three.

Recruitment window months for *M. pyrifera* range from 1-3 as opposed to 2-3 without competition from *S. horneri* (Fig. 3-6). These windows now only occur during the summertime when *S. horneri* is dominated by recruits (low shading effect) and *M. pyrifera* canopy density is low (Fig. 3-6B).

Interspecific competition with *M. pyrifera* nearly caused local extinction of *S. horneri*, with *S. horneri* stages reduced by ~95% during years 1-3 with competition from *M. pyrifera* as compared to without interspecific competition (Fig. 3-7A, B; note scale changes between

panels). Further, following a significant peak in *M. pyrifera* canopy in years 3-4, all *S. horneri* stages were reduced even further, with reductions of ~99% relative to values without competition.

Introduction scenarios: Introduction of S. horneri *into a* M. pyrifera *population*

Following a single introduction event during peak *S. horneri* recruitment months, *S. horneri* was eventually driven to local extinction by a naturally cycling population of *M. pyrifera* in all introduction scenarios, with little effect on the *M. pyrifera* population (Fig. 3-8). However, *S. horneri* persisted longer and/or at higher densities depending on *M. pyrifera* adult and canopy densities at the time of and just following each introduction event. In the first scenario, when *S. horneri* recruits were introduced during a period with intermediate *M. pyrifera* adult and canopy densities, *S. horneri* sustained a second, lower magnitude recruitment event in the second year that propagated through the size classes (Fig. 3-8A). This second recruitment event was likely due to low *M. pyrifera* adult and canopy density following this invasion. However, all *S. horneri* densities subsequently dropped to almost zero by year four, likely due to the accumulation of *M. pyrifera* adults and canopy fronds. Despite a slight decrease in all stage densities during the introduction event, *M. pyrifera* population dynamics were otherwise unaffected.

In the second scenario with low *M. pyrifera* adult and canopy density, *S. horneri* became locally extinct following the introduction event in year two, likely because *M. pyrifera* adult and canopy density rose to a peak just after the introduction, which prevented a subsequent year of recruitment of *S. horneri* (Fig. 3-8B). All *M. pyrifera* stages were seemingly unaffected by the introduction event. In the third scenario with high *M. pyrifera* adult and canopy density, *S. horneri* successfully recruited for three years, likely due to plunging *M. pyrifera* adult and canopy density just after initial introduction (Fig. 3-8C). However, all stages become locally

extinct during the subsequent peak in *M. pyrifera* adults and canopy fronds during year six. The peak densities of *M. pyrifera* recruits and blade sporophytes were lower in years four and five compared to other years, but larger *M. pyrifera* stages were seemingly unaffected by the introduction event. Overall, our model predicts that *S. horneri* cannot successfully invade from a single introduction event without reductions in *M. pyrifera*.

Introduction scenarios: Introduction of M. pyrifera *into a* S. horneri *population*

M. pyrifera long-term recolonization was unsuccessful in scenarios where either immature or adult *S. horneri* densities were high, but successful at intermediate or low immature and adult densities (Fig. 3-9). In the first scenario evaluating *M. pyrifera* introduction during a period with low immature and high adult *S. horneri* densities, *M. pyrifera* was not able to establish and *S. horneri* remained unaffected by the introduction event in year three (Fig. 3-9A). Equivalent dynamics occurred in the third scenario with high immature and low adult *S. horneri* densities (Fig. 3-9C). In the second scenario with intermediate immature and low adult *S. horneri* densities, *M. pyrifera* was able to reestablish recruitment and successfully colonize with large peaks in all stages following the introduction event in year three and all stages reestablishing through year eight (Fig. 3-9B). Following the introduction event, all stages of *S. horneri* substantially declined and became locally extinct by year seven.

M. pyrifera was more likely to successfully recolonize and persist for 10 years when the density of large *S. horneri* stages (immature and adult) was low, and thus bottom light was not reduced by shading by these stages, during the introduction event (Fig. 3-10). The density of *M. pyrifera* adults after 10 years was zero at densities of large *S. horneri* greater than ~10 thalli m^{-2} during the introduction event (Fig. 3-10A). The density of *M. pyrifera* adults after 10 years was zero if bottom light was reduced by ~35% or more due to shading by *S. horneri* during the

introduction event (Fig. 3-10B), likely because shading was not favorable for a recruitment window to occur. The bimodal pattern observed in maximum *M. pyrifera* densities >0 is likely due to offset population cycles resulting in different *M. pyrifera* adult densities at the end of year 10.

Discussion

Here we present the first models of *S. horneri* population dynamics and species-species interactions with the foundational species *M. pyrifera*. We found that a stage-structured model of *S. horneri*, with survival and growth parameters governed by empirical relationships with light and temperature, resulted in model outputs that were highly aligned with field data. Further, while growth of recruit stages occurred over a wide range of temperatures, rapid growth of immature and adult *S. horneri* occurred during the lowest seasonal temperatures. Analyzing single-species models, we found that intraspecific competition for light strongly influenced both *M. pyrifera* and *S. horneri* population dynamics. *M. pyrifera* population structure was controlled by the density of adults and canopy fronds that limited recruitment via shading. In contrast, bottlenecks for *S. horneri* occurred via competition for light at both the recruit and immature stages. Considering the model that combined the two species, we found that interspecific competition for light was another strong driver of population dynamics of both species. When *M. pyrifera* and *S. horneri* were initially both at high densities, *M. pyrifera* drove *S. horneri* to local extinction while *S. horneri* influenced the timing and intensity of *M. pyrifera* recruitment but had minimal impact on its overall dynamics. When exploring the mutual invasibility of these species, specifically the consequences of introducing one into an established population of the other, we found that, once dominant, both species resisted invasion, albeit differentially. Our model suggests *S. horneri* requires disturbance that removes *M. pyrifera* to invade, as *S. horneri*

persisted longer when invasion preceded minimums in large *M. pyrifera*. In contrast, *M. pyrifera* may require continuous gametophyte supply to successfully recolonize *S. horneri* stands in order to take advantage of times when light was abundant and, ultimately, driving *S. horneri* to local extinction.

Resistance to invasion is mediated by differences in life histories

Our model predicts that *S. horneri* is unable to invade established forests of *M. pyrifera*, likely because *S. horneri* is tightly constrained by seasonal recruitment in our model. Specifically, we found that *M. pyrifera* forests with dense adults and canopy are resistant to *S. horneri*, implying that disturbances such as storms, heatwaves, El Niño Southern Oscillation (ENSO), and herbivory that impact *M. pyrifera* (Cavanaugh et al. 2019; Edwards 2019; Steneck et al. 2002) may facilitate *S. horneri* invasion. This hypothesis is supported by the increased prevalence of *S. horneri* in southern California observed following a prolonged heatwave and intense ENSO in 2014-2016 that decimated many *M. pyrifera* canopies (Cavanaugh et al. 2019; Edwards 2019; Reed et al. 2016). Others found recruitment of native understory (Foster 1982b; Reed and Foster 1984) and invasive algae (Ambrose and Nelson 1982; South and Thomsen 2016; Valentine and Johnson 2003) was only possible when *M. pyrifera* canopy was sparse or absent. More broadly, invasive establishment was enhanced when disturbance removed other native canopy-forming macrophytes (Connolly et al. 2017) and dominant native competitors (Minchinton and Bertness 2003). Highly seasonal reproduction and recruitment in *S. horneri* may constrain its ability to exploit episodic favorable events (Reed et al. 1996), as peaks in *S. horneri* recruitment often occur when *M. pyrifera* is at or approaching maximum biomass in southern California (Harrer et al. 2013; Marks et al. 2018; Reed et al. 2009). Therefore, it is important for future model scenarios to explore whether reduced recruitment during the

shoulders of seasonal peaks is sufficient for invasion when *M. pyrifera* is at a seasonal low. As disturbances are predicted to increase in frequency and intensity with global change (Carnell and Keough 2020; DiLorenzo et al. 2010; Doney et al. 2012; Smale et al. 2019), our results suggest *S. horneri* may increase in prevalence if *M. pyrifera* is disproportionately impacted.

Our model also predicts that established beds of *S. horneri* can resist reestablishment of *M. pyrifera*, although the strength of this resistance may depend on the life history of *M. pyrifera* recruitment. *S. horneri* can form dense monocultures with shaded understories (Kaplanis et al. 2016; Marks et al. 2017; Marks et al. 2020a) that may inhibit *M. pyrifera* colonization, as has been found for *M. pyrifera* and the invasive congener, *S. muticum* (Ambrose and Nelson 1982). Our results suggest that year-round reproduction may allow *M. pyrifera* to reestablish during favorable recruitment windows, such as when immature and adult *S. horneri* densities are low and light is readily available during the summer. Similar strategies are seen in terrestrial perennials that vary timing of flowering in response to fluctuating resource availability (Evenari and Gutterman 1985; Jozwik 1970). However, *M. pyrifera* gametophyte production and sporophyte recruitment are adversely impacted by warm temperatures (Dayton and Tegner 1984; Deysher and Dean 1986; Hollarsmith et al. 2020; Reed et al. 1996), indicating that favorable conditions need to coincide with low interspecific competition with *S. horneri* in order for *M. pyrifera* to successfully reestablish. For example, *M. pyrifera* recruitment was not observed following *S. horneri* removals during a period with anomalously warm water temperatures (Marks et al. 2017) but removals during cooler, more favorable temperatures resulted in significant *M. pyrifera* recruitment (Sullaway and Edwards 2020). Our results suggest that *S. horneri* may remain resistant to *M. pyrifera* reestablishment unless favorable environmental conditions for *M. pyrifera* recruitment coincide with low interspecific competition for light.

Life history, intraspecific competition for light, and temperature drive population structure

Incorporating the well-studied relationships between light and temperature and *M. pyrifera* (Dean and Jacobsen 1984; Dean and Jacobsen 1986; Deysher and Dean 1986; Gerard 1984b) into our population model replicated *M. pyrifera* size structure and temporal dynamics in the field. Temperature drives the formation or degradation of a dense surface canopy (Burgman and Gerard 1990; Gerard 1984b), which in turn dictates light availability, recruitment, and subsequent population structure. Characteristic of a perennial life history, *M. pyrifera* adults and the associated canopy persisted for multiple years in our model, which consequently resulted in limited light and recruitment. This relationship of intraspecific competition for light between perennial adults and recruitment has been well-documented in natural *M. pyrifera* forests (Dayton et al. 1984; Ebeling et al. 1985; Reed and Foster 1984), as well as with other dominant perennial algal species (Lubchenco and Menge 1978). *M. pyrifera* may also be able to buffer changes in seasonal temperature and light availability by persisting multiple years and reproducing/recruiting during optimal times, a "bet-hedging" strategy that is observed in terrestrial perennials (Friedman 2020). Overall, our model predictions confirm empirical work demonstrating that changes in light and temperature due to disturbance and/or global change will likely influence *M. pyrifera* population structure and abundance.

Our single-species *S. horneri* model, built upon light and temperature relationships similar to *M. pyrifera* and parameterized with field data (SBC LTER et al. 2018), resulted in realistic *S. horneri* population abundance and structure through time. In our model, shading by conspecifics and natural variability influenced the seasonal availability of light, which in turn influenced *S. horneri* population structure. As in other algal populations (Andrew and Viejo 1998; Arenas and Fernández 2000; Dean et al. 1989; Schiel and Choat 1980), self-shading is an

important density-dependent mechanism regulating *S. horneri* populations (Marks et al. 2017). Therefore, increased light availability during the annual senescence of *S. horneri* is likely critical for successful recruitment. In contrast to *M. pyrifera*, relationships with light and temperature are not well-established for *S. horneri*. However, evidence across *S. horneri*'s native and invasive range suggests it can grow under a variety of light levels (Choi et al. 2008; Aguilar-Rosas et al. 2007; Yoshida 1983) and temperatures (Chu et al. 1998; Marks et al. 2015). Others have found that *S. horneri* exhibited rapid growth and peak biomass when seasonal water temperatures were at their minimum (Choi et al. 2020), a pattern we also observed in our analysis. While *S. horneri* may be able to grow in a variety of environmental conditions, the onset of certain life history events, such as rapid growth and reproduction, may be dictated by critical levels of certain abiotic factors, as has been found for other seasonal algal species (De Wreede 1976; Deysher 1984) and terrestrial plants (Arft et al. 1999; Cleland et al. 2006; Dunne et al. 2003). Our study suggests that light and temperature may be important drivers of *S. horneri* seasonality and timing of life-history events. However, more empirical research is need to refine these relationships.

Competitive asymmetries result from differences in size, life-history, and abiotic conditions

In our model, *S. horneri* is limited by life history constraints on size, as this makes it a competitive inferior for light compared to adult *M. pyrifera*. Thallus size has been cited as the best indicator that an alga (or other sessile species) exerts strong community-wide effects (Edwards and Connell 2012) due to preemption of resources. Therefore, although *S. horneri* is capable of forming dense understory canopies when established (Marks et al. 2017), *M. pyrifera* will always exclude *S. horneri* if it is able to achieve a larger size and form a surface canopy (Dayton and Tegner 1984; Olson and Lubchenco 1990), as we observed in our model. Others have speculated that the invasion success of *S. horneri* is not due to competitive superiority and

instead is a result of exploiting open niches (Caselle et al. 2017; Marks et al. 2020a; Sullaway and Edwards 2020). Therefore, *S. horneri* is not likely to outcompete large *M. pyrifera* for light but will likely take advantage of points in time and space when *M. pyrifera* is low to invade.

Asymmetries in the competitive abilities of *M. pyrifera* and *S. horneri* may be modified by life history differences in addition to size and reproduction, such as life-span and responses to environmental conditions. For example, *S. horneri* has been observed to tolerate a wider range of temperatures (Chu et al. 1998; Marks et al. 2015) than *M. pyrifera* (North et al. 1986; Schiel and Foster 2015). Therefore, *S. horneri* may have a competitive advantage over *M. pyrifera* in elevated temperatures, a scenario that warrants further exploration, particularly given projected changes in oceanographic conditions due to climate change (Carnell and Keough 2020; DiLorenzo et al. 2010; Doney et al. 2012; Smale et al. 2019). Further, *M. pyrifera* may be able to competitively exclude *S. horneri* for multiple years, as it does for conspecifics (Deysher and Dean 1986) and other understory algal species (Foster 1982b; Reed and Foster 1984). This contrasts with the highly seasonal annual life-history of *S. horneri*, where a strong competitive advantage is likely ephemeral and associated with the dominance of large individuals. Therefore, understanding how interspecific competition strength varies with life-history and abiotic factors is important to predict whether such interactions promote or limit invasion.

Future directions

Our models have provided insight into the influence of species-species interactions, life history differences, and abiotic factors in determining the population structure and persistence of *M. pyrifera* and *S. horneri*, as well as developed a framework to explore several important research avenues in the future. For example, invasion scenarios could be evaluated under varying levels of propagule pressure, a factor known to be an important driver of establishment success

in invasive (Grevstad 1999; Panetta and Randall 1994; Britton-Simmons and Abbott 2008) and native species (Mason et al. 2008). Further, *S. horneri* invasion success and the probability of *M. pyrifera* recovery could be evaluated under different disturbance scenarios that disproportionately impact *M. pyrifera* such as extreme temperatures, storm events, and herbivory. One important topic to explore in this model framework is whether the prolonged heatwave and intense 2014-2016 ENSO experienced in California is a possible explanation for increased *S. horneri* prevalence during *M. pyrifera* declines. Additionally, this model makes specific predictions that could be tested in the field, such as evaluating whether supplementing *M. pyrifera* gametophytes and/or recruits when interspecific competition with *S. horneri* is low facilitates *M. pyrifera* population recovery. Finally, this model may provide a useful framework to investigate interactions between other stage-structured populations where light is the limiting resource.

Table 3-1. Equations, state variables, initial conditions, and parameters used in single-species and combined *Macrocystis pyrifera* population model adapted from Burgman and Gerard (1990).

Equations:

"Recruitment windows"

$$G_{P21} = 0.1, if\ T_{bot} \leq 16.3℃\ and\ L_{Ri} \geq 0.7\ mol\ photons\ m^{-2}d^{-1} \quad (2)$$
$$else\ G_{P21} = 0$$

Growth of immature sporophytes (recruit, blade-stage, and subadult)

$$Gmax_i = 1 + 22{S_i}^{-0.5} \quad (3)$$

$$G_{ji} = Gmax_i\left(1 - e^{-k(L_{Ri} - C_i)}\right), if\ L_{Ri} > C_i \quad (4)$$

$$G_{ji} = 0, if\ L_{Ri} \leq C_i$$

$$If\ T_{bot} \leq 13.5, k = 1.5 \quad (5)$$
$$If\ 13.5 < T_{bot} < 18, then\ C_i = 1.5C_i, Gmax_i = 0.67Gmax_i, and\ k = k + 0.5$$
$$or\ if\ T_{bot} \geq 18, then\ C_i = 2C_i, Gmax_i = 0.5Gmax_i, and\ k = k + 1$$

Growth of adult sporophytes

$$A_{Pji} = 0.5 - 0.0625D - F \quad (6)$$

$$If\ T_{surf} \leq 13, F = 0 \quad (7)$$
$$If\ 13 < T_{surf} < 19, F = 0.5\left(\frac{e^{(T_{surf}-13)}}{e^6}\right)$$
$$or\ if\ T_{surf} \geq 19, F = 0.5$$

$$D = N_{P5} * 5 + N_{P6} * 6 + N_{P7} * 7 + N_{P8} * 8 + N_{P9} * 9 \quad (8)$$

Light penetration (competition)

$$P_{Li} = e^{-0.00045N_i{S_i}^{1.1}}\ for\ immature\ sporophytes\ (recruit, blade-stage, and\ subadult) \quad (9)$$

$$P_{Li} = e^{-0.34D}\ for\ the\ surface\ canopy \quad (10)$$

$$L_{Ri} = L * P_{Li}\ for\ each\ stage \quad (11)$$

State variables:

P1 = Gametophytes	P2 = Recruit sporophytes	P3 = Blade-stage sporophytes
P4 = Subadult sporophytes	P5-9 = Adult sporophytes	

Initial condition values (# m^{-2}):

$P1_0$ = 1201.9	$P2_0$ = 100	$P3_0$ = 10
$P4_0$ = 1	$P5\text{-}9_0$ = 0.1	

Parameter:	Description:	Value:
X_{ii}	Survival probability for immature sporophyte stage *I* (mo^{-1})	0.21 (X_{P22}), 0.51 (X_{P33}), 0.75 (X_{P44})
T_{bot}	Monthly mean bottom temperature (˚C)	Variable, see Fig. 3-2D
$Gmax_i$	Maximum potential growth probability (mo^{-1}) for stage *i*	Calculated
S_i	Median length (cm) of immature sporophyte stage *i*	0.55 (S_{P2}), 51 (S_{P3}), 550 (S_{P4})
k	Immature sporophyte growth coefficient	1.5
G_{ji}	Realized growth probability from immature sporophyte stage *i* to stage *j* (mo^{-1})	Calculated
A_{Pji}	Adult growth probability from adult subclass *j* to subclass *i*	Calculated
L_{Ri}	Realized light reaching stage *i* (mol photons m^{-2} day^{-1})	Calculated
C_i	Growth-compensation light level (mol photons m^{-2} day^{-1}) for immature sporophyte stage *i*	0.35 (C_{P2}), 0.4 (C_{P3}), 0.45 (C_{P4})
D	Canopy density (fronds m^{-2})	Calculated
N_i	Density of stage *i* (m^{-2})	Calculated
F	Rate of frond loss for adult sporophytes (# mo^{-1})	Calculated
T_{surf}	Monthly mean surface temperature (˚C)	Variable, see Fig. 3-2D
P_{Li}	Shading parameter for stage *i*	Calculated
L	Monthly mean bottom light (mol photons m^{-2} day^{-1})	Variable, see Fig. 3-2C

Table 3-2. Monthly mean densities (# m^{-2}) with associated standard error (SE) and sample size (N) of different *Sargassum horneri* life-history stages, adapted from SBC LTER et al. (2018). Densities and months are divided into three *Sargassum* life-history phases (Ang and De Wreede (1990)) defined as FG=Fast Growth, RSR=Reproduction, Senescence, Recruitment, and SG=Slow Growth. Asterisks denote months when data are interpolated.

Stage	*Value*	**Jan**	**Feb**	**Mar**	**Apr**	**May**	**Jun**	**Jul***	**Aug***	**Sep**	**Oct***	**Nov***	**Dec**
Recruit	Mean	29.05	12.89	11.24	19.36	22.49	130.4	103.78	77.16	50.54	42.45	34.36	26.27
	SE	NA	6.73	7.12	16.79	19.27	27.81	NA	NA	NA	NA	NA	8.26
	N	1	2	2	2	2	3	NA	NA	1	NA	NA	2
Immat-ure	Mean	17.11	25.01	8.01	2.8	0.6	0.21	3.44	6.67	9.89	19.85	29.8	39.75
	SE	NA	16.52	2.94	0.52	0.03	0.08	NA	NA	NA	NA	NA	16.34
	N	1	2	2	2	2	3	NA	NA	1	NA	NA	2
Stage I adult	Mean	2.41	3.6	10.4	3.68	1.39	0.46	0.37	0.28	0.19	0.19	0.2	0.21
	SE	NA	7.4	9.16	1.48	0.61	0.39	NA	NA	NA	NA	NA	0.11
	N	1	2	2	2	2	3	NA	NA	1	NA	NA	2
Stage II Adult	Mean	0	0	1.83	8.14	1.86	0.25	0.17	0.08	0	0	0	0
	SE	NA	0	0.05	6.57	0.36	0.2	NA	NA	NA	NA	NA	0
	N	1	2	2	2	2	3	NA	NA	1	NA	NA	2
Senes-cent	Mean	0.56	0.82	1.48	3.37	7.6	1.81	1.22	0.64	0.04	0.03	0.03	0.02
	SE	NA	0.82	1.48	0.45	4.71	0.99	NA	NA	NA	NA	NA	0.02
	N	1	2	2	2	2	3	NA	NA	1	NA	NA	2
Phase		**FG**			**RSR**				**SG**				**FG**

Table 3-3. Equations, state variables, initial conditions, and parameters used in single-species and combined *Sargassum horneri* population models.

Equations:

Growth of recruit *S. horneri:* G_{S21}

$If\ L_{RS1} > C_{S1}$: (12)

$G_{S21} = G_{S21}\ (Fig. 2C)$

$Else\ G_{S21} = 0$

Growth of immature *S. horneri:* G_{S32}

$If\ L_{RS2} > C_{S2}$: (13)

$If\ 14 \leq T_{bot} \leq 15, then\ G_{S32} = 0.055$

$If\ T_{bot} < 14, then\ G_{S32} = 0.45$

$Else\ G_{S32} = 0$

Growth of stage I adult *S. horneri:* G_{S43}

$If\ L_{RS3} > C_{S3}$: (14)

$If\ 14 \leq T_{bot} \leq 15, then\ G_{S43} = 0.3$

$If\ T_{bot} < 14, then\ G_{S43} = 0.9$

$Else\ G_{S43} = 0$

Light penetration (competition)

$P_{LS1} = e^{-0.00001 N_{s1} {S_{s1}}^{1.1}}\ for\ recruits$ (15)

$P_{LS2} = e^{-0.00012 N_{s2} {S_{s2}}^{1.1}}\ for\ immature$ (16)

$P_{Li} = e^{-0.00045 N_i {S_i}^{1.1}}\ for\ stage\ I\ and\ II\ adults$ (17)

$L_{Ri} = L * P_{Li}\ for\ each\ stages$ (18)

State variables:

S1 = Recruit; S2 = Immature; S3 = Stage I adult; S4 = Stage II adult; S5 = Senescent

Initial condition values (# m^{-2}):

$S1_0 = 29.05$; $S2_0 = 17.11$; $S3_0 = 2.41$; $S4_0 = 0$; $S5_0 = 0.56$

Parameter:	Description:	Value:
X_{ii}	Survival probability for stage *i* (mo^{-1})	Variable, see Fig. 3-4C
b_S	Recruitment (# m^{-2} mo^{-1})	Variable, see Fig. 3-4D
T_{bot}	Monthly mean bottom temperature (˚C)	Variable, see Fig. 3-2D
S_i	Median length (cm) of stage *i*	2.5 (S_{S1}), 150 (S_{S2}), 150 (S_{S3}), 170 (S_{S4})
G_{ji}	Realized growth probability from stage *j* to stage *i* (mo^{-1})	Variable, see Fig. 3-4C for G_{S21} and G_{S54}
L_{Ri}	Realized light reaching stage *i* (mol photons m^{-2} day^{-1})	Calculated
C_i	Growth-compensation light level (mol photons m^{-2} day^{-1}) for stage *i*	0.28 (C_{S1}), 0.1 (C_{S2}), 0.1 (C_{S3}), 0.1(C_{S4})
N_i	Density of stage *i* (# m^{-2})	Calculated
P_{Li}	Shading parameter for stage *i*	Calculated
L	Monthly mean bottom light (mol photons m^{-2} day^{-1})	Variable, see Fig. 3-2C

Figures captions

Fig. 3-1. Stage-structured state variables and transition matrices for *Macrocystis pyrifera* and *Sargassum horneri*. In (A), circles represent different stages (sizes) of *M. pyrifera*, with gametophytes (microscopic), recruit (0.05-2cm), blade-stage (2-100cm), subadult (100cm-10m), and adult (>10m with canopy fronds) sporophytes. In (C), circles represent different stages (sizes) of *S. horneri,* with recruit (<5cm), immature (5-280cm; no receptacles), stage I adult (5-280cm; with receptacles), stage II adult (5-300cm; with reproductive receptacles), and senescent (5-220cm) thalli. Stage I and II adults have higher biomass than immature stages (SBC LTER et al. 2018). In both (A) and (C) G_{ji} represents the monthly growth probability of i to stage j, X_{ii} represents the survival, or the probability stage i will remain in that stage each month, b represents recruitment, or the number of new individuals in the smallest stage produced per month. b_P is provided as an extrinsic input in the model and cycles yearly according to Fig. 3-2B. In (A), A_{Pji} represents monthly growth of adult sporophytes between 5 subclasses with different numbers of canopy fronds. In (B) and (D), parameters are incorporated into Leslie transition matrices (M) and accompanying population vectors (N_t) at time t for the single-species *M. pyrifera* and *S. horneri* models, respectively. In (E), single-species matrices were combined to form M and N_t for the combined model evaluating interspecific competition between *M. pyrifera* and *S. horneri*.

Fig. 3-2. Monthly mean values of *Macrocystis pyrifera* (A) adult survival and (B) b_P or recruitment of gametophytes, (C) bottom light in open water, and (D) bottom and surface temperature. All parameters collected *in situ* in southern California (T. Dean unpublished data; Rosenthal et al. 1974; Dayton et al. 1984; Dean 1985; Burgman and Gerard 1990).

Fig. 3-3. Diagram illustrating how intraspecific competition for light was incorporated into (A) the single-species *Macrocystis pyrifera* model, (B) the single-species *Sargassum horneri* model, and (C) how intra- and interspecific competition for light was incorporated into the combined model. The total amount of available bottom light in open water (L; Fig. 3-2C) is sequentially reduced by the shading coefficients (P_{Li}) of larger stages as well as stages within the same size class.

Fig. 3-4. Monthly values of (A) *Sargassum horneri* growth between immature and stage 1 adults (G_{S32}) and (B) growth between stage I and stage II adults (G_{S43}) in relation to bottom temperature with horizontal dashed lines denoting temperature thresholds used for the single-species *S. horneri* model (Table 3-2, eq. 13-14). (C) displays monthly values of survival (X_{Sii}) for all stages, the transition between recruit and immature stages (G_{S21}), and the transition between stage II adults and the senescent stage (G_{S54}), and (D) displays recruitment (b_S) values.

Fig. 3-5. *Macrocystis pyrifera* (A) single-species model output (intraspecific competition only) adapted from Burgman and Gerard (1990) ("original") and (B) combined model output (intra- and interspecific competition; same model run as Fig. 3-7B). Densities for each life-history stage and the canopy (fronds m^{-2}) are displayed monthly for five years.

Fig. 3-6. *Macrocystis pyrifera* recruitment in the (A) single-species (intraspecific competition only) and (B) combined model (intra- and interspecific competition; same model run as Fig. 3-

7B) in relation to bottom light and bottom temperature (red bar denotes months within suitable temperature threshold for recruitment (≤16.3˚C)). Values are displayed per month over a period of five years. Asterisks denote recruitment windows, or months when bottom light is ≥0.7 mol photons m^{-2} day^{-1} and bottom temperature is ≤16.3˚C.

Fig. 3-7. *Sargassum horneri* (A) single-species model output (intraspecific competition only) and (B) combined model output (intra- and interspecific competition; same model run as Fig. 3-5B). Stage densities are displayed monthly for five years. Note that scale of the Y-axes in A and B are not the same.

Fig. 3-8. Model predictions in scenarios where *Sargassum horneri* is introduced into *Macrocystis pyrifera* forests at different densities of *M. pyrifera* adults and canopy fronds. Stage densities over eight years are displayed for *M. pyrifera* (left) and *S. horneri* densities (right). Dashed grey vertical lines denote when the introduction event occurs for each scenario.

Fig. 3-9. Model predictions in scenarios where *Macrocystis pyrifera* is introduced into *Sargassum horneri* stands at different densities of immature and adult *S. horneri*. Stage densities over eight years are displayed for *M. pyrifera* (left) and *S. horneri* densities (right). Dashed grey lines denote when the introduction event occurs for each scenario.

Fig. 3-10. Maximum density of *Macrocystis pyrifera* adults in model scenarios with (A) different initial densities of larger (immature and adult) *S. horneri* stages during the introduction event by *M. pyrifera* ($t_{invasion}$) and (B) levels of *S. horneri* shading at $t_{invasion}$ for all scenarios. N=60 scenarios, though many points are overlapping.

Figures

Fig. 3-1

A.

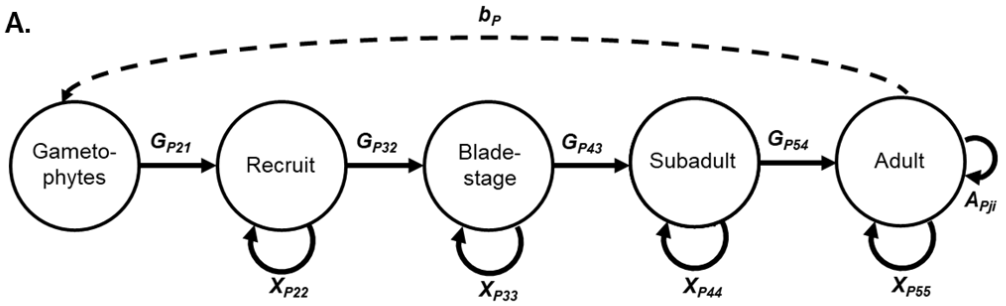

B.

$$\begin{bmatrix} 0 & 0 & 0 & 0 & b_P & b_P & b_P & b_P & b_P \\ G_{P21} & X_{P22} & 0 & 0 & 0 & 0 & 0 & 0 & 0 \\ 0 & G_{P32} & X_{P33} & 0 & 0 & 0 & 0 & 0 & 0 \\ 0 & 0 & G_{P43} & X_{P44} & 0 & 0 & 0 & 0 & 0 \\ 0 & 0 & 0 & G_{P54} & X_{P55} & 0 & 0 & 0 & 0 \\ 0 & 0 & 0 & 0 & A_{P65} & X_{P55} & 0 & 0 & 0 \\ 0 & 0 & 0 & 0 & 0 & A_{P76} & X_{P55} & 0 & 0 \\ 0 & 0 & 0 & 0 & 0 & 0 & A_{P87} & X_{P55} & 0 \\ 0 & 0 & 0 & 0 & 0 & 0 & 0 & A_{P98} & X_{P55} \end{bmatrix} = M \begin{bmatrix} P1 \\ P2 \\ P3 \\ P4 \\ P5 \\ P6 \\ P7 \\ P8 \\ P9 \end{bmatrix} = N_t$$

C.

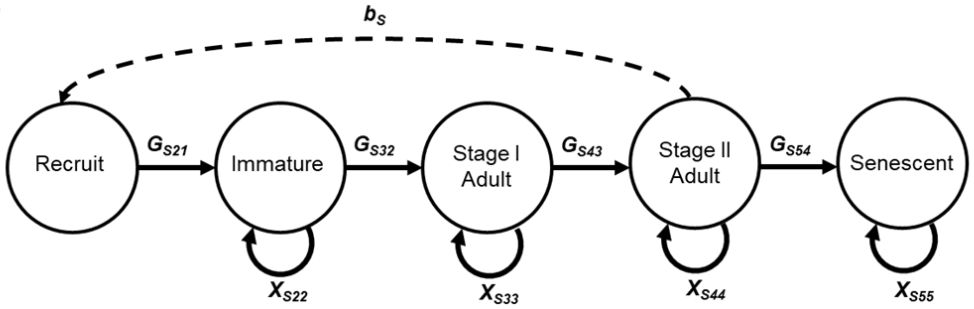

D.

$$\begin{bmatrix} X_{S11} & 0 & 0 & b_S & 0 \\ G_{S21} & X_{S22} & 0 & 0 & 0 \\ 0 & G_{S32} & X_{S33} & 0 & 0 \\ 0 & 0 & G_{S43} & X_{S44} & 0 \\ 0 & 0 & 0 & G_{S54} & X_{S55} \end{bmatrix} = M \begin{bmatrix} S1 \\ S2 \\ S3 \\ S4 \\ S5 \end{bmatrix} = N_t$$

E.

$$\begin{bmatrix} 0 & 0 & 0 & 0 & b_P & b_P & b_P & b_P & b_P & 0 & 0 & 0 & 0 & 0 \\ G_{P21} & X_{P22} & 0 & 0 & 0 & 0 & 0 & 0 & 0 & 0 & 0 & 0 & 0 & 0 \\ 0 & G_{P32} & X_{P33} & 0 & 0 & 0 & 0 & 0 & 0 & 0 & 0 & 0 & 0 & 0 \\ 0 & 0 & G_{P43} & X_{P44} & 0 & 0 & 0 & 0 & 0 & 0 & 0 & 0 & 0 & 0 \\ 0 & 0 & 0 & G_{P54} & X_{P55} & 0 & 0 & 0 & 0 & 0 & 0 & 0 & 0 & 0 \\ 0 & 0 & 0 & 0 & A_{P65} & X_{P55} & 0 & 0 & 0 & 0 & 0 & 0 & 0 & 0 \\ 0 & 0 & 0 & 0 & 0 & A_{P76} & X_{P55} & 0 & 0 & 0 & 0 & 0 & 0 & 0 \\ 0 & 0 & 0 & 0 & 0 & 0 & A_{P87} & X_{P55} & 0 & 0 & 0 & 0 & 0 & 0 \\ 0 & 0 & 0 & 0 & 0 & 0 & 0 & A_{P98} & X_{P55} & 0 & 0 & 0 & 0 & 0 \\ 0 & 0 & 0 & 0 & 0 & 0 & 0 & 0 & 0 & X_{S11} & 0 & 0 & b_S & 0 \\ 0 & 0 & 0 & 0 & 0 & 0 & 0 & 0 & 0 & G_{S21} & X_{S22} & 0 & 0 & 0 \\ 0 & 0 & 0 & 0 & 0 & 0 & 0 & 0 & 0 & 0 & G_{S32} & X_{S33} & 0 & 0 \\ 0 & 0 & 0 & 0 & 0 & 0 & 0 & 0 & 0 & 0 & 0 & G_{S43} & X_{S44} & 0 \\ 0 & 0 & 0 & 0 & 0 & 0 & 0 & 0 & 0 & 0 & 0 & 0 & G_{S54} & X_{S55} \end{bmatrix} = M \begin{bmatrix} P1 \\ P2 \\ P3 \\ P4 \\ P5 \\ P6 \\ P7 \\ P8 \\ P9 \\ S1 \\ S2 \\ S3 \\ S4 \\ S5 \end{bmatrix} = N_t$$

Fig. 3-2

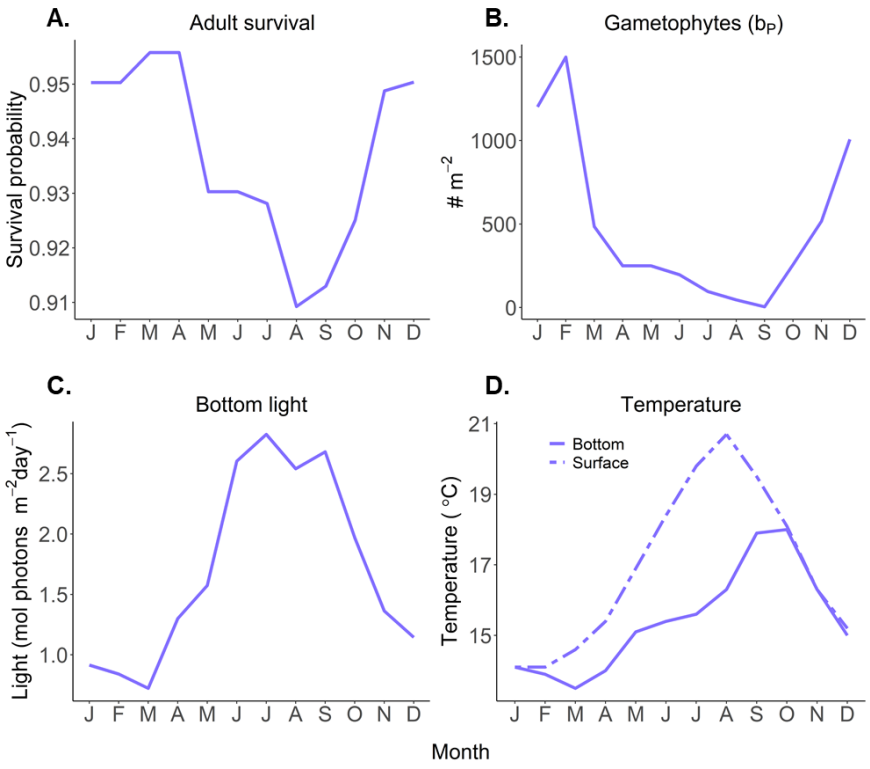
A.
Adult survival
Survival probability
0.95
0.94
0.93
0.92
0.91
J F M A M J J A S O N D
B.
Gametophytes (b_P)
m^{-2}
1500
1000
500
0
J F M A M J J A S O N D
C.
Bottom light
Light (mol photons $m^{-2}day^{-1}$)
2.5
2.0
1.5
1.0
J F M A M J J A S O N D
D.
Temperature
Bottom
Surface
Temperature (°C)
21
19
17
15
J F M A M J J A S O N D
Month

Fig. 3-3

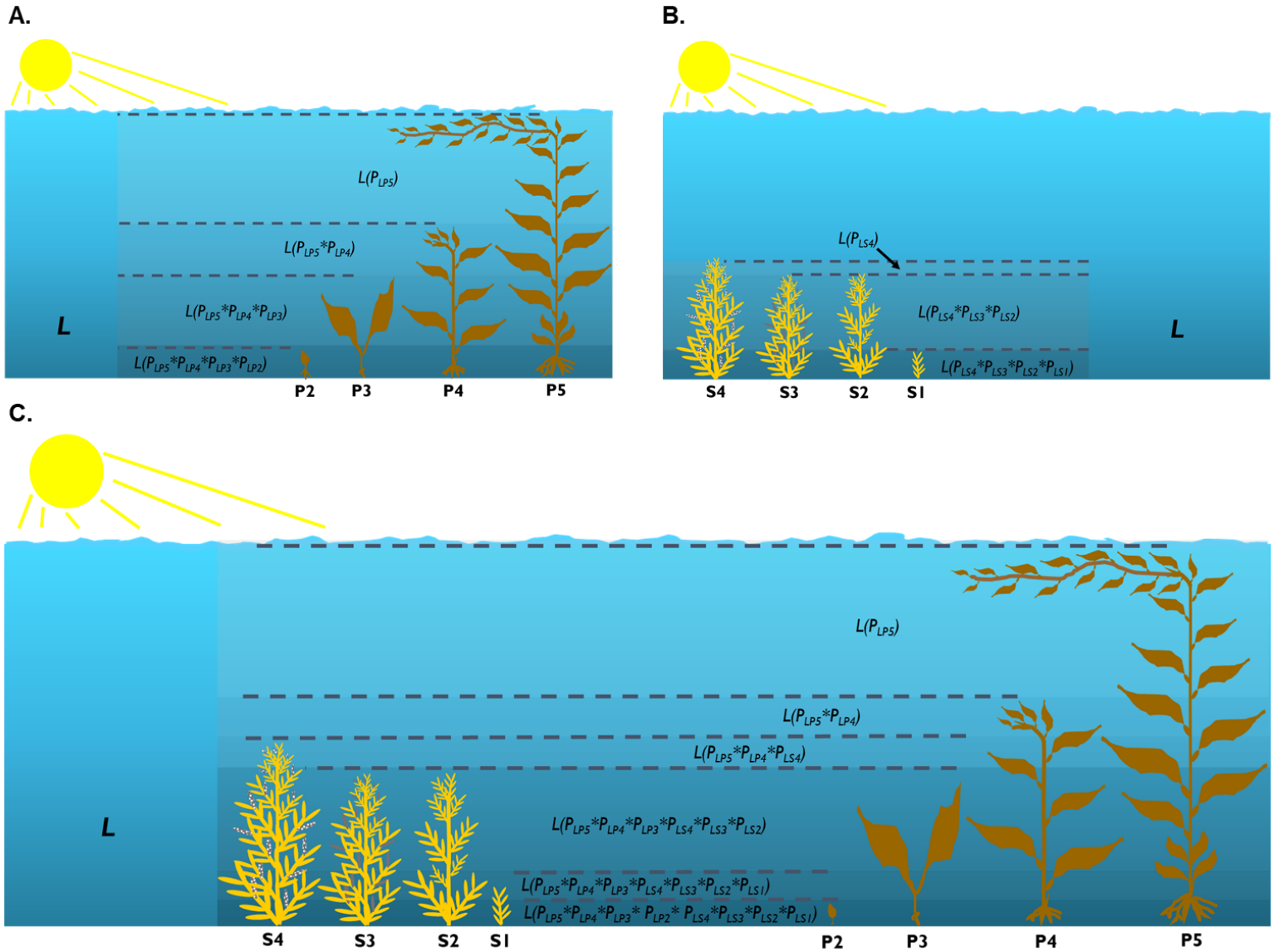
A.
B.
C.
L
$L(P_{LP5})$
$L(P_{LP5}*P_{LP4})$
$L(P_{LP5}*P_{LP4}*P_{LP3})$
$L(P_{LP5}*P_{LP4}*P_{LP3}*P_{LP2})$
P2
P3
P4
P5
$L(P_{LS4})$
$L(P_{LS4}*P_{LS3}*P_{LS2})$
$L(P_{LS4}*P_{LS3}*P_{LS2}*P_{LS1})$
S4
S3
S2
S1
$L(P_{LP5}*P_{LP4}*P_{LS4})$
$L(P_{LP5}*P_{LP4}*P_{LP3}*P_{LS4}*P_{LS3}*P_{LS2})$
$L(P_{LP5}*P_{LP4}*P_{LP3}*P_{LS4}*P_{LS3}*P_{LS2}*P_{LS1})$
$L(P_{LP5}*P_{LP4}*P_{LP3}*P_{LP2}*P_{LS4}*P_{LS3}*P_{LS2}*P_{LS1})$

Fig. 3-4

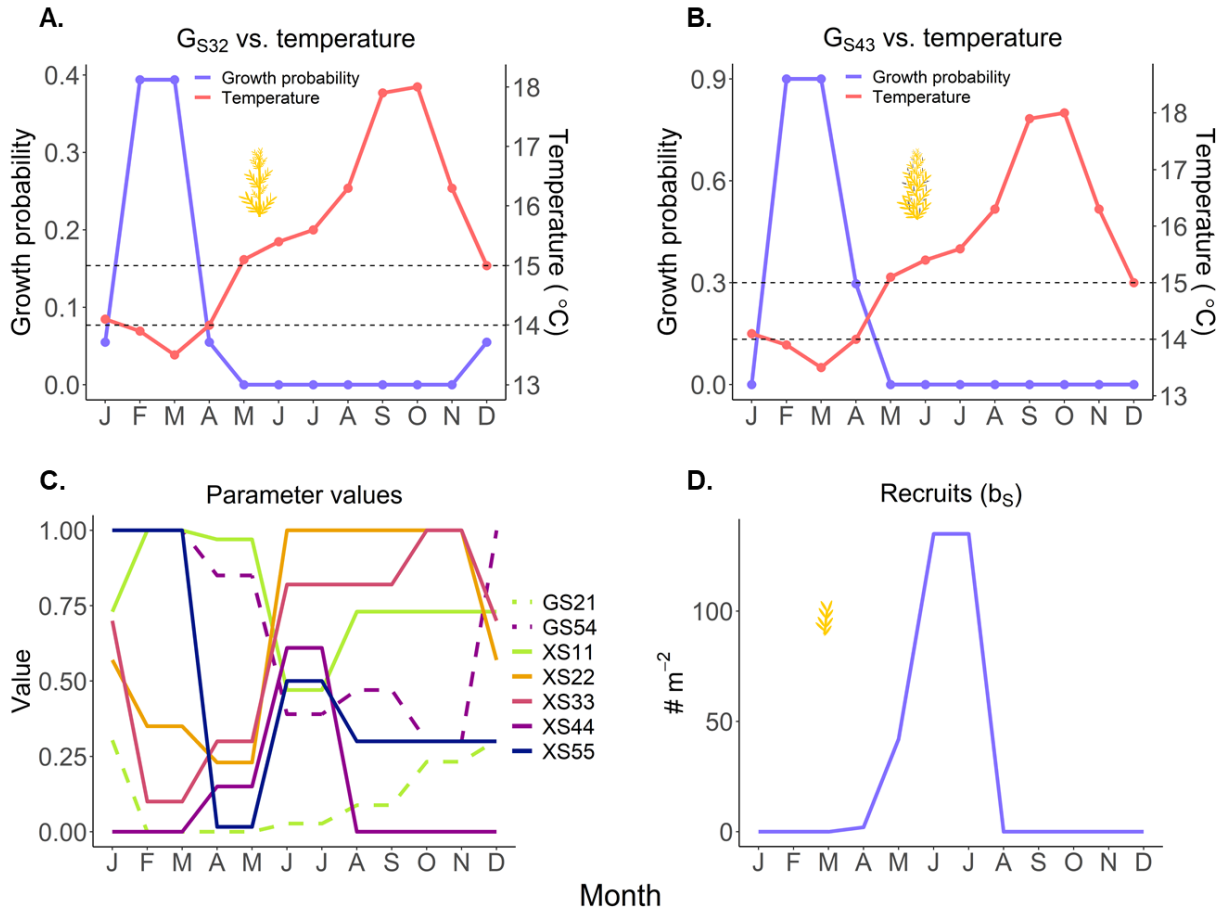
A.
G_{S32} vs. temperature
Growth probability
Temperature
Growth probability
Temperature (°C)
B.
G_{S43} vs. temperature
C.
Parameter values
Value
GS21
GS54
XS11
XS22
XS33
XS44
XS55
D.
Recruits (b_S)
m^{-2}
J F M A M J J A S O N D
Month

Fig. 3-5

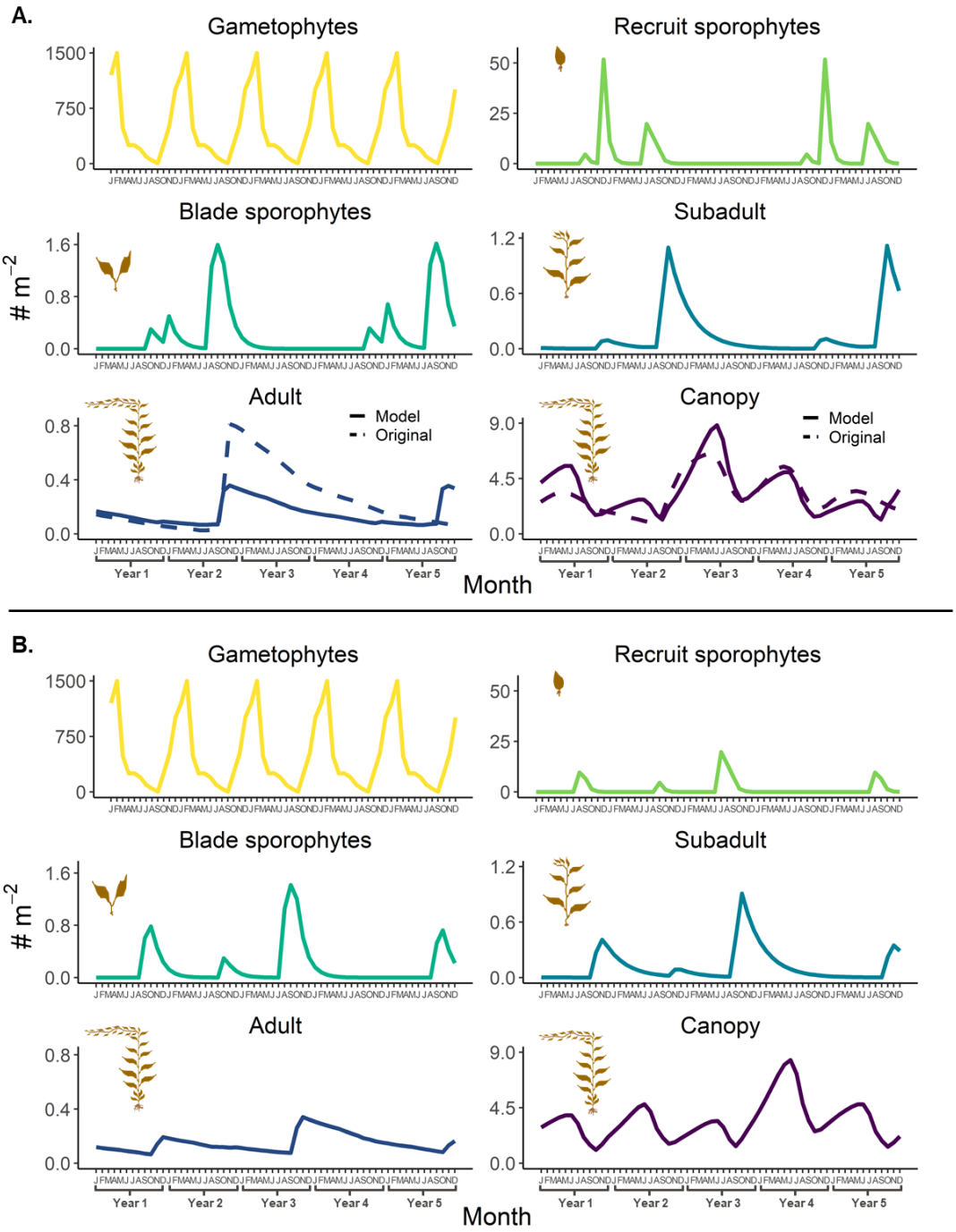
A.
Gametophytes
Recruit sporophytes
Blade sporophytes
Subadult
Adult
Canopy
Model
Original
m^{-2}
Year 1
Year 2
Year 3
Year 4
Year 5
Month
B.
Gametophytes
Recruit sporophytes
Blade sporophytes
Subadult
Adult
Canopy
m^{-2}
Year 1
Year 2
Year 3
Year 4
Year 5
Month

Fig. 3-6

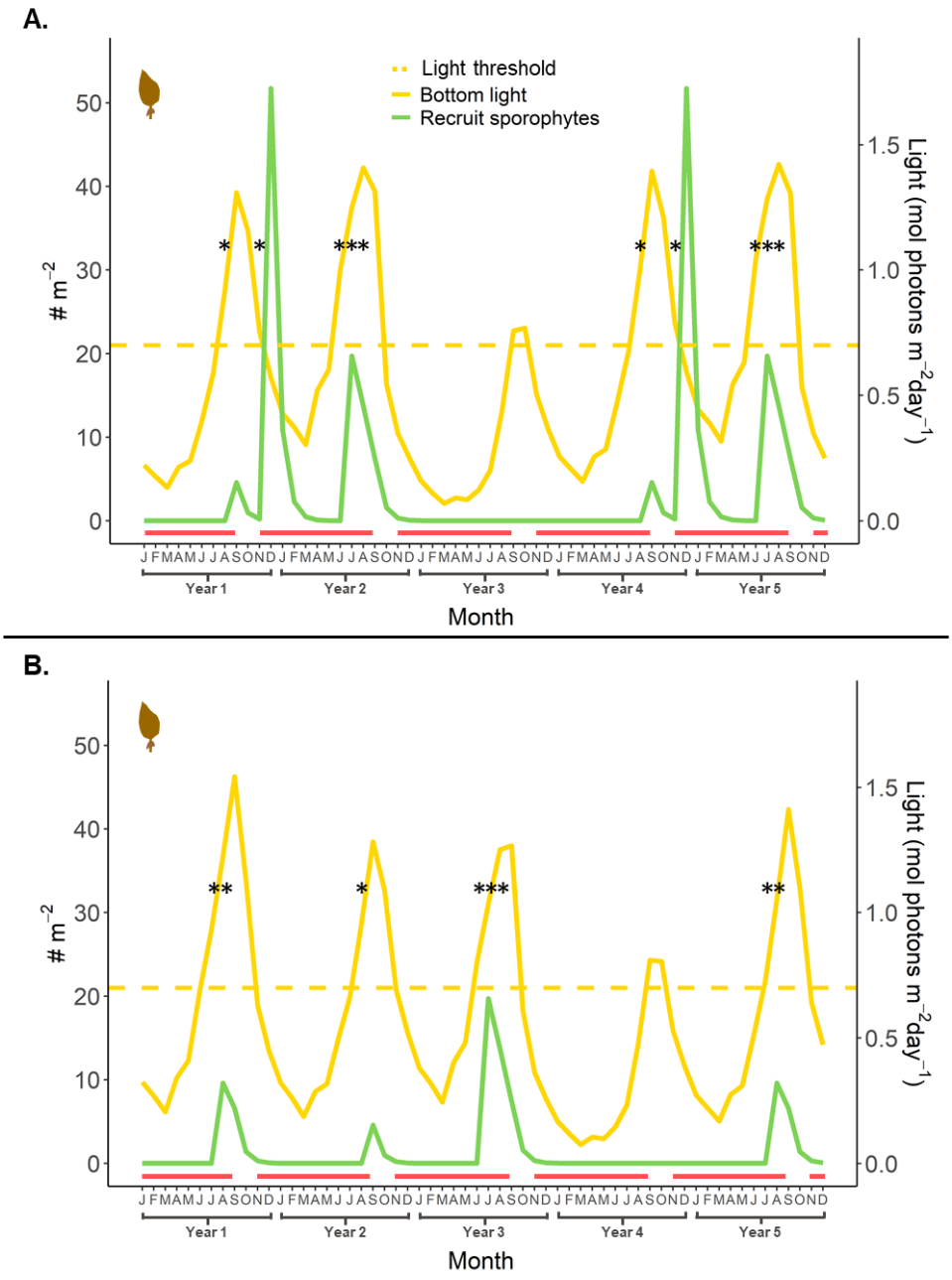
A.
Light threshold
Bottom light
Recruit sporophytes
m^{-2}
Light (mol photons m^{-2}day^{-1})
J F M A M J J A S O N D J F M A M J J A S O N D J F M A M J J A S O N D J F M A M J J A S O N D J F M A M J J A S O N D
Year 1
Year 2
Year 3
Year 4
Year 5
Month
B.
m^{-2}
Light (mol photons m^{-2}day^{-1})
J F M A M J J A S O N D J F M A M J J A S O N D J F M A M J J A S O N D J F M A M J J A S O N D J F M A M J J A S O N D
Year 1
Year 2
Year 3
Year 4
Year 5
Month

Fig. 3-7

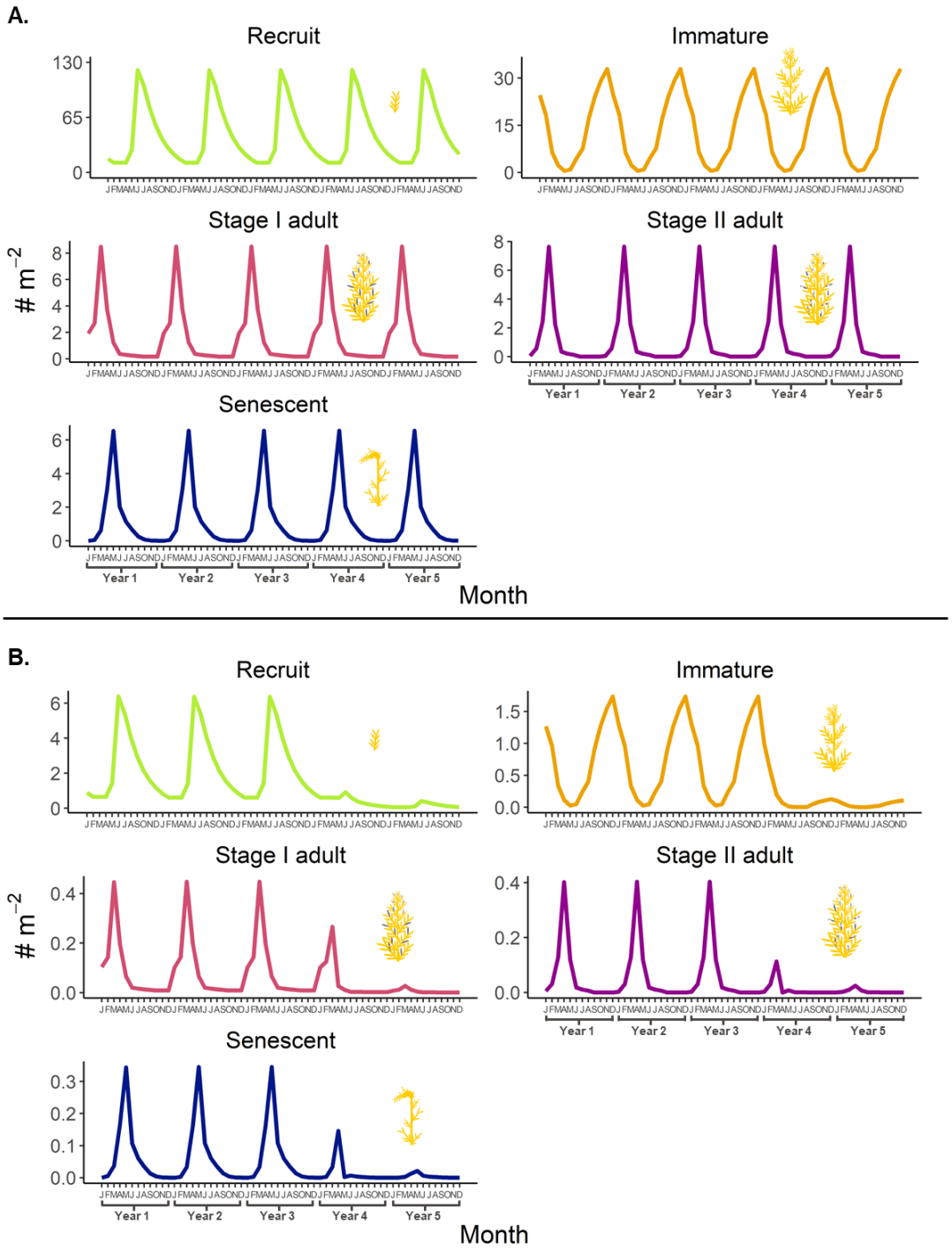
A.
Recruit
Immature
Stage I adult
Stage II adult
Senescent
m^{-2}
Year 1
Year 2
Year 3
Year 4
Year 5
Month
B.
Recruit
Immature
Stage I adult
Stage II adult
Senescent
m^{-2}
Year 1
Year 2
Year 3
Year 4
Year 5
Month

Fig. 3-8

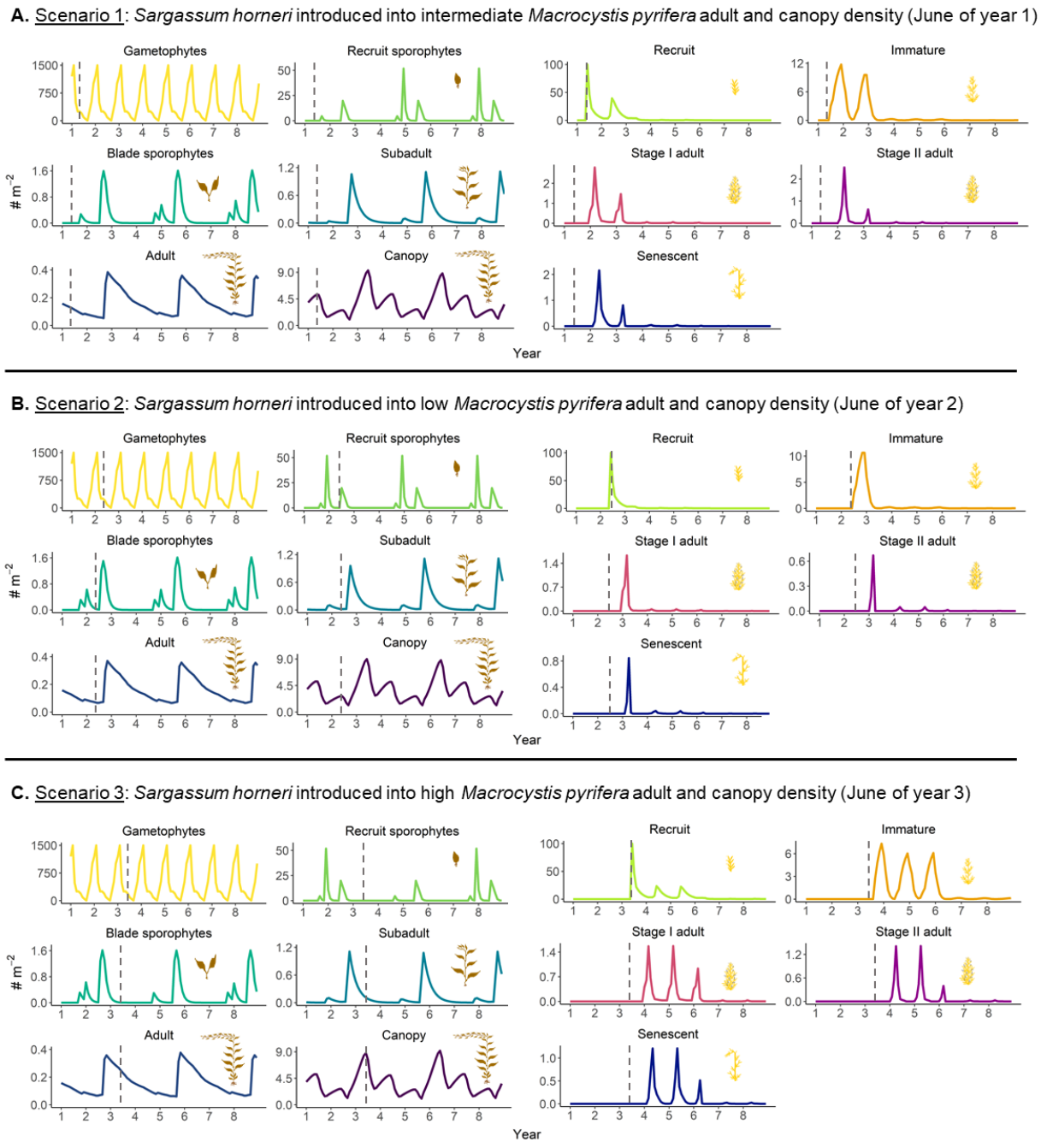
A. Scenario 1: Sargassum horneri introduced into intermediate Macrocystis pyrifera adult and canopy density (June of year 1)
B. Scenario 2: Sargassum horneri introduced into low Macrocystis pyrifera adult and canopy density (June of year 2)
C. Scenario 3: Sargassum horneri introduced into high Macrocystis pyrifera adult and canopy density (June of year 3)
Gametophytes
Recruit sporophytes
Recruit
Immature
Blade sporophytes
Subadult
Stage I adult
Stage II adult
Adult
Canopy
Senescent
m-2
Year

Fig. 3-9

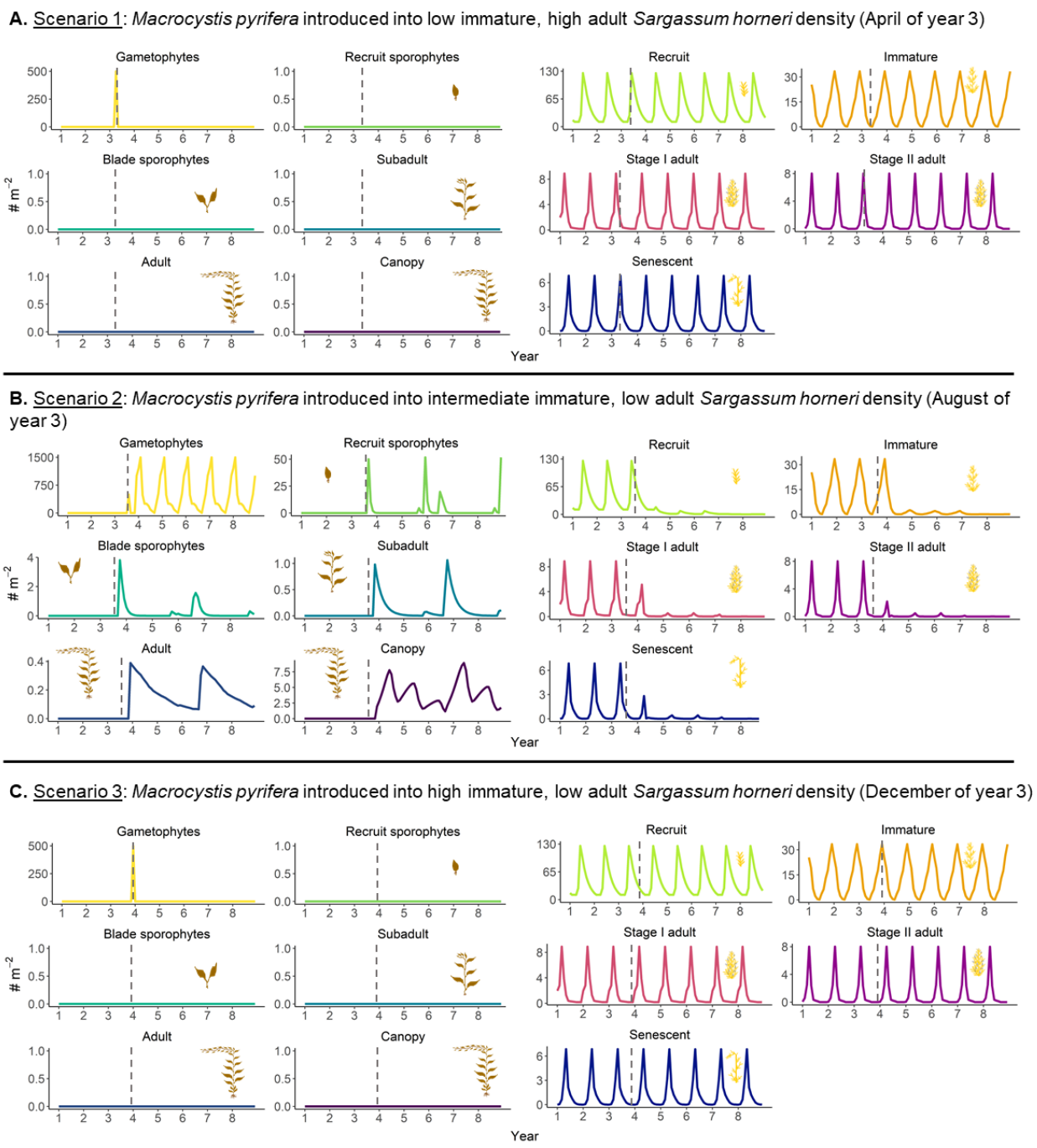
A. Scenario 1: Macrocystis pyrifera introduced into low immature, high adult Sargassum horneri density (April of year 3)
Gametophytes
Recruit sporophytes
Recruit
Immature
Blade sporophytes
Subadult
Stage I adult
Stage II adult
Adult
Canopy
Senescent
m-2
Year
B. Scenario 2: Macrocystis pyrifera introduced into intermediate immature, low adult Sargassum horneri density (August of year 3)
Gametophytes
Recruit sporophytes
Recruit
Immature
Blade sporophytes
Subadult
Stage I adult
Stage II adult
Adult
Canopy
Senescent
m-2
Year
C. Scenario 3: Macrocystis pyrifera introduced into high immature, low adult Sargassum horneri density (December of year 3)
Gametophytes
Recruit sporophytes
Recruit
Immature
Blade sporophytes
Subadult
Stage I adult
Stage II adult
Adult
Canopy
Senescent
m-2
Year

Fig. 3-10

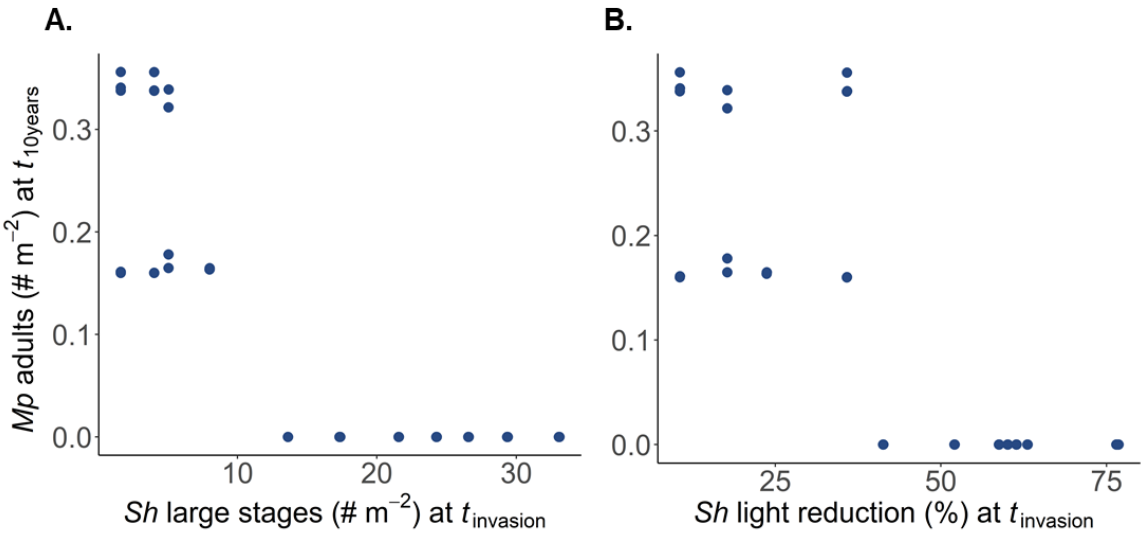

References

Aguilar-Rosas, L.E., Aguilar-Rosas, R., Kawai, H., Uwai, S., and Valenzuela-Espinoza, E. 2007. New record of *Sargasssum filicinum* Harvey (Fucales, Phaeophyceae) in the Pacific Coast of Mexico. *Algae* 22: 17-21. doi: 10.4490/ALGAE.2007.22.1.017

Anderson, E.K., and North, W.J. 1966. In situ studies of spore production and dispersal in the giant kelp, *Macrocystis. Proceedings of the 5th International Seaweed Symposium* (Halifax) 5: 73-86[Young, E.G., McLachlan, J.L. (eds.) Pergamon Press, Oxford]

Anderson, E.K., and North, W.J. 1967. Zoospore release rates in giant kelp, *Macrocystis*. *Bulletin of the Southern California Academy of Sciences* 66: 223-232.

Andrew, N.L., and Viejo, R.M. 1998. Ecological limits to the invasion of *Sargassum muticum* in northern Spain. *Aquatic Botany* 60: 251-263. doi: 10.1016/S0304-3770(97)00088-0

Ang Jr., P.O., and De Wreede, R.E. 1990. Matrix models for algal life history stages. *Marine Ecology Progress Series* 59:171-181. doi: 10.3354/meps059171

Arenas, F., and Fernández, C. 2000. Size structure and dynamics in a population of *Sargassum muticum* (Phaeophyceae). *Journal of Phycology* 36: 1012-1020. doi: 10.1046/j.1529-8817.2000.99235.x

Arenas, F., Vieja, R.M., and Fernández, C. 2002. Density-dependent regulation in an invasive seaweed: responses at plant and modular levels. *Journal of Ecology* 90: 820-829. doi: 10.1046/j.1365-2745.2002.00720.x

Arft, A.M., Walker, M.D., Gurevitch, J., Alatalo, J.M., Bret-Harte, M.S., Dale, M., Diemer, M.,…Wookey, P.A. 1999. Responses of tundra plants to experimental warming: a meta-analysis of the international tundra experiment. *Ecological Monographs* 69(4): 491-511. doi: 10.1890/0012-9615(1999)069[0491:ROTPTE]2.0.CO;2

Balata, D., Piazzi, L., and Cinelli, F. 2004. A comparison among assemblages in areas invaded by *Caulerpa taxifolia* and *C. racemosa* on a subtidal Mediterranean rocky bottom. *Marine Ecology* 25:1–13. doi: 10.1111/j.1439-0485.2004.00013.x

Bax, N., Williamson, A., Aguero, M., Gonzalez, E., and Geeves, W. 2003. Marine invasive alien species: a threat to global biodiversity. *Marine Policy* 27: 313-323. doi: 10.1016/S0308-597X(03)00041-1

Bonsall, M.B., Jansen, V.A.A., and Hassell, M.P. 2004. Life history trade-offs assemble ecological guilds. *Science* 306: 111-114. doi: 10.1126/science.1100680

Britton-Simmons, K.H., and Abbott, K.C. 2008. Short- and long-term effects of disturbance and propagule pressure on a biological invasion. *Journal of Ecology* 96: 68-77. doi: 10.1111 /j.1365-2745.2007.0

Burgman, M.A., and Gerard, V.A. 1990. A stage-structured, stochastic population model for the giant kelp *Macrocystis pyrifera*. Marine Biology 105: 15-23. doi: 10.1007/BF01344266

Carpenter, R.C. 1990. Competition among marine macroalgae: a physiological perspective. *Journal of Phycology* 26: 6-12. doi: 10.1111/j.0022-3646.1990.00006.x

Caselle, J.E., Davis, K., and Marks, L.M. 2018. Marine management affects the invasion success of a non-native species in a temperate reef system in California, USA. *Ecology Letters* 21:43-53. doi: 10.1111/ele.12869

Caswell, H. 2001. Matrix population models: construction, analysis and interpretation. Sinauer Associates, Inc: 2001. p. 713.

Carnell, P.E., and Keough, M.J. 2020. More severe disturbances regimes drive the shift of a kelp forest to a sea urchin barren in south-eastern Australia. *Scientific Reports* 10(1): 11272. doi: 10.1038/s41598-020-67962-y

Cavanaugh, K.C., Reed, D.C., Bell, T.W. Castorani, M.C.N., and Beas-Luna, R. 2019. Spatial variability in the resistance and resilience of giant kelp in Southern and Baja California to a multiyear heatwave. *Frontiers in Marine Science* 6: 413. doi:10.3389/fmars.2019.00413

Chan, F.T., and Briski, E. 2017. An overview of recent research in marine biological invasions. *Marine Biology* 164: 121. doi: 10.1007/s00227-017-3155-4

Chisholm, J.R.M. and Moulin, P. 2003. Stimulation of nitrogen fixation in refractory organic sediments by *Caulerpa taxifolia*. *Limnology and Oceanography* 48:787–94. doi:

10.4319/lo.2003.48.2.0787

Choi, C.G., Kim, H.G., and Sohn, C.H. 2003. Transplantation of young fronds of *Sargassum horneri* for construction of seaweed beds. *Korean Journal of Fisheries and Aquatic Sciences* 36: 469-473. doi: 10.5657/kfas.2003.36.5.469

Choi, H.G., Lee, K.H., Yoo, H.I., Kang, P.J., Kim, Y.S., and Nam, K.W. 2007. Physiological differences in the growth of *Sargassum horneri* between germling and adult stages. *Journal of Applied Phycology* 20: 729-735. doi: 10.1007/s10811-007-9281-5

Choi, S.K., Oh, H.J., Yun, S.H., Lee, H.J., Lee, K., Han, Y.K., Kim, S., and Park, S.R. 2020. Population dynamics of the 'Golden Tides' seaweed, *Sargassum horneri*, on the Southwestern coast of Korea: the extent and formation of golden tides. *Sustainability* 12: 2903. doi: 10.3390/su12072903

Chu, P.C., Chen, Y., and Lu, S. 1998. Temporal and spatial variabilities of Japan Sea surface temperature and atmospheric forcings. *Journal of Oceanography* 54: 273-284. doi: 10.10 07/BF02751702

Clark, R.P., Edwards, M.S., and Foster, M.S. 2004. Effects of shade from multiple kelp canopies on an understory algal assemblage. *Marine Ecology Progress Series* 267: 107-119. doi: 10.3354/meps267107

Cleland, E.E., Chiariella, N.R., Loarie, S.R., Mooney, H.A., and Field, C.B. 2006. Diverse responses of phenology to global changes in a grassland ecosystem. *Proceedings of the National Academy of Sciences* 103(37): 13740-13744. doi: 10.1073/pnas.0600815103

Connolly, B.M., Powers, J., and Mack, R.N. 2017. Biotic constraints on the establishment and performance of native, naturalized, and invasive plants in Pacific Northwest (USA) steppe and forest. *NeoBiota* 34: 21-40. doi: 10.3897/neobiota.34.10820

Corbin, J.D., and D'Antonio, C.M. 2004. Competition between native perennial and exotic annual grasses: implications for a historical invasion. *Ecology* 85: 1273-1283. doi: 10.1890/02-0744

Creed, J.C., Kain, J.M., and Norton, T.A. 1998. An experimental evaluation of density and plant size in two large brown seaweeds. *Journal of Phycology* 34:203-209. 10.1046/j.1529-8817.1998.340039.x

Dayton, P.K., Currie, V., Gerrodette, T., Keller, B.D., Rosenthal, R., and Ven Tresca, D. 1984. Patch dynamics and stability of some California kelp communities. *Ecological Monographs* 54: 253-289. doi: 10.2307/1942498

Dayton, P. and Parnell, P.E.1992. Temporal and spatial patterns of disturbance and recovery in a kelp forest community. *Ecological Monographs* 62(3): 421-445. doi: 0.2307/2937118

Dayton, P.K., and Tegner, M.J. 1984. Catastrophic storms, El Niño and patch stability in a southern California kelp community. *Science* 224: 283-285. doi: 10.1126/science.224.4646.283

Dean, T. A., and Jacobsen, F.R. 1986. Nutrient-limited growth of juvenile kelp, Macrocystis pyrifera, during the 1982-1984 "El Niño" in southern California. *Marine Biology* 90:597-601. doi: 10.1007/BF00409280

Dean, T.A., and Jacobsen, F.R. 1984. Growth of juvenile *Macrocystis pyrifera* (Laminariales) in relation to environmental factors. *Marine Biology* 83: 301-311. doi: 10.1007/BF00397463

Dean, T. A., Thies, K., Lagos, S. L. (1989). Survival of juvenile giant kelp: the effects of demographic factors, competitors, and grazers. *Ecology* 70:483-495.

De Wreede, R.E. 1976. The phenology of three species of *Sargassum* (Sargassaceae, Phaeophyta) in Hawaii. *Phycologia* 15: 175-183. doi: 10.2216/i0031-8884-15-2-175.1

Deysher, L.E. 1984. Reproductive phenology of newly introduced populations of the brown alga, *Sargassum muticum* (Yendo) Fensholt. *Hydrobiologia* 116: 403-407. doi: 10.1007/BF00027710

Deysher, L.E., and Dean, T. A. 1986. In situ recruitment of sporophytes of the giant kelp, Macrocystis pyrifera: effects of physical factors. *Journal of Experimental Marine Biology and Ecology* 103:41-63. doi: 10.1016/0022-0981(86)90131-0

DiLorenzo, E., Cobb, K.M., Furtado, J.C., Schneider, N., Anderson, B.T., Bracco, A., Alexander, M.A., and Vimont, D.J. 2010. Central North Pacific El Niño and decadal climate change in the North Pacific Ocean. *Nature Geoscience* 3: 762-765. doi: 10.1038/NGEO 984

Doney, S.C., Ruckelshaus, M., Duffy, J.E., Barry, J.P., Chan, F., English, C.A., Galindo, H.M., … Talley, L.D. 2012. Climate change impacts on marine ecosystems. *Annual Review of Marine Science* 4: 11-37. doi: 10.1146/annurev-marine-041911-111611

Dumay, O., Fernandez, C., and Pergent, G. 2002a. Primary production and vegetative cycle in *Posidonia oceanica* when in competition with the green algae *Caulerpa taxifolia* and *Caulerpa racemosa*. *Journal of the Marine Biological Association of the United Kingdom* 82:379–87. doi: 10.1017/S0025315402005611

Dunne, J.A., Harte, J., and Taylor, K.J. 2003. Subalpine meadow flowering phenology responses to climate change: integrating experimental and gradient methods. *Ecological Monographs* 73(1): 69-86. doi: 10.1890/0012-9615(2003)073[0069:SM FPRT]2.0.CO;2

Ebeling, A.W., Laur, D., and Rowley, R.J. 1985. Severe storm disturbances and reversal of community structure in a southern California kelp forest. *Marine Biology* 84: 287-294. doi: 10.1007/BF00392498

Edwards, M.S. 2019. Comparing the impacts of four ENSO events on giant kelp (*Macrocystis pyrifera*) in the northeast Pacific Ocean. *Algae* 34(2): 141-151. doi: 10.4490/algae.2019. 34.5.4

Edwards, M.S., and Connell, S.D. 2012. Competition. In C. Wiencke and K. Bischof (Eds.), *Seaweed Ecophysiology and Ecology* (pp. 135-156). Springer.

Evenari, M., and Gutterman, Y. 1985. Desert plants. Pages 41-69 in A.H. Halevy (ed). Handbook of flowering plants. Volume 1. CRC Press, Boca Raton, Florida, USA.

Foster, M.S. 1975. Regulation of algal community development in a *Macrocystis pyrifera* forest. *Marine Biology* 32: 331-342.

Foster, M.S. 1982b. The regulation of macroalgal associations in kelp forests. In: Srivastava L (ed) Synthetic and degradative processes in marine macrophytes. Walter de Gruyter, Berlin.

Friedman, J. 2020. The evolution of annual and perennial plant life histories: ecological correlates and genetic mechanisms. *Annual Review of Ecology, Evolution, and Systematics* 51:461-81. doi: 10.1146/annurev-ecolsys-110218- 024638

Gaitán-Espitia, J.D., Hancock, J.R., Padilla-Gamiño, J.L., Rivest, E.B., Blanchette, C.A., Reed, D.C., and Hofmann, G.E. Interactive effects of elevated temperature and pCO_2 on early-life-history stages of the giant kelp *Macrocystis pyrifera*. *Journal of Experimental Marine Biology and Ecology* 457: 51-58. doi: 10.1016/j.jembe.2014.03.018

Gerard, V.A. 1984a. The light environment in a giant kelp forest: influence of *Macrocystis pyrifera* on spatial and temporal variability. *Marine Biology* 84: 189-195. doi: 10.10 07/BF00393004

Gerard, V.A. 1984b. Physiological effects of El Niño on giant kelp in southern California. *Marine Biology Letters* 5: 317-322.

Grevstad, F.S. 1999. Experimental invasions using biological control introductions: the influence of release size on the chance of population establishment. *Biological Invasions* 1: 313-323. doi: 10.1023/A:1010037912369

Grosholz, E.D. 2002. Ecological and evolutionary consequences of coastal invasions. *Trends in Ecology and Evolution* 17: 22-27. doi: 10.1016/S0169-5347(01)02358-8

Harrer, S.L., Reed, D.C., Holbrook, S.J., and Miller, R.J. 2013. Patterns and controls of the dynamics of net primary production by understory macroalgal assemblages in giant kelp forests. *Journal of Phycology* 49: 248-257. doi: 10.1111/jpy.12023

Hollarsmith, J.A., Buschmann, A.H., Camus, C., and Grosholz, E.D. 2020. Varying reproductive success under ocean warming and acidification across giant kelp (*Macrocystis pyrifera*)

populations. *Journal of Experimental Marine Biology and Ecology* 522: 151247. doi: 10.1016/j.jembe.2019.151247

Hooper, D.U., Chapin III, F.S., Ewel, J.J., Hector, A., Inchausti, P., Lavorel, S., Lawton, J.H., Lodge, D.M.,…Wardel, D.A. 2005. Effects of biodiversity on ecosystem functioning: a consensus of current knowledge. *Ecological Monographs* 75(1): 3-35. doi: 10.1890/04-0922

Inderjit, D.C., Ranelletti, M., and Kaushik, S. 2006. Invasive marine algae: an ecological perspective. *The Botanical Review* 72(2): 153–178.

Jozwik, F.X. 1970. Response of Mitchell grasses (*Astrebla* F. Muell) to photoperiod and temperature. *Australian Journal of Agricultural Research* 21: 395-405. doi: 10.1071/AR9 700395

Kaplanis, N.J., Harris, J.L, and Smith, J.E. 2016. Distribution patterns of the non-native seaweeds *Sargassum horneri* (Turner) C. Agardh and *Undaria pinnatifida* (Harvey) Suringar on the San Diego and Pacific coast of North America. *Aquatic Invasions* 11(2): 111-124. doi: 10.33 91/ai.2016.11.2.01

Katsanevakis, S., Wallentinus, I., Zenetos, A., Leppakoski, E., Cinar, M., Ozturk, B., Grabowski, M., Golani, D., and Cardosos, A.C. 2014. Impacts of invasive alien marine species on ecosystem services and biodiversity: a pan-Europena review. *Aquatic Invasions* 9(4): 391-423. doi: 10.3391/ai.2014.9.4.01

Kettenring, K.M., and Adams, C.R. 2011. Lessons learned from invasive plant control experiments: a systematic review and meta-analysis. *Journal of Applied Ecology* 48: 970-979. doi: 10.1111/j.1365-2664.2011.01979.x

Ladah, L.B., and Zertuche-González, J.A. 2007. Survival of microscopic stages of a perennial kelp (*Macrocystis pyrifera*) from the center and the southern extreme of its range in the Northern Hemisphere after exposure to simulated El Niño stress. *Marine Biology* 152: 677-686. doi: 10.1007/s00227-007-0723-z

Lancaster, L.T., Morrison, G., and Fitt, R.N. 2017. Life history trade-offs, the intensity of competition, and coexistence in novel and evolving communities under climate change. *Philosophical Transactions of the Royal Society B* 372: 20160046. doi: 10.1098/rstb.20 16.0046

Leslie, P.H. 1945. On the use of matrices in certain population mathematics. *Biometrika* 35: 183-212.

Lubchenco, J., and Menge, B.A. 1978. Community development and persistence in a low rocky intertidal zone. *Ecological Monographs* 48(1): 67-95. doi: 10.2307/2937360

Mathieson, A. C., Dawes, C.J., Harris, L.G., and Hehre, E.J. 2003. Expansion of the Asiatic

green alga *Codium fragile* ssp. *tomentosoides* in the Gulf of Maine. *Rhodora* 105: 1-53.

Marks, L.M., Reed, D.C. and Holbrook, S.J. 2018. Life history traits of the invasive seaweed *Sargassum horneri* at Santa Catalina Island, California. *Aquatic Invasions* 13(3): 339-350. doi: 10.3391/ai.2018.13.3.03

Marks, L.M., Reed, D.C., and Holbrook, S.J. 2020a. Niche complementarity and resistance to grazing promote the invasion success of *Sargassum horneri* in North America. *Diversity* 12(2): 54. doi: 10.3390/d12020054

Marks, L.M., Reed, D.C., and Obaza, A.K. 2017. Assessment of control methods for the invasive seaweed *Sargassum horneri* in California, USA. *Management of Biological Invasions* 8(2): 205–213. doi: 10.3391/mbi.2017.8.2.08

Marks, L.M., Salinas-Ruiz, P., Reed, D.C., Holbrook, S.J., Culver, C.S., Engle, J.M., Kushner, D.J., Caselle, J.E., Freiwald, J., Williams, J.P., Smith, J.R., Aguilar-Rosas, L.E., and Kaplanis, N.J. 2015. Range expansion of a non-native, invasive macroalga *Sargassum horneri* (Turner) C. Agardh, 1820 in the eastern Pacific. *BioInvasions Records* 4(4): 243–248. doi: 10.3391/bir.2015.4.4.02

Mason, R.A.B., Cooke, J., Moles, A.T., and Leishman, M.R. 2008. Reproductive output of invasive versus native plants. *Global Ecology and Biogeography* 17: 633-640. doi: 10.1111/j.1466-8238.2008.00402.x

Melbourne, B.A., Cornell, H.V., Davies, K.F., Dugaw, C.J., Elmendorf, S., Freestone, A.L., Hall, R.J.,…Yokomizo, H. 2007. Invasion in a heterogenous world: resistance, coexistence or hostile takeover? *Ecology Letters* 10: 77-94. doi: 10.1111/j.1365-2745.2007.0

Mikami, A., Komatsu, T., Aoki, M., Yokohama, Y. 2006. Seasonal changes in growth and photosynthesis-light curves of *Sargassum horneri* (Fucales, Phaeophyta) in Oura Bay on the coast of central Honshu, Japan. La Mer 44: 109-118.

Minchinton, T.E.,and Bertness, M.D. 2003. Disturbance-mediated competition and the spread of *Phragmites australis* in a coastal marsh. *Ecological Applications* 13: 1400–1416. doi: 10. 1890/02-5136

North, W.J., Jackson, G.A., and Manley, S.L. 1986. *Macrocystis* and its environment, knowns and unknowns. *Aquatic Botany* 26: 9-26. doi: 10.1016/0304-3770(86)90003-3

Olson, A., and Lubchenco, J. 1990. Competition in seaweeds: linking plant traits to competitive outcomes. *Journal of Phycology* 26: 1-6. doi: 10.1111/j.0022-3646.1990.00001.x

Paine, R.T. 1990. Benthic macroalgal competition: complications and consequences. *Journal of Phycology* 26: 12-17. doi: 10.1111/j.0022-3646.1990.00012.x

Panetta, F.D., and Randall, R.P. 1994. An assessment of the colonizing ability of *Emex australis.*

Australian Journal of Ecology 19: 76-82. doi: 10.1111/j.1442-9993.1994.tb01546.x

Papacostas, K.J., Rielly-Carroll, E.W., Georgian, S.E., Long, D.J., Princiotta, S.D., Quattrini,A.M., Reuter, K.E., and Freestone, A.L. 2017. Biological mechanisms of marine invasions. *Marine Ecology Progress Series* 565: 251-268. doi: 10.3354/mep s12001

R Core Team. 2017. R: A language and environment for statistical computing. R Foundation for Statistical Computing, Vienna, Austria. www.r-project.org.

Reed, D.C., Ebeling, A.W., Anderson, T.W., and Anghera, M. 1996. Differential reproductive responses to fluctuating resources in two seaweeds with different reproductive strategies. *Ecology* 77(1):300-316. doi: 10.2307/2265679

Reed, D.C., and Foster, M. S. 1984. The effects of canopy shadings on algal recruitment and growth in a giant kelp forest. *Ecology* 65(3): 937-948. doi: 10.2307/1938066

Reed, D.C., Laure, D.R., and Ebeling, A.W. 1988. Variation in algal dispersal and recruitment: the importance of episodic events. *Ecological Monographs* 58: 321-335. doi: 10.2307/1 942543

Reed, D.C., Neushul, M., and Ebeling, A.W. 1992. Role of settlement density on gametophyte growth and reproduction in the kelps *Pteryogophora californica* and *Macrocystis pyrifera* (Phaeophyceae). *Journal of Phycology* 27(3): 361-366. doi: 10.1111/j.0022-3646.1991.00 361.x

Reed, D.C., Washburn, L., Rassweiler, A., Miller, R., Bell, T., and Harrer, S. 2016. Extreme warming challenges sentinel status of kelp forests as indicators of climate change. *Nature Communications* 7: 13747. doi: 10.1038/ncomms13757

Reed, D., Rassweiler, A., and Arkema, K. 2009. Density derived estimates of standing crop and net primary production in the giant kelp *Macrocystis pyrifera*. *Marine Biology* 156: 2077-2083. doi: 10.1007/s00227-009-1238-6

Rilov, G., Mant, R., Lyons, D., Bulleri, F., Benedetti-Cechi, L., Kotta, J., Quierós, A.M,…Guy-Haim, T. 2012. How strong is the effect of invasive ecosystem engineers on the distribution patters of local species, the local and regional biodiversity and ecosystem functions? *Environmental Evidence* 1: 1-10. doi: 10.1186/2047-2382-1-10

Rosenthal, R.J., Clarke, W.D., and Dayton, P.K. 1974. Ecology and natural history of a stand of giant kelp, *Macrocystis pyrifera*, off Del Mar, California. *Fisheries Bulletin US* 72: 670-684.

Sánchez, I., and Fernández, C. 2005. Impact of the invasive seaweed *Sargassum muticum* (Phaeophyta) on an intertidal macroalgal assemblage. *Journal of Phycology* 41: 923-30. doi: 10.1111/j.1529-8817.2005.00120.x

SBC LTER (Santa Barbara Coastal LTER), Marks, L., Reed, D., and Holbrook, S. 2018. SBC LTER: Sargassum horneri life history in southern California ver 1. Environmental Data Initiative. doi: 10.6073/pasta/d684a982c9154fbcc70805ad360534d9

Schiel, D.R., and Choat, J.H. 1980. Effects of density on monospecific stands of marine algae. *Nature* 285: 324-326. doi: 10.1038/285324a0

Schiel, D.R., and Foster, M.S. 2015. *The biology and ecology of giant kelp forests.* University of California Press.

Seebens, H., Gastner, M.T., and Blasius, B. 2013. The risk of marine bioinvasion caused by global shipping. *Ecology Letters* 16: 782-790. doi: 10.1111/ele.12111

Simberloff, D., Martin, J.L., Genovesi, P., Maris, V., Wardle, D.A., Aronson, J., Courchamp, F., Galil, B.,…Vilá, M. 2013. Impacts of biological invasions: what's what and the way forward. *Trends in Ecology and Evolution* 28(1): 58-66. doi: 10.1016/j.tree.2012.07.013

Smale, D.A., Wernberg, T., Oliver, E.C.J., Thomsen, M., Harvey, B.P., Straub, S.C., and Burrows, M.T. 2019. Marine heatwaves threaten global biodiversity and the provision of ecosystem services. *Nature Climate Change* 9: 306-12. doi: 10.1038/s41558-019-0412-1

South, P.M., and Thomsen, M.S. 2016. The ecological role of invading *Undaria pinnatifida*: an experimental test of the driver-passenger models. *Marine Biology* 163: 175. doi: 10.100 7/s00227-016-2948-1

Stachowicz, J.J., Terwin, J.R., Whitlatch, R.B., and Osman, R.W. 2002. Linking climate change and biological invasions: ocean warming facilitates nonindigenous species invasions. *Proceedings of the National Academy of Sciences* 99: 15497-15500. doi: 10.1073/pnas .2424374 99

Steneck, R., Graham, M.H., Bourque, B.J., Corbett, D., Erlandson, J.M., Estes, J.A., and Tegner, M.J. Kelp forest ecosystems: biodiversity, stability, resilience, and future. *Marine Sciences Faculty Scholarship* 65.

Sullaway, G., and Edwards, M. 2020. Impacts of the non-native alga, *Sargassum horneri*, on benthic community production in a California kelp forest. *Marine Ecology Progress Series* 637: 45-57. doi: 10.3354/meps13231

Tait, L.W., South, P.M., Lilley, S.A., Thomsen, M.S., and Schiel, D.R. 2015. Assemblage and understory carbon production of native and invasive canopy-forming macroalgae. *Journal of Experimental Marine Biology and Ecology* 469: 10-17. doi: 10.1016/j.jembe .2015.04.007

Title 14§Section 650, California Code of Regulations

Trowbridge C.D. 2002. Coexistence of introduced and native congeneric algae: *Codium fragile* and *Codium fragile* spp. *tomentosoides* on Irish rocky intertidal shores. *Journal of the Marine Biological Association of the United Kingdom* 81: 931–937. doi: 10.1017/S0025315401004854

Vaz-Pinto, F., Martínez, B., Olabarria, C., and Arenas, F. 2014. Neighborhood competition in coexisting species: the native *Cystoseira humilis* vs. the invasive *Sargassum muticum*. *Journal of Experimental Marine Biology and Ecology* 454: 32-41. doi: 10.1016/j.jembe.2014.02.001

Wickham, H. 2016. ggplot2: Elegant graphics for data analysis. Springer-Verlag New York.

Williams, S.L. and Smith, J.E. 2007. A global review of the distribution, taxonomy, and impacts of introduced seaweeds. *Annual Review of Ecology, Evolution, and Systematics* 38(1): 327–359. doi: 10.1146/annurev.ecolsys.38.091206.095543

Wood, S.N. 1997. Inverse problems and structured-population dynamics. In: Tuljapurkar, S., Caswell, H. (eds.). Structured-population models in marine, terrestrial, and freshwater systems SE-19. Springer US; pp.55-586. doi: 10.1007/978-1-4615-5973-3_19

Yoshida, T. 1983. Japanese species of *Sargassum* subgenus *Bactrophycus* (Phaeophyta, Fucales). *Journal of the Faculty of Science, Hokkaido University. Series 5, Botany* 13: 99-246.

Yoshida, G., Yoshikawa, K., and Terawaki, T. 2001. Growth and maturation of two populations of *Sargassum horneri*, (Fucales, Phaeophyta) in Hiroshima Bay, the Seto Inland Sea. *Fisheries Science* 67: 1023-1029. doi: 10.1046/j.1444-2906.2001.00357.x

APPENDIX 1 – CHAPTER 1 SUPPLEMENT

Supplementary results

Table 1-S1. Statistical results of 1-factor ANOVA (for non-parametric equivalent, see Table 1-S2) for algal functional groups and species. Tests conducted for thallus toughness, thallus tensile strength, and relative growth for tropical and temperate algal species. *P*-values lower than Bonferroni's corrected alpha are statistically significant (denoted in bold).

	Source of Variation	*Df*	*SS*	*MS*	*F*	*P*
A.	**Toughness**					
ANOVA	<u>Tropical</u>					
	Functional Group	4	471.97	117.99	327.61	**<0.001**
	Residuals	125	45.02	0.36		
	Species	12	16.24	1.35	321.3	**<0.001**
	Residuals	117	0.49	0.01		
	<u>Temperate</u>					
	Functional Group	3	15.05	5.02	165.75	**<0.001**
	Residuals	196	5.93	0.03		
B.	**Tensile**					
ANOVA	<u>Tropical</u>					
	Functional Group	4	8.98	2.24	13.43	**<0.001**
	Residuals	112	18.72	0.17		
	Species	12	645.66	53.80	46.47	**<0.001**
	Residuals	104	120.42	1.16		
	<u>Temperate</u>					
	Functional Group	3	14.22	4.74	53.7	**<0.001**
	Residuals	196	17.30	0.09		
C.	**Growth**					
ANOVA	<u>Tropical</u>					
	Functional Group	2	3.17	1.58	17.75	**<0.001**
	Residuals	45	4.02	0.09		
	Species	5	22.58	4.52	56.26	**<0.001**
	Residuals	42	3.37	0.08		
	<u>Temperate</u>					
	Functional Group	2	0.81	0.41	6.46	**<0.001**
	Residuals	37	2.32	0.06		
	Species	4	1.40	0.35	7.08	**0.004**
	Residuals	35	1.73	0.05		

Table 1-S2. Statistical results of 1-factor Kruskal-Wallis test (for parametric equivalent, see Table 1-S1) for algal species. Tests conducted for thallus toughness, thallus tensile strength, and relative growth for tropical and temperate algal species. *P*-values lower than Bonferroni's corrected alpha are statistically significant (denoted in bold).

	Source of Variation	***Df***	***ChiSquare***	***Prob>ChiSq***
A.	**Toughness**			
	Temperate Species	19	188.76	**<0.001**
B.	**Tensile**			
	Temperate Species	19	192.07	**<0.001**

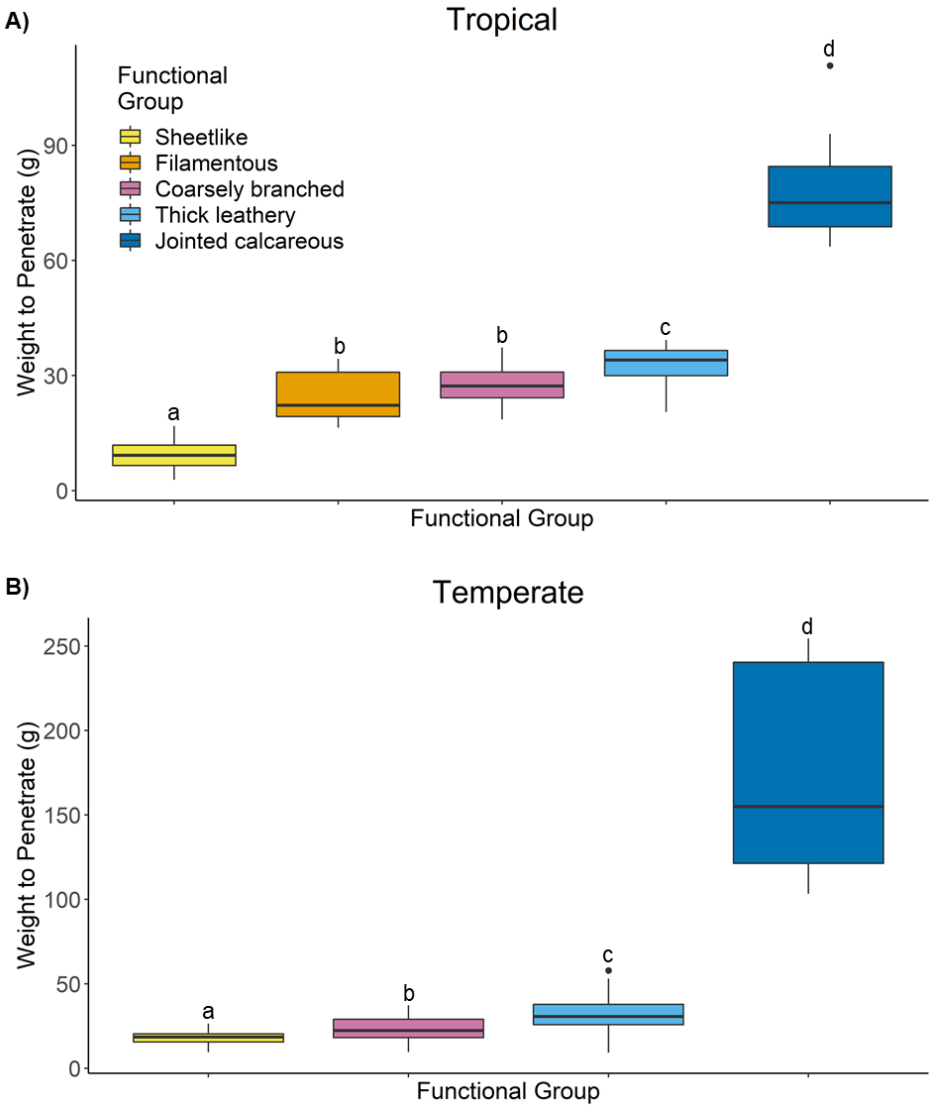

Fig. 1-S1. Thallus toughness by functional group for tropical (panel A) and temperate (panel B) algae. Individual bars represent weight to penetrate (g), colors represent functional group designations. Lower and upper box boundaries are 25th and 75th percentiles, respectively, line inside box designate medians, lower and upper error lines represent ±1.5*IQR (interquartile range), respectively, with filled circles designating data falling outside ±1.5*IQR. Note difference in scales.

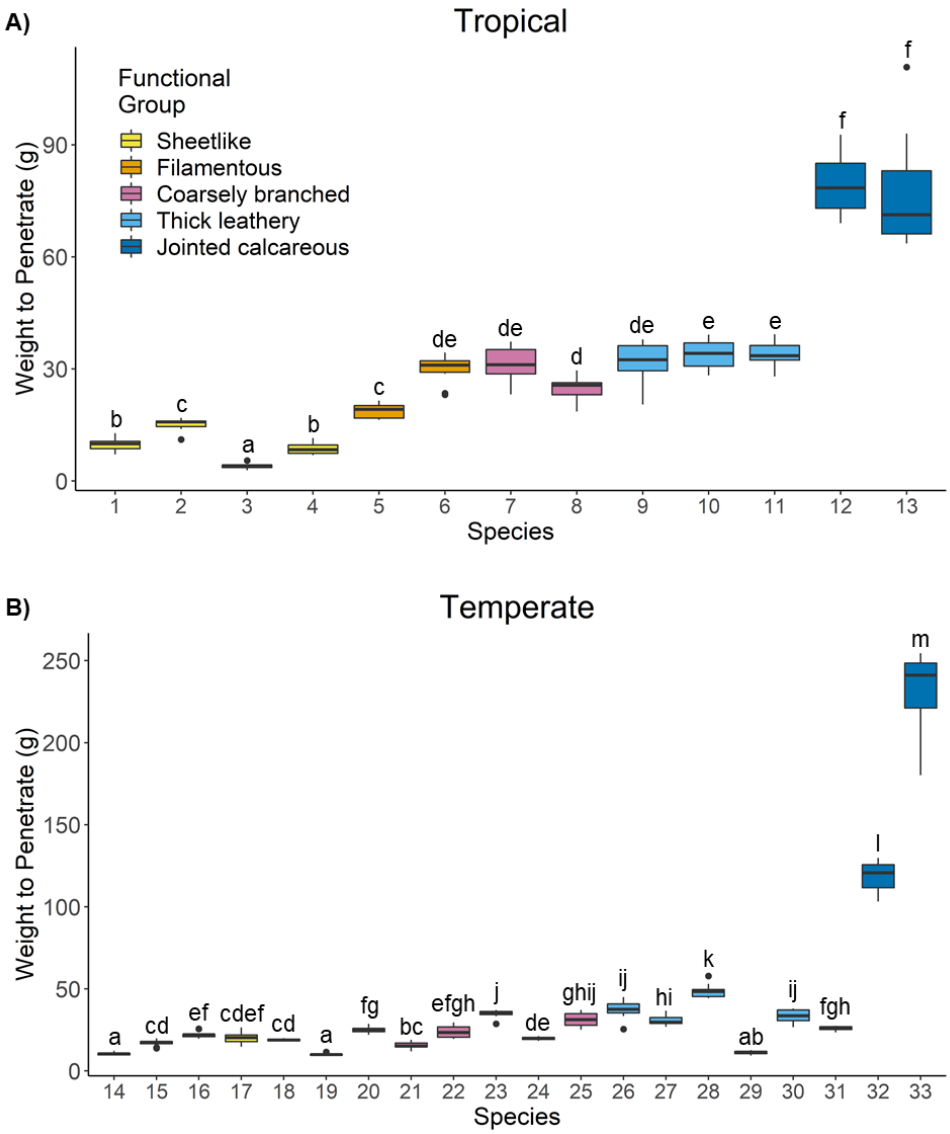

Fig. 1-S2. Thallus toughness by species for tropical (panel A) and temperate (panel B) algae. Individual bars represent weight to penetrate (g) each species' thallus, colors represent each species' functional group designation. For species numbers on x-axis, refer to Table 1-2. Lower and upper box boundaries are 25th and 75th percentiles, respectively, line inside box designate medians, lower and upper error lines represent ±1.5*IQR (interquartile range), respectively, with filled circles designating data falling outside ±1.5*IQR. Note difference in scales.

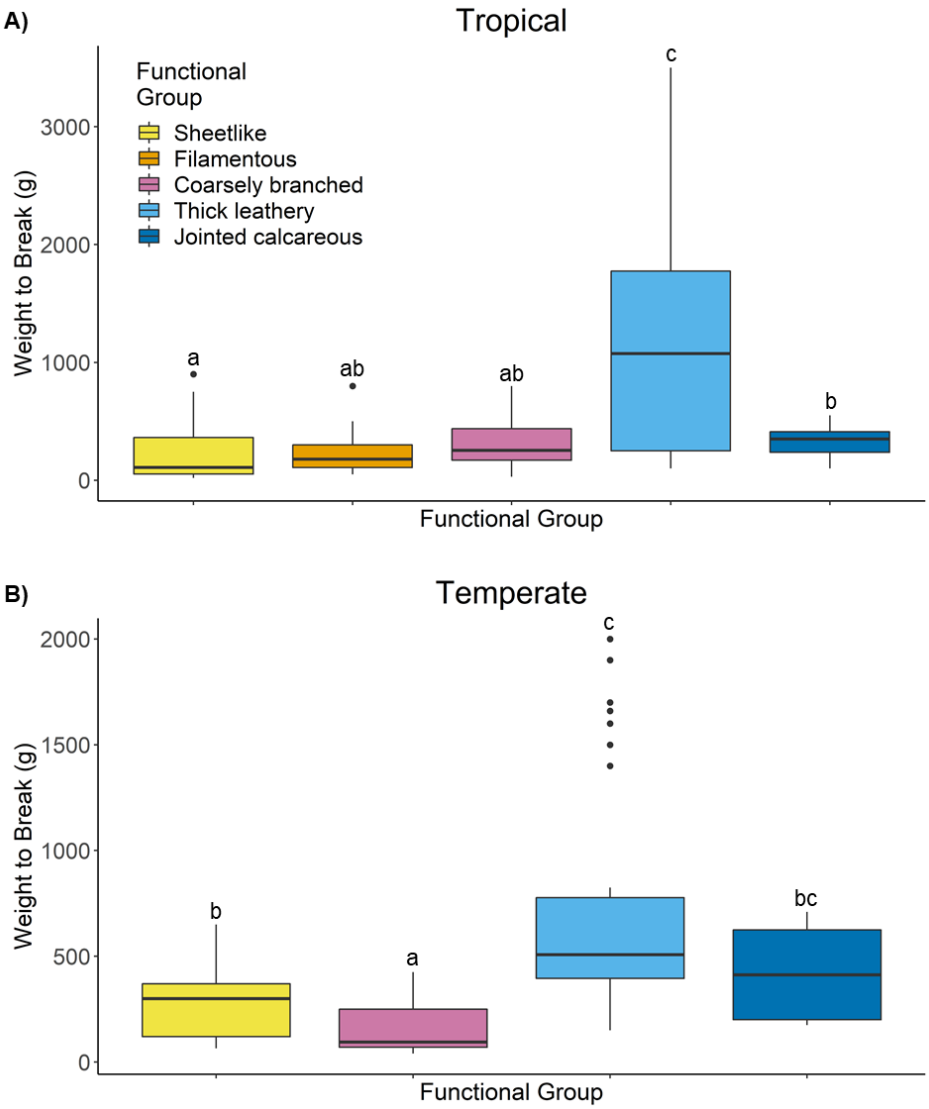

Fig. 1-S3. Thallus tensile strength by functional group for tropical (panel A) and temperate (panel B) algae. Individual bars represent weight to break (g), colors represent functional group designations. Lower and upper box boundaries are 25th and 75th percentiles, respectively, line inside box designate medians, lower and upper error lines represent ±1.5*IQR (interquartile range), respectively, with filled circles designating data falling outside ±1.5*IQR. Note difference in scales.

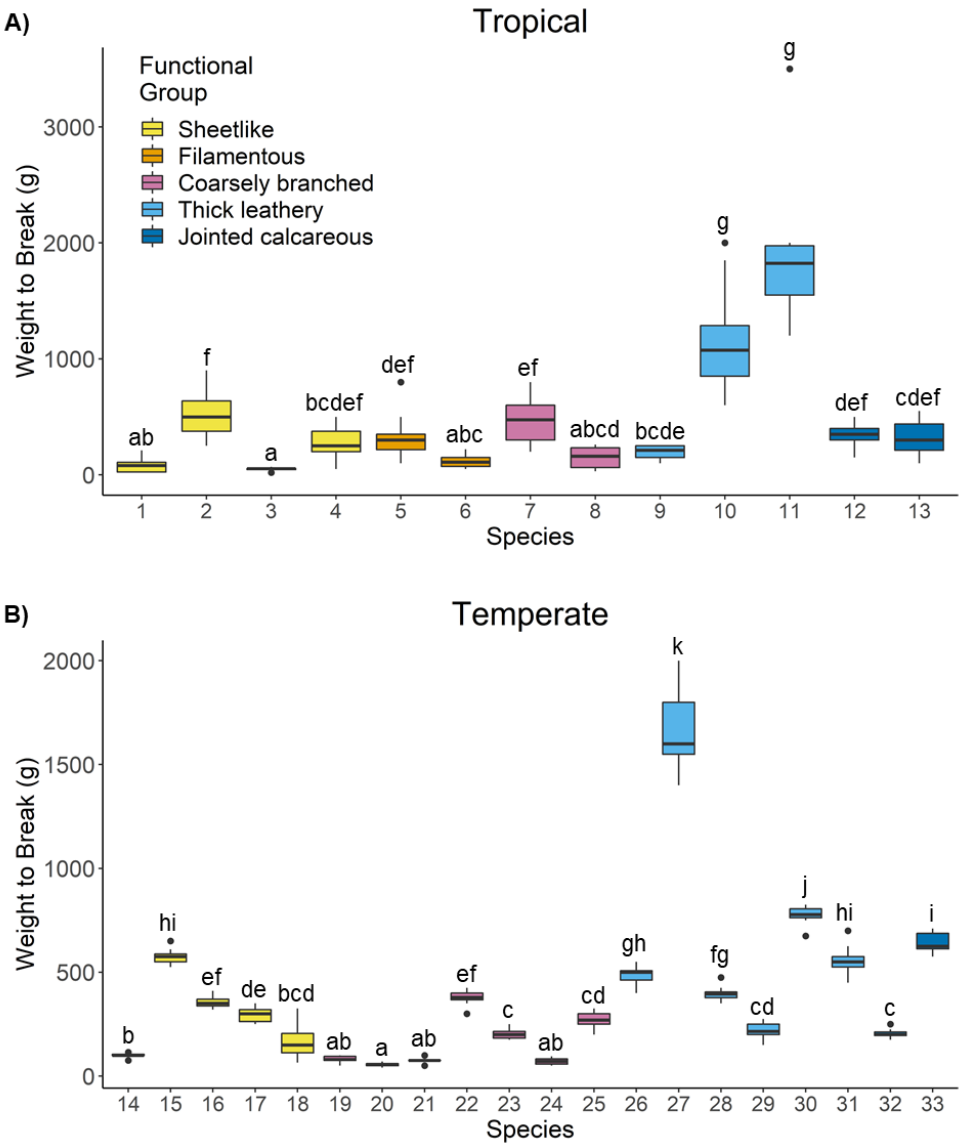

Fig. 1-S4. Thallus tensile strength by species for tropical (panel A) and temperate (panel B) algae. Individual bars represent weight to break (g) each species' thallus, colors represent each species' functional group designation. For species numbers on x-axis, refer to Table 1-2. Lower and upper box boundaries are 25th and 75th percentiles, respectively, line inside box designate medians, lower and upper error lines represent ±1.5*IQR (interquartile range), respectively, with filled circles designating data falling outside ±1.5*IQR. Note difference in scales.

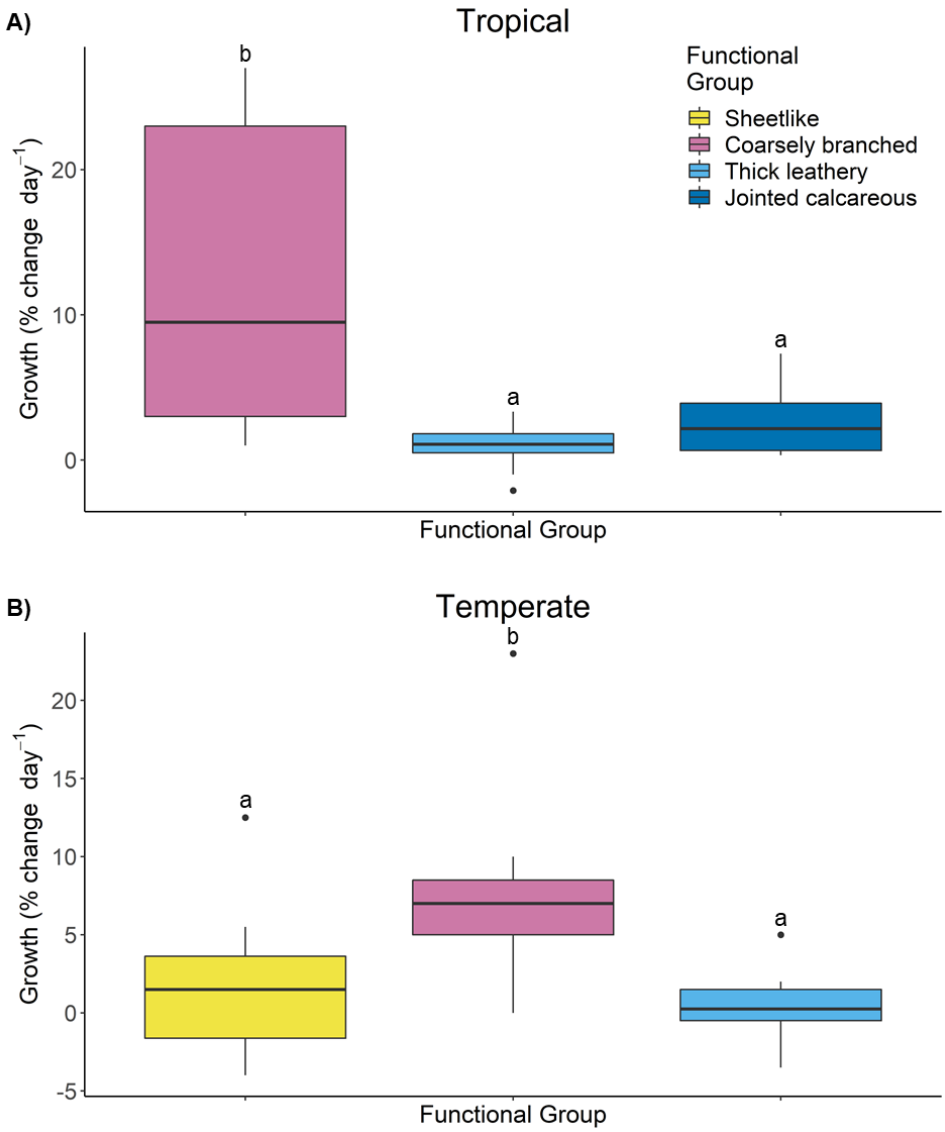

Fig. 1-S5. Relative growth by functional group for tropical (panel A) and temperate (panel B) algae. Individual bars represent growth, colors represent functional group designations. Lower and upper box boundaries are 25th and 75th percentiles, respectively, line inside box designate medians, lower and upper error lines represent ±1.5*IQR (interquartile range), respectively, with filled circles designating data falling outside ±1.5*IQR. Note difference in scales.

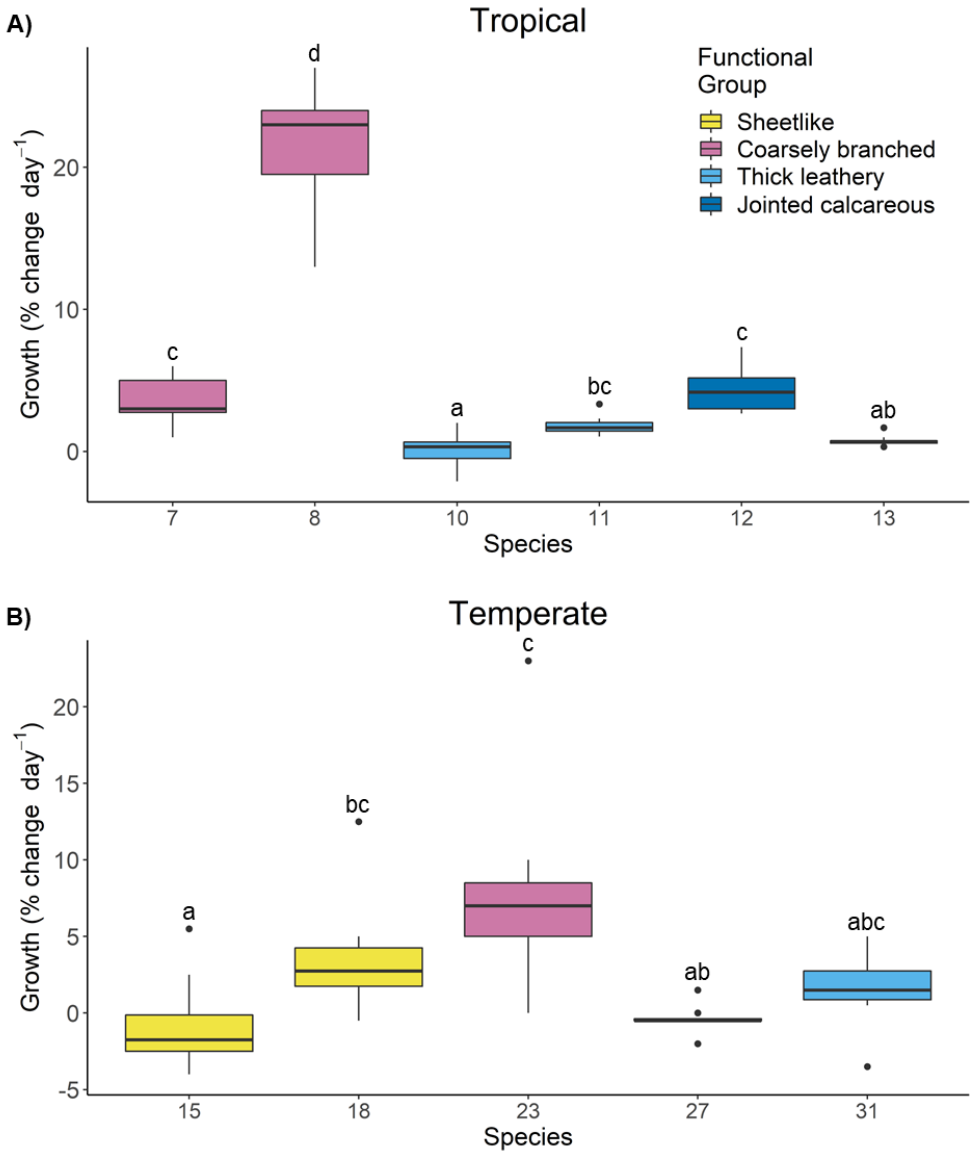

Fig. 1-S6. Relative growth by species for tropical (panel A) and temperate (panel B) algae. Individual bars represent growth, colors represent each species' functional group designation. For species numbers on x-axis, refer to Table 1-2. Lower and upper box boundaries are 25th and 75th percentiles, respectively, line inside box designate medians, lower and upper error lines represent ±1.5*IQR (interquartile range), respectively, with filled circles designating data falling outside ±1.5*IQR. Note difference in scales.

APPENDIX 2 – CHAPTER 2 SUPPLEMENT

Supplementary methods

Site characterization (relief and inanimate cover) methods

Relief type (high, medium, or low) was characterized for each quadrat. Relief was determined by estimating the difference in height between the highest and lowest points within each quadrat, with the differences being ~0-0.5m for low relief, ~0.5-1.5m for medium relief, and ~>1.5m for high relief. Additionally, using the point-intercept method, the principal cover categories (algae, inanimate, non-mobile invertebrate) were identified under 45 intersecting points within each $1m^2$ quadrat. Inanimate substrate categories were classified as rock, sand, sediment/mud, or shell debris.

The number of quadrats characterized for each relief type were divided by the total number of quadrats for each site to calculate the proportion of each relief type at each site (n=20, N=80). Mean percent cover per m^2 of each inanimate category by averaging percent cover by category for each quadrat for each site (n=20, N=80). We analyzed inanimate cover by site via a 1-factor PERMANOVA as data did not meet assumptions for parametric statistics and significant tests were followed by a Pillai post-hoc comparison.

Supplementary results

Site characterization (relief and substrate) results

Sites were generally characterized as medium relief (Fig. 2-S1), and inanimate percent cover was significantly different among sites (PERMANOVA, *pseudo-F*(3,71)=6.4, $p<0.001$). Post-hocs revealed all sites were statistically similar in inanimate cover except for -D+U. Inanimate percent cover was generally low across all sites, with rock percent cover highest in -

D+U and +D+U and the other sites characterized by a more even distribution of inanimate categories (Fig. 2-S2).

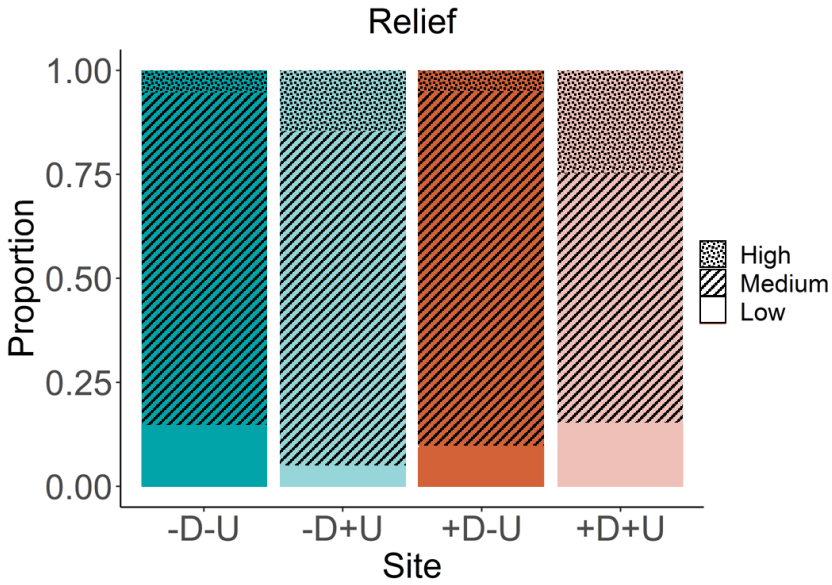

Fig. 2-S1. Proportion of relief types (low=0-0.5m, medium=0.5-1.5m, high=>1.5m) across sites, with different patterns representing the different relief types.

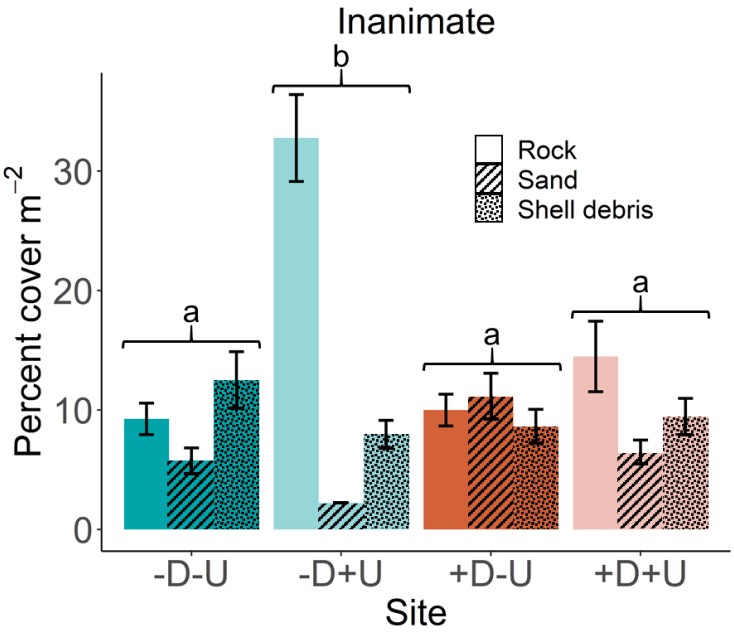

Fig. 2-S2. Mean percent cover (±SE) of different inanimate categories across sites, with different pattern representing different inanimate categories. Sites with different lowercase are significantly different.

APPENDIX 3 – CHAPTER 3 SUPPLEMENT

S1: Marks et al. (2018) field survey methods

Marks et al. (2018) surveyed *S. horneri* populations at 31 sites on the leeward side of Santa Catalina Island every 1-3 months from June 2013-June 2015. At each site, divers counted all *S. horneri* individuals in eight, $1m^2$ quadrats regularly spaced every 5m along a 40m transect following a 7m depth contour. The height of every individual was measured and classified by life history stage. Finally, the biomass of each stage was quantified to develop height/weight relationships by collecting representative samples of each life stage (n=35, 85, 104, 65, and 29 for recruit, immature, stage I adults, stage II adults, and senescent stages, respectively). These data are publicly available via the Santa Barbara Long-Term Ecological Research Network Data Portal (SBC LTER et al. 2018) and were the primary data source for developing the single-species *S. horneri* model.

S2: *S. horneri* model parameterization information

Ang and De Wreede (1990) describe a generalized *Sargassum* life-history as occurring in three distinct phases lasting approximately four months each. First is a slow growth phase where only the smallest individuals are present. This is followed by a period of fast growth, where small individuals rapidly transition into larger, more mature stages. The final phase is characterized by reproduction, senescence, and recruitment, where, following embryo release, mature individuals decay and new individuals begin to appear in the population. Ang and De Wreede (1990) used these phases to inform parameterization of a stage-structured model for *Sargassum siliquosum*, a tropical species, where each phase was characterized by two unique transition matrices representing two months with parameter values derived from field surveys.

We estimated transition probabilities with unique values of G_{ji}, X_{ii}, and b_S from

field data (SBC LTER et al. 2018) for each of the six 2-month matrices (two matrices for each 4-month phase in Table 3-2, main text) so that:

$$D(t+1) = MD(t) \quad \text{(S1)}$$

Where D corresponds to the field data at time t and M corresponds to the transition matrix of parameters we wanted to estimate; in these simulations, timesteps were two months. Thus, we sought parameter values for elements of M that, when multiplied by $D(t)$ or the observed field densities at time t, result in the observed field densities in the next month $D(t+1)$ within each phase. To do so, we utilized Wood's quadratic programming method (Wood 1997) as described by Caswell (2001, section 6.2.2.), that seeks to minimize the sum of squared deviations between $D(t+1)$ and $MD(t)$ to estimate values of M when subject to certain value constraints. The general notation for the quadratic programming method is as follows:

$$minimize\ \frac{p^T G p}{2} + f^T p \quad \text{(S2)}$$

$$subject\ to\ Cp \leq b$$

$$where\ G = D^T D\ and\ f^T = -z^T D$$

Where D represents $D(t)$, z corresponds to $D(t+1)$, C corresponds to the matrix of parameter constraints, p corresponds to positions of non-zero elements in matrix M, or the parameters we are trying to estimate, and b corresponds to the vector of parameter constraints. Superscript T denotes the transpose of an element. To utilize quadratic programming to generate parameter estimates for our transition matrix (M), we used the *QPmat* function from the "popbio" package (Stubben and Milligan 2007) along with the "quadprog" package (Turlach et al. 2019) in R, which takes C, p, b, and the field data matrix (D(t) and $D(t+1)$ combined), as arguments to generate parameter estimations for our transition matrix (M). To do so, we first defined the vector of non-zero elements (p) (Fig. 3-S1A) corresponding to the positions in our transition

matrix (*M*; Fig. 3-4, main text) that were non-zero, as described in Caswell (2001, section 6.2.2.) and Bordehore et al. 2015. Next, we defined a matrix of parameter constraints (*C*), constraining all parameters to be ≥0 and column sums of survival and growth parameters to be ≤1 (Fig. 3-S1B). In matrix *C*, the first 10 rows correspond to parameter constraints ≥0, with the principal diagonal corresponding to each parameter in matrix *M*. The last five rows in matrix *C* guarantee that $X_{S11}+G_{S21}$, $X_{S22}+G_{S32}$, $X_{S33}+G_{S43}$, $X_{S44}+G_{S54}$, and X_{S55} are all ≤1. The recruitment rate (b_S) is omitted from the last five rows of matrix *C* because it can be >1. Finally, we defined vector constraints (*b*) (Fig. 3-S1C), which is equivalent to the maximum value of each row in matrix *C*. We then input *C, p, b,* along with the first two-month field data matrix (December-January) as arguments in the *QPmat* R function to generate parameter estimations for our transition matrix (*M*). We repeated this process for each two-month field data matrix until we had six transition matrices with unique values of G_{ji}, X_{ii}, and b_S (see Fig. 3-4, main text).

A.

$$p = (1\ 2\ 7\ 8\ 13\ 14\ 16\ 19\ 20\ 25)$$

B.

$$C = \begin{bmatrix} -1 & 0 & 0 & 0 & 0 & 0 & 0 & 0 & 0 & 0 \\ 0 & -1 & 0 & 0 & 0 & 0 & 0 & 0 & 0 & 0 \\ 0 & 0 & -1 & 0 & 0 & 0 & 0 & 0 & 0 & 0 \\ 0 & 0 & 0 & -1 & 0 & 0 & 0 & 0 & 0 & 0 \\ 0 & 0 & 0 & 0 & -1 & 0 & 0 & 0 & 0 & 0 \\ 0 & 0 & 0 & 0 & 0 & -1 & 0 & 0 & 0 & 0 \\ 0 & 0 & 0 & 0 & 0 & 0 & -1 & 0 & 0 & 0 \\ 0 & 0 & 0 & 0 & 0 & 0 & 0 & -1 & 0 & 0 \\ 0 & 0 & 0 & 0 & 0 & 0 & 0 & 0 & -1 & 0 \\ 0 & 0 & 0 & 0 & 0 & 0 & 0 & 0 & 0 & -1 \\ 1 & 1 & 0 & 0 & 0 & 0 & 0 & 0 & 0 & 0 \\ 0 & 0 & 1 & 1 & 0 & 0 & 0 & 0 & 0 & 0 \\ 0 & 0 & 0 & 0 & 1 & 1 & 0 & 0 & 0 & 0 \\ 0 & 0 & 0 & 0 & 0 & 0 & 0 & 1 & 1 & 0 \\ 0 & 0 & 0 & 0 & 0 & 0 & 0 & 0 & 0 & 1 \end{bmatrix}$$

C.

$$b = (0\ 0\ 0\ 0\ 0\ 0\ 0\ 0\ 0\ 0\ 1\ 1\ 1\ 1\ 1)$$

Fig. 3-S1. Vector of non-zero elements (A), matrix of parameter constraints (B), and vector of parameter constraints (C) utilized to estimate parameters in

S3: Lack of a clear relationship for temperature and growth of recruits to immature stages

Monthly estimates of transition probabilities between recruit and immature *S. horneri* (G_{S21}) were plotted against monthly values of bottom temperature (Fig. 3-S2) to evaluate whether generalized relationships could be established between growth and temperature. However, there was not a clear relationship, suggesting that observed rates were governed by other factors, and therefore we did not specify a growth-temperature relationship for G_{S21} in the model and instead used values derived from quadratic programming estimates (Fig. 3-4C, main text).

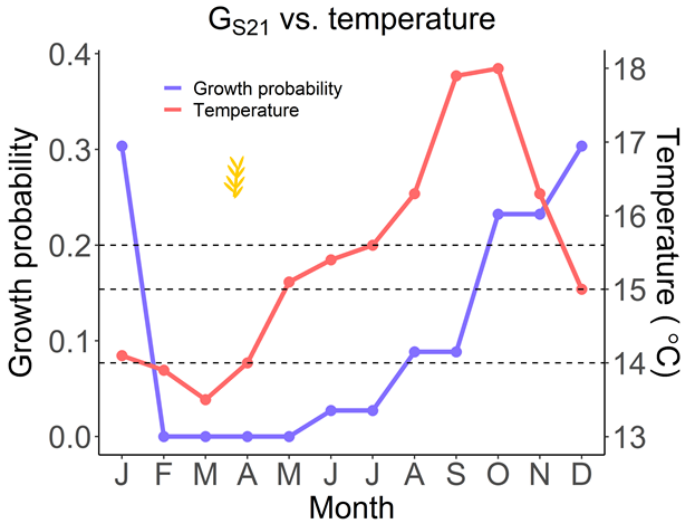

Fig. 3-S2. Values of *Sargassum horneri* growth between recruit and immature stages (G_{S21}) in relation to bottom temperature, with horizontal dashed lines denoting proposed temperature thresholds illustrating there is not a clear relationship between G_{S21} and temperature

S4: Estimating the growth-compensation light level (C_i) for each *S. horneri* stage

To evaluate *S. horneri*'s relationship with light, we estimated the growth-compensation light level (C_i) for each *S. horneri* stage by calculating the light level at which no growth occurred using linear regression equations (Eq. S3-S5) derived from field data in southern California (Ryznar et al., unpublished data).

Recruits

$$y = 0.009367x - 1.656673 \quad \text{(S3)}$$

$$p < 0.05,\ R^2 = 0.15$$

Immature

$$y = 0.04161x - 1.15507 \quad \text{(S4)}$$

$$p < 0.001,\ R^2 = 0.58$$

Stage I and II adults

$$y = 0.01656x + 0.44506 \quad \text{(S5)}$$

$$p < 0.001,\ R^2 = 0.44$$

S5: Comparing stochastic model predictions (Burgman and Gerard 1990) to our single-species *M. pyrifera* model predictions

To incorporate stochasticity, the original stochastic model in Burgman and Gerard (1990) samples from a distribution that incorporates a coefficient of variation around the mean of every monthly demographic and environmental parameter simultaneously. In our deterministic model, we used parameter means. As expected, there were considerable differences between our deterministic model predictions and the stochastic model. Overall, our model approximated the temporal pattern of stochastic stage densities from the original model, albeit the magnitude and timing of the predicted population fluctuations were not identical (Fig. 3-S3). Recruit sporophyte densities observed in the single-species model output are in the lower range of what is observed in the original stochastic model output. The original stochastic model predicts the largest peaks occurring at around 150 individuals m^{-2} whereas the maximum density in our model output is around 50 individuals m^{-2}. The densities of blade sporophytes are overall lower in the single-species model than what is predicted by the stochastic original output. Densities of subadult sporophytes observed in the single-species model fall within the range of what is observed in the

stochastic model, except for a large peak between in the original model that was not observed in the single-species model.

The best fits between the two models occur for the subadults and adults. This is intuitive as the cumulative nature of the demography likely smoothed out stochastic fluctuations to seem more deterministic, resulting in a better fit between the original stochastic and our deterministic outputs in later stages. Maximum density of adults observed in single-species model is slightly less than what is observed in the original model but both occur in the middle of year three. Densities before and after the peak are slightly higher in the single-species model than what is observed in the original model. Canopy dynamics generally align between the single-species model and the original model, with canopy peaks occurring every year. However, canopy density in the single-species model is generally slightly higher than what is observed in the original model.

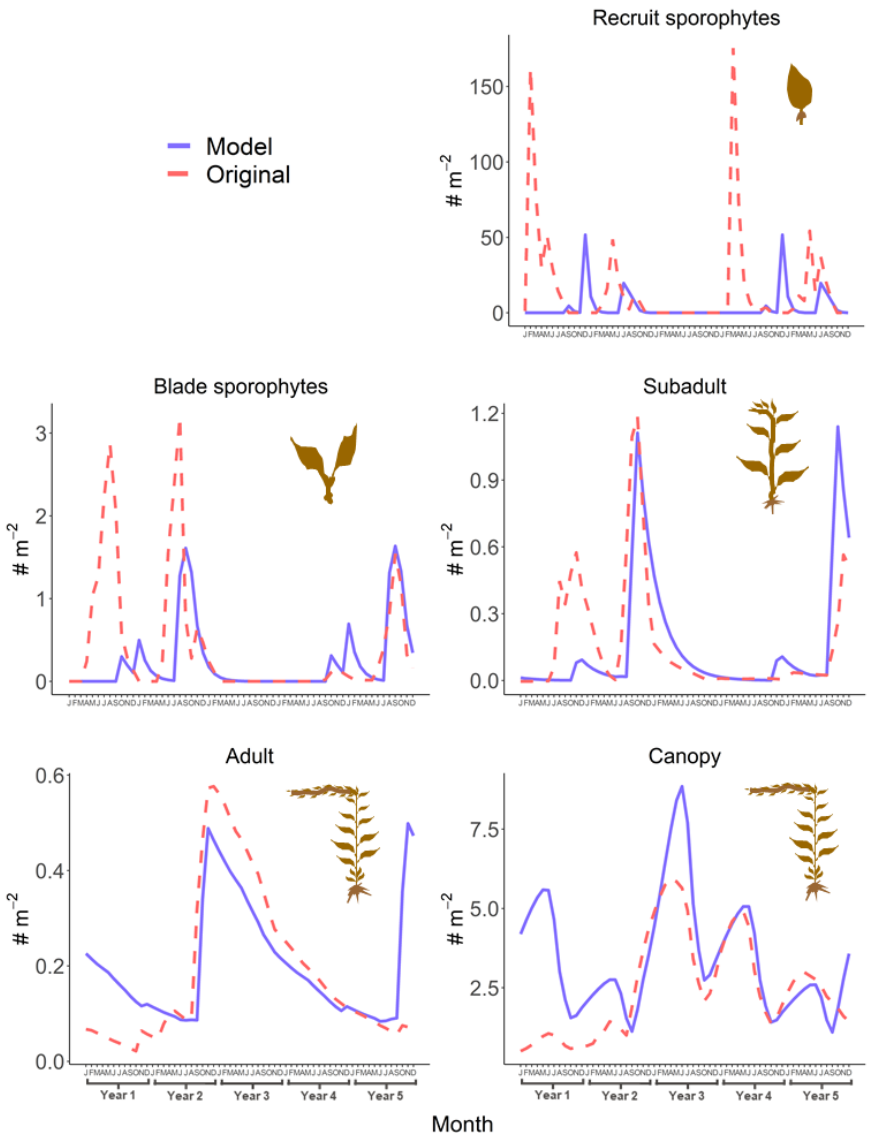

Fig. 3-S3. *Macrocystis pyrifera* single-species model output (intraspecific competition only) for recruit, blade, subadult, and adult stages, and the canopy compared corresponding stochastic model outputs from Fig. 4-5 in the original Burgman and Gerard (1990) model. Canopy and stage densities are displayed per month over a period of five years.

S6: Comparison between the single-species *S. horneri* model output and the field data upon which it was built.

We compared single-species model outputs for *S. horneri* for one year with the field data used to estimate transition parameters (SBC LTER et al. 2018). Overall, the model output closely approximated the field data upon which it was built (Fig. 3-S4).

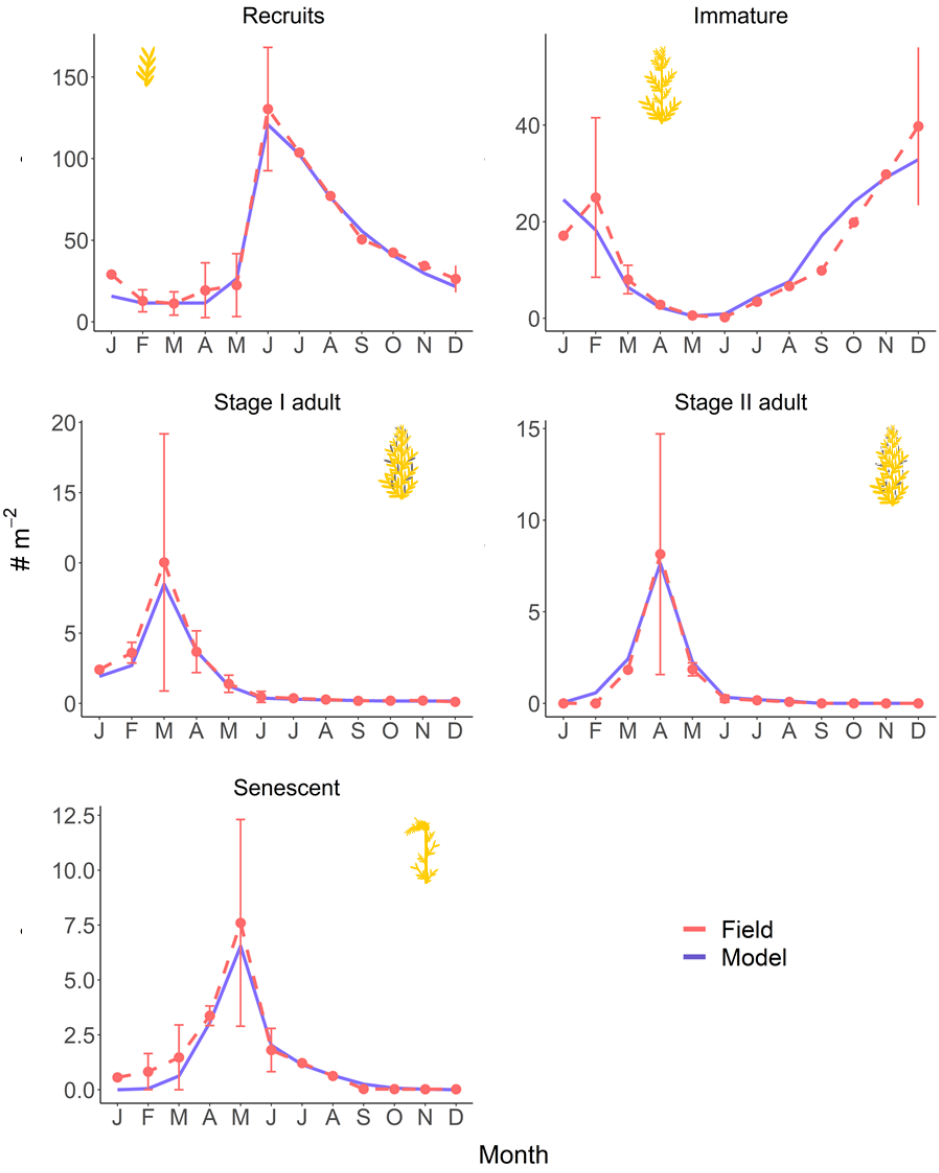

Fig. 3-S4. *Sargassum horneri* single-species model output (intraspecific competition only) for all stages compared to field data (SBC LTER et al. 2018) in southern California. Stage densities are displayed per month over one year, with field data displayed as densities averaged over all survey sites and years (±SE).